

# **Modelling and Simulation of Hybrid Membrane Separation System**

*By*

**PAYEL SARKAR**

(Enrolment No:-ENGG01200704013)

**Bhabha Atomic Research Centre  
Mumbai – 400 085  
INDIA**

*A thesis submitted to the Board of Studies  
In Engineering Sciences*

*In partial fulfilment of requirements For the Degree of*

**DOCTOR OF PHILOSOPHY**

*Of*

**HOMI BHABHA NATIONAL INSTITUTE, MUMBAI**



**July, 2014**

## Homi Bhabha National Institute

### Recommendations of the Viva Voce Board

As members of the Viva Voce Board, we recommend that the dissertation prepared by Payel Sarkar entitled "Modeling and simulation of hybrid membrane separation system" may be accepted as fulfilling the dissertation requirements for the Degree of Doctor of Philosophy.

Srikumar Banerjee 18.6.2014  
Chairman (Prof. S. Banerjee) Date-18.06.14

P.K. Tewari  
Covener(Guide) (Prof. P.K.Tewari) Date-18.06.14

G.K. Dey  
Member (Prof. G.K.Dey) Date-18.06.14

Smt. S.B. Roy  
Member ( Prof. (Smt.) S.B. Roy) Date-18.06.14

N.K. Maheswari  
Member (Prof. N.K. Maheswari) Date-18.06.14

Shri D. Goswami 18/06/14  
Technology adviser (Shri D. Goswami) Date-18.06.14

Madhu Vinjamur  
External Examiner (Prof. Madhu Vinjamur, IIT Powai) Date-18.06.14

Final approval and acceptance of this dissertation is contingent upon the candidate's submission of the final copies of the dissertation to HBNI.

I hereby certify that I have read this dissertation prepared under my direction and recommend that it may be accepted as fulfilling the dissertation requirement.

P.K. Tewari  
Guide- Prof. P.K.Tewari Date: 18.06.14

## STATEMENT BY AUTHOR

This dissertation has been submitted in partial fulfillment of requirements for an advanced degree at Homi Bhabha National Institute (HBNI) and is deposited in the Library to be made available to borrowers under rules of the HBNI.

Brief quotations from this dissertation are allowable without special permission, provided that accurate acknowledgement of source is made. Requests for permission for extended quotation from or reproduction of this manuscript in whole or in part may be granted by the Competent Authority of HBNI when in his or her judgment the proposed use of the material is in the interests of scholarship. In all other instances, however, permission must be obtained from the author.

**Date:** 18.06.14

*Payel Sarkar*  
**Signature**

## DECLARATION

This thesis is a presentation of my original research work. Wherever contributions of others are involved, every effort is made to indicate this clearly, with due reference to the literature, and acknowledgement of collaborative research and discussions.

**Date:** 18.06.14

*Payel Sarkar*  
**Signature**

## List of publications arising from the Thesis

1. Payel Sarkar, D. Goswami, S. Prabhakar, P.K. Tewari, Optimized design of a reverse osmosis system with a recycle, *Desalination*, 230 (2008) pp128-139
2. Payel Sarkar, S. Prabhakar, Sushil Tiwari, D. Goswami and P.K. Tewari, Recovery of water from saturated solutions by membrane process, *Desalination and Water Treatment*, 36(2011), pp65-74
3. Payel Sarkar, S. Prabhakar, D. Goswami and P.K. Tewari, Mathematical model for removal of trace metal by complexation ultrafiltration, *Desalination and Water Treatment*, March (2013), pp1-12
4. Payel Sarkar, S. Prabhakar, D. Goswami and P.K. Tewari, Mathematical modelling of hybrid NF membrane system for the volume reduction of sulphate bearing mining effluent. *International Journal of Chemistry* 2 1 (2013) pp103-111

Date: 18.06.14

*Payel Sarkar*  
Signature

# ACKNOWLEDGEMENT

The first person, to whom I would like to express my most sincere gratitude is my guide, Prof. P.K.Tewari. His enlightening guidance, critical observations and intellectual support have enriched me throughout my research work.

I acknowledge the immense contribution of Dr.S.Prabhakar without whom this thesis would have never come into existence. His academic supervision, encouragement and patience have always sustained me through all my research work. The association with a person of his level of monumental erudition and dedication will always strongly influence me as a researcher and a human being.

I take this opportunity to extend my heartfelt thanks to Mr. D. Goswami for his valuable suggestions and making time for technical discussion with me whenever asked, however busy his schedule be. I remain grateful to Dr. P.A. Hassan of Chemistry Division for his sincere help in Dynamic Light Scattering experiment. The members of the doctoral committee are gratefully acknowledged for their critical review and suggestions during progress review and pre-synopsis viva-voce.

I also wish to record my thanks to my colleague Ms.Avilasha Singha for her sincere contribution to experimental work. Special thanks go to my friends, Mr.G.Kishore, Mr. Sushil Tiwari, Mr.AbhijitRaha, Mr.Soumitra Kar and Mr. Amit Sur for being with me whenever I need them the most. I fondly acknowledge my best friend for last 25 years, Dr. Sumana SenGupta, for being one of my strengths. All my colleagues of Desalination Division are also gratefully acknowledged for their help and support.

My heart warms up while mentioning the people who have made me the person that I am today, my parents, my sister and my brother in law. Words are not enough for expressing

my gratitude to my in-laws, especially my father-in-law, who has always shown keen interest about my progress of work.

Finally I reserve my deepest gratitude to my husband Dr. Subhashis Sarkar for being the pillar of support in my life. His encouragement, inspiration, and diligence for hard work continuously inspire me. Our bundle of joy, Ron (Srijan) also motivates me in a great way to see the positive side of life from a different angle.

# ABSTRACT

Membrane processes are continuously gaining importance owing to several advantages including eco-friendliness, modularity, low chemical intervention, low maintenance and uni-phase operation. One step pressure driven membrane processes such as reverse osmosis, nano-filtration and ultra-filtration are the work horses in the water treatment industry today meeting the objective of providing purified water but they do not lead to absolute separation. They have still some environmental challenges to overcome with regard to the disposal reject streams. In this context, it is felt appropriate to use hybrid membrane processes which combine two membrane processes with same or different characteristics operating in tandem. Accordingly it was decided to take up the study of hybrid membrane separations in detail which forms the subject matter of the doctoral work. The various studies and developments were presented in four chapters.

The introductory chapter describes various membrane based separation processes with emphasis on pressure driven processes. The different mechanisms of the processes proposed for the pressure driven processes such as sieve mechanism, wetted surface mechanism, solution-diffusion mechanism and preferential sorption capillary flow mechanism are reviewed in detail. The various mathematical models which describe the transport of solute through the membranes were then presented. The concept of irreversible thermodynamics model has been analysed in detail particularly based on Kedem-Katchalsky and Spiegler-Kedem approaches. Even though the whole range of pore-sizes are covered from molecular size in RO to about a few microns in MF, absolute separation is hardly possible particularly from homogeneous systems. Highlighting the necessity to look for a combination of processes to achieve near absolute separations, two challenging industrial problems particularly relevant to nuclear industry namely

**‘Removal or separation of trace contaminant from effluent stream’** and **‘Recovery of water from near saturated sparingly soluble effluent stream for reuse’** have been chosen as the subject matter of the thesis with specific objectives on experimental studies to generate separation characteristics and thereafter modeling and simulation of the same based on the membrane characteristics, solute characteristics and hydrodynamics.

The second chapter describes the work carried out with respect to the ‘Removal or separation of trace contaminant from effluent stream’. Starting from the literature model based on irreversible thermodynamic approach, the modifications carried out step by step are described. The base model treats membrane as a black box and describes the water flux and solute flux through two coefficients  $\sigma$  (reflection coefficient),  $\omega$  (solute permeability) respectively. The experimental studies were carried out using complexation-ultrafiltration. The complexation-ultrafiltration operates on the principle of increasing the size of the species to be removed followed by ultrafiltration. In the studies the separation of copper was investigated with polyethyleneimine (PEI) as a complexing ligand, using UF with different MWCO (6,20 and 100KD). The detailed studies indicated that the separation depends on pore size distribution of the membranes, molecular weight distribution of complexing ligand and stability constant of Cu-PEI complex ( $K_d$ ) of the metal ligand complex. The model was developed incorporating the discretised pore size distribution of the membrane and molecular weight distribution of ligand and stability constant into the basic Kedem Katchalsky model and validated based on the experimental studies with copper. The model equations were applied to predict the removal of cobalt and iron as single contaminants and later fractionation of cobalt-iron mixed solute. The combination two UF membranes with different MWCOs were optimized to provide higher separation of Co and iron. The experimental results were found to be in good agreement with the model predictions.

The third chapter deals with the experimental studies on the use of hybrid membrane system to recover water and value from mining effluent circumventing the scaling of  $\text{CaSO}_4$  and the development of a simulation model. Application of NF prior to RO is a critical step in which most bivalent load was eliminated by high flux NF keeping RO at minimum scale threat. Experimental studies were conducted to locate the critical point of flux decline owing to calcium sulphate scale formation in NF. Further it was established that the critical point was only dependent on feed concentration and recovery and is independent of flow rates. From the experimental data, empirical correlation of resistance as a function of feed flow, product flow, operating pressure and reject concentration were developed using least square regression method. Based on the correlation and experimental observations, a simulation model was developed to optimise the operating parameters namely the feed flow rate and operating pressure for a given feed composition. A mathematical model of reverse osmosis for optimizing, the operating pressure, required product quality and quantity have been incorporated. Studies pertaining to optimising the hydrodynamic parameters by thermodynamic exergy calculation and reject management were also carried out. Reject management studies with reference to NF concentrates using lime column has been carried out to demonstrate the approach to zero liquid discharge.

The last chapter provides the summary and conclusions indicating that it was possible to remove trace contaminants particularly heavy metals by complexation UF. With judicious combination of two UF systems it was demonstrated that the mixed systems also can be fractionated. The model developed incorporating the pore-size distribution of the membrane and molecular weight distribution of the complexing ligand along with the stability constant of the metal – ligand complex could reasonably predict the behaviour

not only for single component but also for mixed solute systems. In the case of saturated calcium sulphate effluent stream it was indicated that a NF-RO system combined with lime column could lead to near zero liquid discharge.

# TABLE OF CONTENTS

<b>SYNOPSIS</b> .....	v
<b>LIST OF FIGURES</b> .....	xiv
<b>LIST OF TABLES</b> .....	xix
<b>CHAPTER -1</b> .....	1
<b>INTRODUCTION</b> .....	1
1.1. Separation Processes.....	2
1.2. Membrane Separations .....	3
1.2.1. Membranes.....	3
1.2.2. Membrane Separation Processes.....	11
1.2.3. Relative Characteristics of Membrane Processes .....	15
1.2.4. Hybrid Membrane Systems.....	16
1.2.5. System configuration .....	17
1.3. Mechanisms of Membrane Performance .....	18
1.4. Mathematical model development of membrane based system .....	22
1.5. Objective of present work.....	26
<b>CHAPTER 2</b> .....	28
<b>MATHEMATICAL MODEL FOR THE REMOVAL OF TRACE CONTAMINATION</b>	28
2.1 Theoretical consideration .....	31
2.2 Objective.....	32
2.3 Experimental and Theoretical work carried out .....	32

2.3.1	Materials and Methods.....	33
2.3.2	Estimation of mean pore diameter $r_p$ of membranes .....	37
2.3.3	Mathematical model for separation of single component.....	39
2.3.3.1	Modifications carried out in current studies.....	41
2.3.3.2	Incorporation of pore theory in rejection model .....	42
2.3.4	Results and Discussion .....	44
2.3.4.1	Basic Membrane and ligand characteristics .....	44
2.3.4.2	Discretisation of the pore sizes: .....	48
2.3.4.3	Molecular weight distribution of ligands .....	49
2.3.5	Experimental rejection data .....	52
2.3.5.1	Rejection information of pure copper and pure ligand .....	52
2.3.5.2	Experimental rejection of Copper by complexation with Polyethylene imine (PEI) .....	53
2.4	Model Validation.....	54
2.4.1	Assuming pure ligand rejection 100% and pure metal rejection 0% .....	56
2.4.2	Validation of experimental rejection data of copper with incorporation of mean pore sizes of membrane .....	57
2.4.3	Validation of experimental rejection data of copper with incorporation of discretised pore sizes of membrane and size distribution of ligand.....	58
2.5	Percentage error calculation .....	64
2.6	Prediction of rejection behaviour of single system by mathematical model.....	65
2.6.1	Prediction of rejection behaviour of cobalt system.....	65

2.6.2	Prediction of rejection behaviour of Iron system.....	66
2.7	Prediction of rejection behaviour of multicomponent system.....	69
2.7.1	Rejection of multicomponent solute in 100 KD membrane .....	70
2.7.2	Rejection of mixed solute in 20 KD membrane.....	71
2.7.3	Rejection of mixed solute in 6 KD membrane.....	72
2.8	Fractionation of multi-solute components .....	73
2.8.1	Reject staging of 100 KD followed by 6 KD membrane.....	74
2.8.2	Reject staging of 100 KD followed by 100 KD membrane.....	75
2.8.3	Reject staging of 6 KD followed by 6 KD membrane.....	76
2.8.4	Product staging of 6 KD followed by 100 KD membrane.....	77
2.8.5	Product staging of 100 KD followed by 100 KD membrane.....	78
2.8.6	Product staging of 6 KD followed by 6 KD membrane.....	79
2.8.7	Experimental validation of fractionation result .....	80
CHAPTER-3 .....		82
DEVELOPMENT OF SIMULATION MODEL OF HYBRID MEMBRANE SYSTEM .		82
3.1	Theoretical Considerations .....	86
3.2	Objective.....	88
3.3	Experimental and Theoretical work carried out .....	89
3.3.1	Experimental studies to observe the critical point of scale formation and other performance characteristics in nanofiltration.....	90
3.3.2	Development of mathematical model .....	103
3.3.3	Modification of flux term incorporating cake resistance.....	110

3.3.4	Validation of nanofiltration model.....	116
3.3.5	Optimised feed flow and feed pressure.....	118
3.3.6	Optimization of operating parameters nanofiltration membrane by thermodynamic efficiency analysis (exergy).....	121
3.3.7	Reject Management .....	133
3.3.8	Reverse Osmosis model.....	136
3.3.9	Identification of the overall scheme for the approach to Zero Liquid Discharge.. .....	137
3.4	Conclusion.....	139
CHAPTER-4.....		141
SUMMARY AND CONCLUSION .....		141
<b>Nomenclature</b> .....		147
<b>Reference</b> .....		151

# SYNOPSIS

Membrane processes introduce a new era in the world of separation and are continuously gaining importance owing to several advantages including eco-friendliness, modularity, low chemical intervention, low maintenance and uni-phase operation. A variety of membranes are available with different physical characteristics such as pore size distribution, membrane material, morphology, physico-chemical characteristics (such as surface charge, and solute-membrane interaction etc.) enabling a variety of separations in process industries. Depending on the driving force, the membrane processes can be classified into different subgroups. In each subgroup, membranes of different inherent characteristics can be tailor made by varying their starting raw material, preparation conditions or by incorporating some specific functional groups. Among them, the pressure driven membrane processes have been well established. These pressure driven membrane processes inherently cannot lead to absolute separations because of the pore-size distribution of the membrane and process limitation of osmotic pressure. The concept of hybrid membrane process i.e. judicious selection and use of membrane processes of same or different characteristics in tandem has been conceived to approach towards absolute separation in low energy intensive and highly selective way. The present thesis entitled 'Development of Mathematical Model and Simulation of Hybrid Membrane System' aims at development of validated mathematical model for the removal of trace contaminants using different molecular weight cutoff UltraFiltration (UF) membranes and removal of bulk contaminants using hybrid Nano Filtration-Reverse Osmosis (NF-RO) systems.

The thesis is divided into four chapters for the convenience of presentation. Chapter 1 contains introduction to the present work leading to the objectives. Chapter 2 is devoted to the studies pertaining to 'Development and validation of mathematical model for the removal

of trace contamination and fractionation of mixed solute systems' while Chapter 3 is devoted to 'development of simulation model of hybrid membrane system using RO-NF for water recovery and demonstration of approach to zero liquid discharge'. Both the chapters (Chapter 2 and Chapter 3) contain the theoretical basis for the model development along with the experimental results leading to the validation. Chapter 4 gives conclusions followed by suggestions & recommendation for future work.

### ***Chapter I : Introduction***

This chapter provides a general introduction to different membrane based separation processes and their characteristics. The advantages of membrane separation processes over other separation processes are briefly described. Following a brief description of the characteristics of different membrane processes, an in-depth analysis of the pressure driven membrane processes is presented. The hybrid membrane processes are further discussed highlighting the advantages, with examples from industries. The different mechanisms of salt rejection are described in detail. Sieve mechanism, wetted surface mechanism, solution-diffusion mechanism and preferential sorption of capillary flow mechanisms are described. The descriptions of mathematical models which are used to describe the transport phenomenon of solute through the membrane are elaborated. The concept of irreversible thermodynamics model has been described particularly based on Kedem Katchalsky and Spiegler Kedem approaches as the present work uses this as base model for incorporating the new concepts envisaged in the present thesis.

The family of pressure driven membrane system comprises of microfiltration (MF), ultrafiltration (UF), nanofiltration (NF) and hyperfiltration i.e. reverse osmosis (RO). Depending on separation mechanism the pressure driven membranes are again subdivided into two groups-size exclusion based membranes (MF, UF) and size exclusion as well as

electrostatic interaction based membranes (NF,RO). Membrane processes cannot give absolute separation for contaminants owing to its pore size distribution. Decreasing trend for mean pore sizes has been observed from MF to RO. RO is the finest barrier which can remove monovalent to the tune of above 95%. Removal of trace contaminants or radioactive contaminants from effluent stream demands almost absolute separation of contaminants as the environmental safe limits of these contaminants are low and stringent. This chapter highlights the necessity to look for some other means such as chemical addition or combination of two or more processes- hybrid membrane processes (can be different membrane processes or membrane and conventional processes) to achieve the objectives. With this background the specific objectives of the present study has been derived.

The present work has picked up two challenging industrial problems, particularly relevant to nuclear industry, for which mathematical model has been developed for predicting the membrane performance viz. '**Removal or separation of trace contaminant from effluent stream**' and '**Recovery of water from near saturated sparingly soluble effluent stream for reuse**'.

***Chapter-2 Development and validation of mathematical model for the removal of trace contamination and fractionation of mixed solute systems:***

This chapter describes the work carried out with respect to the 'Removal or separation of trace contaminant from effluent stream'. Starting from the literature model based on irreversible thermodynamic approach, the modifications carried out step by step are described. The base model treats membrane as a black box and describes the water flux and solute flux through two coefficients  $\sigma$  (reflection coefficient),  $\omega$  (solute permeability) respectively. The present work attempts to modify these coefficients by incorporating the membrane properties and polymer-ligand characteristics. The improvements in each step are

indicated in comparison to the experimental results ultimately leading to validation of the model.

The specific challenge is the recovery of trace metals from simulated solution by complexation ultrafiltration process. The pressure driven membranes which operate in size exclusion based separation mechanism are basically low energy intensive process. In industrial effluents valuable metals like copper, cobalt, lead which are present in trace amount are discharged as a waste. For recovering these trace metal from industrial waste in low energy intensive manner, the size of trace metal has been enhanced by complexing it with ligand of higher molecular weight. The macromolecular metal-ligand complex can be easily removed by UF in low energy intensive way. In the present work, complexation ultrafiltration process has been selected for recovery of trace metal. The advantages of complexation ultrafiltration over reverse osmosis for removal of trace contaminant, possibility of recovery of complexing agent are discussed elaborately. RO, the work horse of desalination industry is capable of giving high separation of solutes in the process of producing potable water. However, when the same process is applied to removal of trace contaminants (even though most of the trace contaminants are multivalent species), it is difficult to obtain desirable results as the membrane would operate under 'solution controlled' regime. In addition to being energy intensive, the recovery is limited by the osmotic pressure of the concentrate and operating pressure. On the contrary, if the size of the contaminant species is increased by complexation, then it is possible to obtain high recovery and high removal rates at much less energy. The removal efficiency of UF is not solely dependent on UF pore size distribution. It is a function of metal ligand complex equilibrium and molecular weight distribution of ligand. There is a possibility to pass small molecular weight metal-ligand complex through the smallest pore size of membrane provided size of metal-ligand complex is smaller than smallest pore of membrane. In literature, the most of

the mathematical models developed for complexation ultrafiltration are validated using test cell experimental data [1, 2]. All the studies have assumed 100% rejection for complexed species and 0% rejection for free metal with reference to average molecular weight cut off (MWCO) of the membrane. Consequently the models do not consider transport of complexed species which are dependent on the actual characteristics of the membrane and polymeric ligand besides the equilibrium that exist between the free metal ions and the polymeric ligand. This chapter highlights the present work which involves extensive modification of the irreversible thermodynamic transport model [3] by incorporating the discretised pore size distribution of the membrane and molecular weight distribution of ligand for validation of model in practical system where the recovery is high. For development of model, by virtue of collecting experimental input; Copper –polyethyleneimine (PEI) complex system has been selected owing to its high stability constant and three UF membranes (6KD, 20 KD and 100 KD) of different molecular weight cutoff has been selected . In the experimental set up, the simulated solution of different concentration of metal with constant concentration of ligand has been prepared and it is sent to UF system at 2.5 bar pressure. Both the reject stream and product stream are recycled back to actual feed tank to keep the concentration of feed tank constant. Guided by the experimental observations with respect to solute rejection of Cu-PEI system under different operating conditions with different UF membranes, the base mathematical model proposed by Javier Llanos et.al[1]is initially modified by incorporating mean pore sizes of three membranes. It is further modified by incorporating discretised pore size distribution of membrane and molecular weight distribution of ligand in irreversible thermodynamic model. The modification has been done step by step to reduce the error between the model prediction and actual results. Each discerning trend is analysed conceptually and mathematically corrected in the model. Further the model takes into account the equilibrium conditions and the possibility wherein the number of complexing sites of the

ligand are saturated when excess metal ions are present. After developing mathematical model for single component-single membrane system, mathematical model has been developed for cobalt-PEI and iron-PEI system and they are validated experimentally. By applying different molecular weight cut off (MWCO) ultrafiltration membrane in tandem (intra membrane hybrid system) the possibility of fractionation of multiple solute mixtures has also been envisaged through 6 KD and 100 KD membrane systems.

### ***Chapter-3 Development of simulation model of hybrid membrane system using RO-NF for water recovery and demonstration of approach to zero liquid discharge***

This chapter deals with the study pertaining to recovery of water from nearly saturated sparingly soluble salt solution by inter hybrid membrane process (i.e. nanofiltration followed by reverse osmosis). Recovery of water from near saturated sparingly salt solution by membrane process is a great challenge owing to scale threat on the surface of membrane. In literature, there are instances where addition of antiscalant for sparingly soluble salt separation is suggested [4]. In the present work, addition of antiscalant is not considered as it complicates the reject management. The application of reverse osmosis is constrained by the increasing osmotic pressure in achieving decent recovery. It may be difficult to use UF for separation as complexing would involve large quantities of dosage chemicals. Under these conditions, use of hybrid membrane systems such as NF -RO in combination with the physics of scaling process would help in achieving the desired separation. However, the application of NF followed by RO is considered as the NF has very low solute rejection for monovalents, less tendency for scaling due to surface charge and provides an opportunity to recover water for reuse and approach to zero liquid discharge. Accordingly, studies were carried out with uranium mining effluents which have calcium sulphate near saturation levels besides sodium chloride. Nanofiltration membrane with surface negative charge has been chosen to reduce

the surface attraction of sulphate species which in turn minimizes scale formation. Calcium sulphate precipitation demands significant induction time depending on degree of supersaturation. This chapter comprises of experimental studies pertaining to locating the critical point of flux decline owing to scale formation of calcium sulphate in nanofiltration. By incorporating this experimental input, mathematical model for nanofiltration membrane has been developed to evaluate the operating flow and operating pressure at optimized scale safe recovery. Evaluation of resistances to product flow (intrinsic membrane resistance, osmotic and scale resistance) by experimental flux decline data and developed an empirical correlation of resistance as a function of feed flow, product flow, operating pressure and reject concentration by least square regression method has been carried out. The innovation of present work is development of mathematical model to optimize the super-saturation in tune with the induction time required for precipitation. In practical terms, the hydrodynamics in terms of feed velocity and operating pressure requires to be controlled in addition to the length of the membrane through which the feed has to traverse. One metre length module (commercially available NF90-4040 module) has been used with batch mode of operation involving recirculation of the reject stream. The product stream from nanofiltration membrane has been sent to reverse osmosis module for further refinement of product quality. For achieving zero liquid discharge, reject stream from reverse osmosis module which is less concentrated compared to actual feed is recycled back to nanofiltration feed tank. Mathematical model predicts the product flow and product quality at scale safe recovery for nanofiltration membrane. This model has been validated before and after incorporation of resistance term by experimental flux decline data of nanofiltration. This chapter also presents the optimization study of operating flow and operating pressure of nanofiltration by exergy analysis. Reject management study of nanofiltration by lime column has been also discussed. By this reject management, the sparingly soluble salt can be converted into solid sludge in

lime column and the effluent of lime column can be recycled back to NF feed tank. By this reject management, the potentiality of zero liquid discharge has been envisaged. Development of mathematical model for reverse osmosis for optimizing the operating pressure for obtaining required product quality and quantity has also been discussed.

#### ***Chapter-4 Summary and Conclusion:***

The present thesis deals with development and simulation of mathematical model for hybrid membrane system. Mathematical model developed for complexation ultrafiltration in order to remove trace contaminants from industrial waste is made more realistic by predicting the rejection of macromolecular complex through irreversible thermodynamic transport model. Mathematical models reported in literature are valid for test cell data under zero recovery condition. For predicting the rejection performance of ultrafiltration in real industrial scenario, i.e. at moderate recovery condition; parameters of transport model i.e. solute permeability ( $\omega$ ) and reflection coefficient ( $\sigma$ ) are expressed in terms of discretised pore size distribution of membranes and molecular weight distribution of ligand. The mathematical model developed in this present thesis can predict the experimental rejection value of different trace metals (copper, cobalt and iron) complexed with polyethyleneimine within 3% error range. This model can also predict the fractionation potential of intra membrane hybrid membrane system by predicting the rejection behavior of multicomponent solute mixture through different molecular weight cut-off membranes. Mathematical model developed for water recovery and reuse from near saturated sparingly soluble mine effluents by hybrid NF-RO system is unique for its novel attempt to demonstrate the potential of membrane for sparingly soluble salt removal by optimizing the hydrodynamics, without addition of antiscalant. Application of NF prior to RO is critical step in which most bivalent load can be eliminated by high flux NF keeping RO at minimum scale threat. Incorporation

of resistance terms for evaluation of flux decline in NF improves the model predictability. Studies pertaining to optimising the hydrodynamic parameters by thermodynamic exergy calculation and reject management have also been carried out.

It is concluded that complexation ultrafiltration can be used for the removal of trace contaminants even in highly complex solutions such as seawater. Detailed studies can be undertaken in this regard. Similarly, hybrid systems can be used for fractionation of industrial effluents by judicious selection of membrane processes to recover value.

## References

1. Javier Llanos et.al., Polymer supported ultrafiltration as a technique for selective heavy metal separation and complex formation constants prediction, *Separation and Purification Technology*, 73 (2010) pp126-134
2. Juang, Chen et.al, Measurement of Binding Constants of Poly(ethyleneimine) with metal ions and metal chelates in aqueous media by ultrafiltration, *Ind.Eng.Chem.Res.*, 35(1996) pp1935-1943
3. Gill et.al., Review of Reverse Osmosis Membranes and Transport Models, *Chem. Eng. Commun.*, 12(1981) pp279-363
4. Zahid Amjad, Kinetics of crystal growth of calcium sulphate dihydrate. The influence of polymer composition, molecular weight and solution pH; *Can. J. Chem.*, 66 (1988) pp1529-1536

# LIST OF FIGURES

1.1	Principle of membrane based separations	4
1.2	a) Isotropic membrane; b) Anisotropic membrane; c) Thin film composite membrane	8
1.3	Different membrane element/module configurations	10
1.4	Characteristics of pressure driven membrane processes	14
1.5	Cross Flow filtration and Dead End filtration	18
2.1	Schematic flow sheet of developmental approaches	35
2.2	Schematic diagram of ultrafiltration complexation system	37
2.3	Pure water permeability (PWP)s of different molecular wt. cut off membrane	45
2.4	Variation of pressure drop across UF module during the time of experimentation	45
2.5	Variation of solute rejection in different membranes with different solute molecular weight	46
2.6	Solute mean size of different molecular weight cut off membrane	47
2.7	Cumulative pore size distribution	48
2.8	Linear and branched chain polyethyleneimine	50
2.9	Molecular weight distribution of PEI	51

2.10	Size distribution of PEI	51
2.11	Pure PEI (160 ppm) rejection and pure copper (64 ppm) rejection data	53
2.12	Experimental rejection behaviour of copper as a complex with PEI ligand, concentration 160 ppm	54
2.13	Strategy of validation of experimental data with mathematical model	55
2.14	Validation of model with experimental data by assuming pure ligand rejection 100% and pure metal rejection 0%	56
2.15	Validation of experimental rejection data by incorporating mean pore sizes of membranes in mathematical model	57
2.16	Explanation of calculation procedure for incorporation of mean pore diameter	58
2.17	Validation of experimental metal rejection by incorporating poresize distribution of membrane and size distribution of polyethyleneimine	59
2.18	Prediction of rejection behaviour of cobalt in cobalt –PEI complex by mathematical model at PEI concentration 160 ppm	65
2.19	Validation of rejection behaviour of cobalt by experiments	66
2.20	Prediction of rejection behaviour of iron in iron–PEI complex by mathematical model at PEI concentration 160 ppm	68
2.21	Validation of rejection behaviour of iron by experiments	68
2.22	Rejection study of cobalt and iron in mixed solute containing fixed amount of cobalt (32 ppm) and PEI (160 ppm) in 100 KD membrane	71
2.23	Rejection study of cobalt and iron in mixed solute containing fixed	72

	amount of cobalt (32ppm) and PEI (160 ppm) in 20 KD membrane	
2.24	Rejection of mixed solute (cobalt 32 ppm, PEI 160 ppm) in 6 KD membrane	73
2.25	Fractionation through 100KD-6KD reject staging	74
2.26	Fractionation through 100KD-100KD reject staging	75
2.27	Fractionation through 6KD-6KD reject staging	76
2.28	Fractionation through 6KD-100KD product staging	77
2.29	Fractionation through 100KD-100KD product staging	78
2.30	Fractionation through 6KD-6KD product staging	79
3.1	Flow sheet of integrated membrane system	93
3.2	Effect of operating pressure on recovery at 9.0 lpm feed flow rate	96
3.3	Effect of operating pressure on recovery at 4.5 lpm feed flow rate	97
3.4	Effect of feed flow rate on permeate flow at 9 bar pressure	98
3.5	Normalised Flux as a function of operating pressure at 0.7 recovery for different feed flowrates a) 4.5 lpm b) 7.0 lpm c) 9.0 lpm d.)13.0 lpm [corresponding to apparent Reynold's Number 132, 205, 264 and 381 respectively]	100
3.6	Permeate quality with recovery at (a) constant pressure and (b) constant flow rate	101
3.7	Permeateflow as a function of recovery at 9 bar pressure at different	103

	flowrates	
3.8	Schematic flow sheet of development of mathematical model	104
3.9	Physical model of nanofiltration system	105
3.10	Change of membrane intrinsic resistance with pressure	113
3.11	Change of osmotic resistance with pressure	114
3.12	Change of scale resistance with pressure	115
3.13	Validation of experimental flux decline of nanofiltration by surface crystal growth model	117
3.14	Validation of experimental flux decline of nanofiltration by resistance incorporated surface crystal growth model	118
3.15	Dependence of scaling threat on hydrodynamics	119
3.16	Variation of product flow at different feed flow and different feed pressure	120
3.17	Variation of product quality with feed flow rate at 9 bar pressure	121
3.18	Schematic of nanofiltration process	124
3.19	Variation of specific recovery in different flow rate and pressure	130
3.20	Variation of overall recovery in different flow rate and pressure	131
3.21	Variation of total exergy input in different flow rate and pressure	132
3.22	Variation of total exergy loss in different flow rate and pressure	132

3.23	Thermodynamic efficiency of a system for varying pressure and flow rate	133
3.24	Free settling behaviour of selected reject samples	134
3.25	Settling behavior of concentrates with seeding	135
3.26	Decrease of solid content of reject samples through lime column	136
3.27	Approach towards zero liquid discharge	138

# LIST OF TABLES

1.1	Chemical structure of repeat units of polymeric membrane used in Membrane processes	6
1.2	Relative characteristic of four module configurations	11
1.3	Membrane Processes and their characteristics	13
2.1	Ultrafiltration membrane characteristic	36
2.2	Mean pore size of Ultrafiltration membrane	47
2.3	Discretised pore size distribution	49
2.4	Size distribution of ligand (PEI)	52
2.5a	Explanation of calculation procedure for 6 KD 1:2.5 load ratio of copper and PEI	61
2.5b	Explanation of calculation procedure for 20 KD 1:2.5 load ratio of copper and PEI	62
2.5c	Explanation of calculation procedure for 100 KD 1:2.5 load ratio of copper and PEI	63
2.6	Percentage error calculation	64
2.7	Fractionation of cobalt-Iron Mixture	80
3.1	Evaluation of individual resistance term from flux decline data	112
3.2	Dependance of resistances on parameters	116

3.3	Evaluation of process parameters for exergy analysis	126
3.4	Evaluation of exergy input at state 1 (after pressurization of feed)	127
3.5	Evaluation of exergy at state 2 (reject stream)	128
3.6	Evaluation of exergy at state 3 (product stream)	129



# **CHAPTER -1**

## **INTRODUCTION**

Membrane based separations are gaining importance in the chemical process industries in view of their potential to provide cost effective eco-friendly solutions, following their significant successes in the field of desalination [1] and effluent water treatment [2]. A variety of membranes and membrane processes are being investigated for carrying out challenging separations. The important application areas include provision of purified drinking water from contaminated streams [3] such as micro-organisms, iron, fluoride, arsenic, uranium [4] etc., decontamination of aqueous radioactive effluents [5-6], energy conversion devices like fuel cells [7], concentration of fruit juices in food & beverage industries [8] and environmental management through bipolar electrolysis [9]. and decontamination of aqueous radioactive effluents [4-6]. Innovations in membranes involving polymer blends, nano-materials etc. [10] and membrane processes such as seeded UF, complexation UF etc. have a potential to open up wide range of applications focussing towards recovery of valuable and reuse of spent streams after treatment.

### **1.1. Separation Processes**

The separation processes, in general, involve, either separation of solutes from the solvent as in desalination or separation of a mixture of solutes as done in the petrochemical industries. A separation process [11] is basically a mass transfer operation leading to preferential separation of one or more components from other constituents, which may or may not result in absolute separation. However, at least one component would be enriched in a particular phase. The separation processes can be broadly divided into two categories; equilibrium governed and rate governed. In equilibrium governed processes, the product phase is in equilibrium with the feed (inlet) phases, as in distillation, adsorption, solvent extraction etc. On the other hand, the rate of physical transport of species, governs the separation in the rate governed processes such as reverse osmosis. Generally, the separation is brought out by the

addition of the external component either in the form of energy or matter. In distillation, energy is added to separate one component from the rest while the addition of coagulant aid to a colloidal solution results in the separation of colloids. Adsorption, coagulation, filtration, ion exchange, osmosis etc. are some of the processes where separation is brought about by the addition of external agent, while distillation, crystallisation, drying etc. require energy for effecting the separation. Most of the membrane processes such as reverse osmosis, electro-dialysis, pervaporation etc. require both energy and an external agent.

## **1.2. Membrane Separations**

Membrane is a semipermeable barrier which allows preferentially one of the components to permeate through the membrane. In general to achieve a separation, a membrane with an appropriate driving force is required as shown in Fig.1.1.[12]

### **1.2.1. Membranes**

Membrane is the heart of membrane processes. The membranes are classified in different ways. The first natural classification can be as 'biological' or 'synthetic'. The development of synthetic polymeric membranes such as polyamides and cellulose derivatives has seen an unparalleled growth making the membrane desalination process as an attractive option. Recent research indicates [13] that biomimetic membrane prepared by vesicle fusion on a dense water-permeable support, such as a nanofiltration (NF) membrane can lead to water desalination at less energy intensive manner compared to conventional nano-filtration and reverse osmosis. Of course, issues related to life & stability of the membranes requires to be addressed.

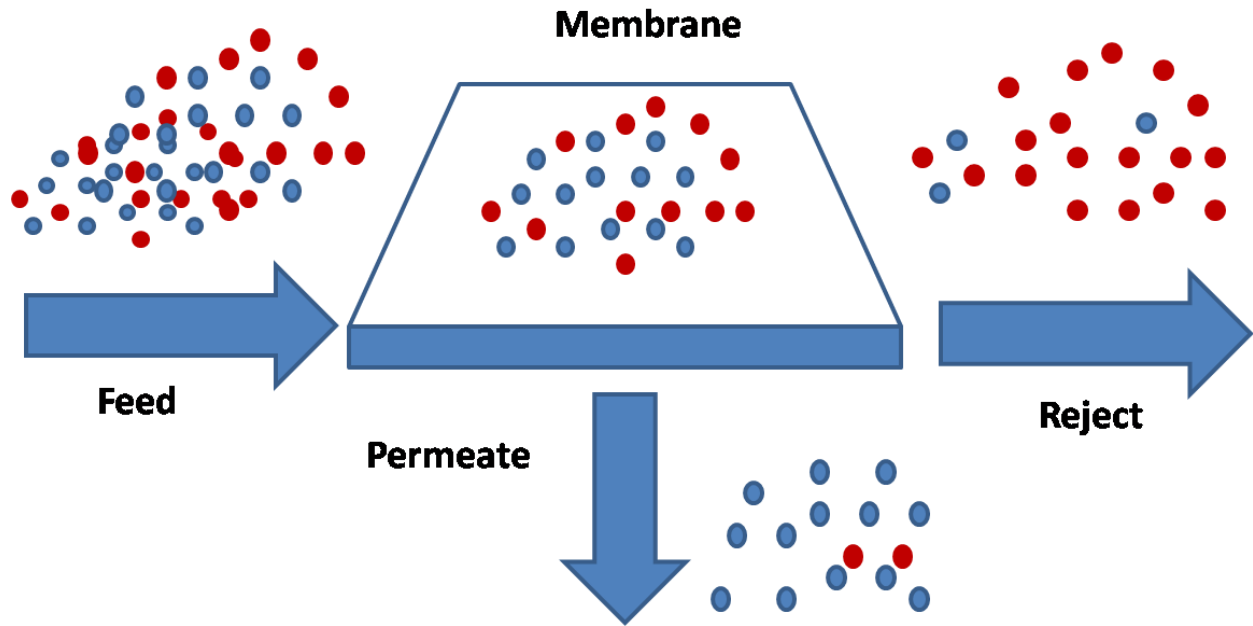


**Fig.1.1. Principle of Membrane Based Separations**

The synthetic membranes can be classified based on their porosity or the other physical characteristics. The material can be inorganic or organic. Inorganic membranes [14] can be of metals such as palladium, silver, metal-alloys or materials such as zeolite, silica, ceramic, carbon, oxides of alumina, titania, zirconia etc. Inorganic membranes have longer life, easy cleanability and withstand high temperatures & harsh environment. However, they are brittle, capital intensive, less compact and exhibit less selectivity.

The synthetic organic membranes [15] are made of either natural polymers, such as cellulose acetates (CTA/CA), nitrates etc. or synthetic polymers such as polyamides (PA), polysulphones (PS/PES), polytetrafluoroethylene (PTFE) etc. The membranes can be neutral or charged. Table.1.1 indicates the chemical structure of the repeating monomer of the widely used polymeric membranes. The membranes can have a dense or porous structure with pores ranging from a few tenths of nano-meters to about a micron. The membranes can be prepared by solution or melt casting method [16]. A number of parameters such as casting solution composition, casting temperature, evaporation period, gelation bath and its temperature,

annealing temperature and post treatment, influence the characteristics of the membranes. Dense membrane dope does not contain any pore forming species. In the case of porous membranes, the pores are incorporated in the membrane matrix by the leaching of the pore forming agent. This being a natural process, there will be a pore-size distribution in the matrix. As only the membrane surface is responsible for the selective permeation and the membrane thickness contributes to the total resistance for flow, thin film composite membranes are made where a porous substrate supports a very thin (about a few hundred nanometers) active polymer membrane. As solution casting [17] is not amenable to formation of such thin films, in-situ polymerisation technique is adopted. In fact, all the commercial membranes used for desalination are prepared based on this technique. Track etched membranes have uniform pores as the pores are formed on thin homogeneous polymer film by the impingement of accelerated nuclear particles such Cu-64 [18].

Based on the structure as shown in Fig.1.2, the membranes are called symmetric (isotropic) or asymmetric (anisotropic) membranes [19]. Isotropic membranes (symmetric membranes) exhibit the same composition as well as structure throughout. They can be dense or porous. Dense membranes also known as homogenous membranes have a dense film through which the species are transported by diffusion under the imposed driving force (electrical potential, pressure, temperature or concentration). The separation is controlled by relative solubility and diffusion rates of the different species present in the mixture. These membranes are suited for separation of species having comparable sizes. Porous membranes can have pore-sizes ranging from about few tenths of nano-meters to about a few microns. Depending on the pore-size, the mechanism of separation can be either only physical (size based) or in combination with physico-chemical interactions. The total membrane thickness determines the resistance to mass transfer. Electrically charged membranes, known as ion-exchange membranes are also dense membranes with fixed positively or negatively charged ions.

**Table.1.1 Chemical structure of repeat units of polymeric membrane used in Membrane processes**

S.No.	Chemical Name	Structure
1.	Polyamide	<p>The structure shows a repeating unit of a polyamide, consisting of a chain of amide groups (-NH-) connected by methylene groups (-CH<sub>2</sub>-). The structure is shown as a zigzag line with dashed lines indicating the continuation of the polymer chain.</p>
2.	Cellulose acetate	<p>The structure shows a repeating unit of cellulose acetate, consisting of a chain of glucose units in a chair conformation, linked by oxygen atoms. Each glucose unit has an acetyl group (-O-C(=O)-CH<sub>3</sub>) attached to the C2 and C6 positions. The structure is enclosed in brackets with a subscript 'n'.</p>
3.	Polysulphone	<p>The structure shows a repeating unit of polysulphone, consisting of a chain of benzene rings connected by oxygen atoms and a central sulfur atom. The structure is enclosed in brackets with a subscript 'n'.</p>
4.	Polycarbonate	<p>The structure shows a repeating unit of polycarbonate, consisting of a chain of benzene rings connected by oxygen atoms and a central carbonyl group (-C(=O)-). The structure is enclosed in brackets with a subscript 'n'.</p>
5.	Polytetrafluoro ethylene	<p>The structure shows a repeating unit of polytetrafluoro ethylene, consisting of a chain of carbon atoms with fluorine atoms attached. The structure is enclosed in brackets with a subscript 'n'.</p>
6.	Nafion membrane	<p>The structure shows a repeating unit of a Nafion membrane, consisting of a chain of fluorinated carbon atoms with a sulfonic acid group (-SO<sub>3</sub>H) attached. The structure is shown as a complex, branched molecule with multiple fluorine atoms and a sulfonic acid group.</p>

Anisotropic (asymmetric) membranes consist of a number of layers each with different structure and permeability characteristics. A typical anisotropic membrane has a relatively dense, extremely thin surface layer (i.e. the "skin", also called the permselective layer) supported on an open, much thicker porous substructure. The separation properties and permeation rates are determined exclusively by the surface layer and the substructure functions as mechanical support with virtually no separating function. The resistance to mass transfer is determined largely or completely by the thin surface layer. These membranes can be made thick enough to withstand the compressive forces used in separation. The thin film is always in contact with the high-pressure feed. Integrally skinned membranes similar to the membranes prepared by Loeb-Sourirajan [20], consist of a single membrane material, but the porosity and pore size change in different layers of the membrane. Anisotropic membranes made by other techniques and used on a large scale often consist of layers of different materials which serve different functions. Interfacial (thin-film) composite membrane which is also anisotropic consists of a thin dense film of highly cross-linked polymer formed on the surface of a thicker microporous support. The dense polymer layer is extremely thin; about a few tens of nanometers. Consequently, the membrane permeability is high and high cross-linking provides better selectivity.

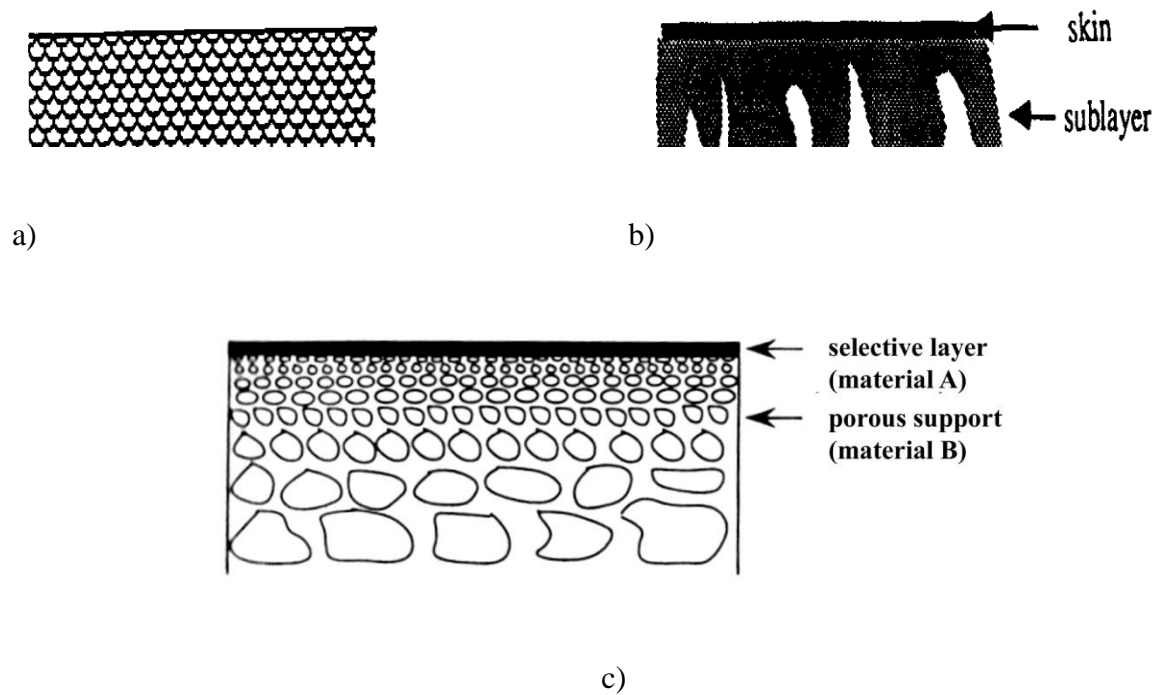


**Fig-1.2 a) Isotropic membrane ; b) Anisotropic membrane; c) Thin film composite membrane**

### **Membrane Configuration**

For using the membranes for separation they have to be packed into elements or modules, which are the building blocks of the overall configuration. Normally membranes are manufactured as sheets or in cylindrical capillaries / tubes. Module or element is the unit into which the membrane is packed. The selection of the type of module depends on the application, quality of feed and the available foot print area.

Commercially four different membrane element configurations exist i.e. tubular, plate & frame, spiral and hollow fibre as shown in Fig.1.3. [21].Hollow fibre configuration has no support for the membrane, while all the other configurations require support for the membrane. The relative characteristics are shown in Table 1.2. Due to practical difficulties such as scaling, hollow fibre elements are not popular for NF & RO applications. Spiral

configuration for RO / NF and hollow fibre/capillary configuration for UF are the workhorses in the water treatment industry

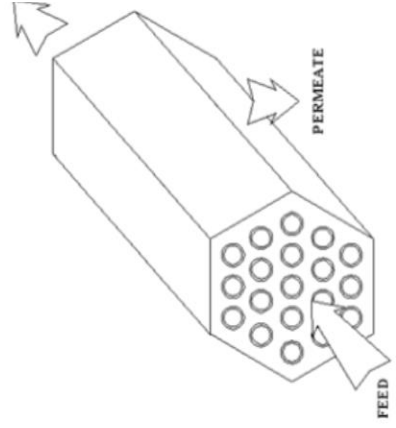
### **Different membrane module and their characteristics:**

Plate and frame modules are easy to clean and replace membranes but less compact having moderate membrane area per volume (100-400 m<sup>2</sup>/m<sup>3</sup>). Plate and frame modules are used in electro dialysis, membrane distillation and mobile units of seawater reverse osmosis.

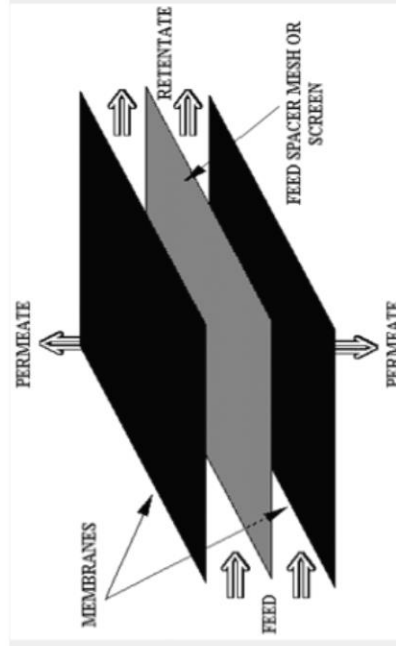
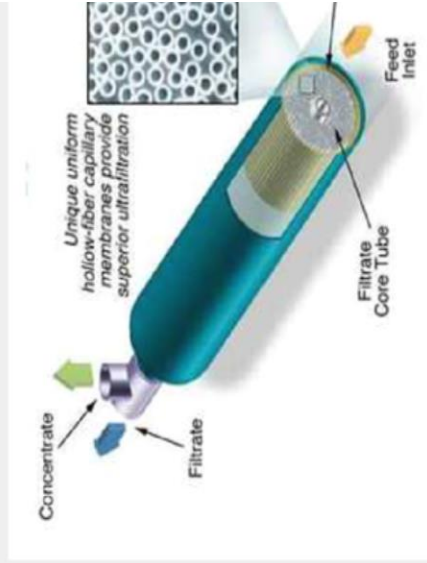
Tubular modules are used while dealing with liquids with high suspended loads as encountered in food industries. The modules are less prone to fouling, and easy to clean but least compact of all the commercial configurations. The tubular configurations are used mainly in ultrafiltration for applications in food industry such as concentration of fruit juices etc.

Spiral wound modules are having high packing density (300-1000 m<sup>2</sup>/m<sup>3</sup>). Maintaining hydrodynamics on top surface of the membrane is easier in this type of module configuration. The spiral wound modules are difficult to clean and sterilise. The pressure drop (100-150 kPa) across the module is on higher side.

Hollow fibre modules are having very high packing density (500-9000 m<sup>2</sup>/m<sup>3</sup>) but poor resistance to fouling and are difficult to clean. Table 1.2 gives a comparative characteristic chart of different module configurations.



## B. Tubular



## A. Plate & Frame

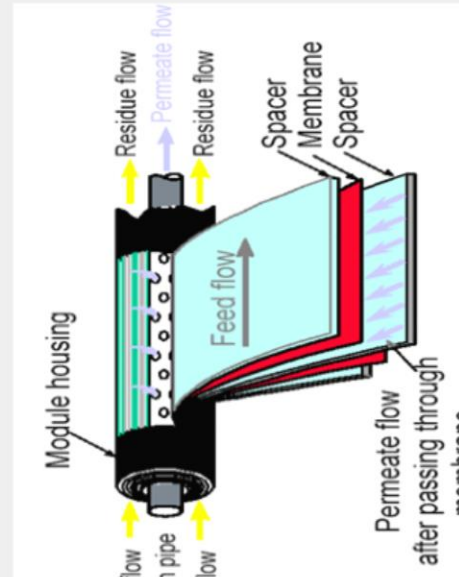


Fig-1.3. Different membrane element/module configurations.[21]

**Table-1.2 Relative characteristic of four module configurations**

	Plate and Frame	Spiral wound	Tubular	Hollow-fibre
Packing density	Moderate	High	Low	Very high
Fouling tendency	Low	High	Low	Very high
Ease of cleaning	High	Low	High	Very low
Pressure drop	High	High	Low	Low
Back washability	Low	Low	High	High
Replacement	Easy	Easy	Difficult	Difficult

### **1.2.2. Membrane Separation Processes**

Membrane separation processes are those which bring about the separation of components using a membrane under an appropriate driving force. A variety of membrane processes have been in use as seen in Table 1.3. The membrane processes can be broadly categorised into concentration driven, electrically driven, pressure driven and others.

Concentration driven membrane processes such as osmosis, haemo-dialysis, diffusion dialysis, etc. are equilibrium controlled processes using either neutral membranes as in osmosis and haemo-dialysis or charged membranes as in diffusion dialysis. Haemo-dialysis uses porous neutral membranes and finds extensive use in medical applications. Osmosis applications have large potential waiting for exploitation and are one of the hot topics of research & development activity at present [22].

Electrically driven processes are based on the transport of charged species through ionic membranes and include electrodialysis (ED), bipolar electrolysis (BPE), membrane electrolysis, electrodeionisation (EDI), electro-electrodialysis (EED) etc [23]. All of them use charged membranes (cationic / anionic). ED has been used for brackish water desalination and clarification of fruit juices. EDI is useful for producing ultrapure water. BPE has

potential in splitting salts present in effluent into their parent acid and base, demonstrated to split salt into their parent acid and base, while EED is being investigated for the concentration of HI in the I-S process for producing hydrogen.

Among the other membrane processes, the R&D studies in the field of membrane distillation (MD) [24] and liquid membranes (LM) [25] are rigorously pursued. MD is thermally driven and uses porous hydrophobic membranes for desalination using waste heat. Liquid membranes (LM) are highly selective membrane process which combines both extraction & stripping with the solvent trapped in pores of the membrane. It is academically well studied but a few practical problems relating to stability of the membrane in the pores of the support membrane and cost of the highly selective solvents need to be addressed.

Among the membrane processes, the pressure-driven membrane processes as seen in Fig.1.4 [26] are the commercially preferred technologies for desalination, water treatment and effluent management. Operating on the applied pressure as the driving force, the membrane preferentially allows certain species to permeate through and retains rest of the components in the concentrate stream such as reverse osmosis, nanofiltration, ultrafiltration and microfiltration. The operating pressure may vary from less than a bar to about 70-80 bars. The mechanism of separation can be purely based on size exclusion as in the case of microfiltration (MF) & ultrafiltration (UF) or size exclusion cum physico-chemical interaction as seen in the cases of nano-filtration (NF) & reverse osmosis (RO).

**Table-1.3 Membrane Processes and their characteristics**

Separation Process	Membrane Type Used	Applied Driving Force	Mode of Separation	Application
Microfiltration	Symmetric porous structure, pore size 0.1 to 5 $\mu$ m	Hydrostatic pressure 0.1-3 bar	Filtration (size exclusion)	Water purification, sterilisation
Ultrafiltration	Asymmetric porous structure, pore size 20 nm-0.1 $\mu$ m	Hydrostatic pressure 2-10 bar	Filtration (size exclusion)	Removal of colloids/suspended solids
Nanofiltration	Asymmetric porous structure, pore size around 1nm	Hydrostatic pressure 5-30 bar	Size exclusion, electrostatic repulsion	Water softening
Reverse Osmosis	Asymmetric porous structure, pore size 0.1 -1nm	Hydrostatic pressure 10-100 bar	Preferential sorption capillary flow method	Sea and brackish water desalination
Electrodialysis	Symmetric ion-exchange membrane	Electrical Potential	Diffusion, Donan-exclusion	Desalination
Diffusion Dialysis	Ion exchange membrane	Concentration gradient	Diffusion, Donan exclusion	Purification/Recovery of acid

Microfiltration (MF) MF membrane uses sieving mechanism with distinct pore sizes for retaining larger size particles than the pore diameter, while the mechanism for conventional depth filtration is mainly adsorption and entrapment. Natural or synthetic polymers, such as cellulose nitrate or acetate, polyvinylidenedifluoride PVDF, polyamides, polysulfones, polycarbonate, polypropylene, PTFE etc. are used for manufacturing MF membranes. Some inorganic materials, such as metal oxides (alumina), glass, zirconia coated carbon etc. are also used for manufacturing MF membranes. MF finds extensive applications in pharmaceutical, food & beverage, chemical and microelectronic industries

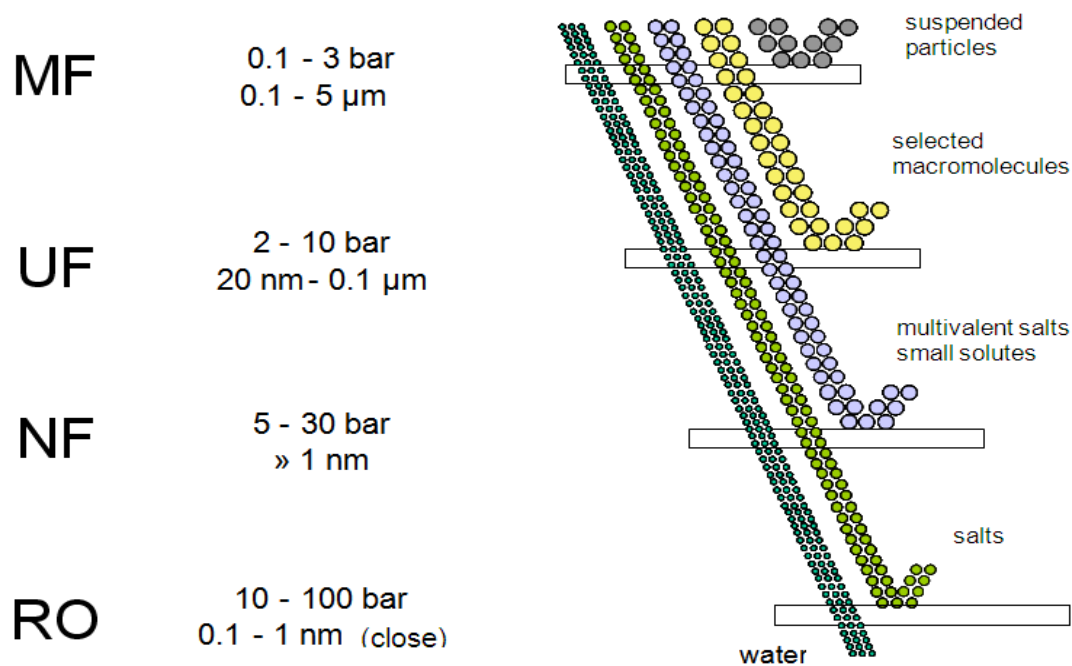


**Fig.1.4. Characteristics of Pressure Driven Membrane Processes**

Ultrafiltration (UF) is a process in which suspended solids and higher molecular weight species are retained. The primary removal mechanism is size exclusion, although the electrical charge and surface chemistry of the particles or membrane may affect the purification efficiency. Ultrafiltration pore ratings ranges from approximately 20 nm-0.1 $\mu\text{m}$  . UF membranes are made of both hydrophilic and hydrophobic polymers. Ultrafiltration finds extensive applications in the field of biotechnology and food processing industries.

Nanofiltration (NF) membrane has pore sizes ranging from about 1nm to about 3 nm. The mechanism of separation is essentially based on surface interactions of membrane top surface with solutes coming as feed subject to size exclusion.NF membrane rejects high molecular weight organic molecules and multivalent ions better than monovalents species. NF processes finds applications in textile and dye industries and softening of hard water. The polymeric material used for membrane for NF applications are similar to RO membrane such as polyamides and cellulose acetates.

Reverse Osmosis (RO) Reverse Osmosis is widely used membrane process particularly for desalination and water treatment. The process uses membranes with very small pore-sizes (i.e) of the order of a few tenths of a nanometer. The mechanism involves preferential flow of water through the membrane and hence requires high operating pressures to counter the solution osmotic pressure.

### **1.2.3. Relative Characteristics of Membrane Processes**

Size exclusion is the primary mechanism through which all the pressure driven membrane processes operate, when the feed stream contains components of distinctly different sizes. This is the case for MF & UF where larger species are separated. Since the retained species would block the pores on accumulation, periodic back wash is carried out to restore the membrane performance. This is possible, as the membranes are largely isotropic and backwash would not lead to any noticeable damage to the membranes. MF is used where the solid phase is to be separated from a solution as in conventional filtration, while UF is useful for separating macromolecules / colloids from solution. NF and RO membranes have relatively smaller pore-size. As NF & RO use asymmetric membranes with top active layer having minute pores, any backwash would lead to the damage of the active layer.

NF & RO membranes preferentially allow water to permeate through due to the surface interactions. NF with relatively larger pore sizes allows monovalent species to pass through in comparison to RO. The permeate fluxes are influenced by the osmotic pressure of the solution. Hence it is difficult to achieve complete separation of water from the feed. Because of the pore-size distribution, the quality of the permeate stream would also deteriorate with increasing separation (recovery), meaning thereby the passage of more solutes along with water.

Even though UF / MF can be operated in dead end mode, they are more often operated in cross-flow mode like NF / RO, excepting 'high value - small volume' operations. Membrane processes when operating in cross flow mode splits the feed stream into two streams: one rich in product i.e. water and the other concentrated stream containing the rejected species. Nearly pure product is possible in UF & MF if the maximum pore-size is smaller than the species to be rejected. In fact 30K Molecular Weight Cut Off (MWCO) UF can provide 5-6 log reduction of bacteria in biologically contaminated water streams. However in NF/RO where membrane duty is to separate water from ionic species which are of comparable sizes, high purity is not possible to obtain because of the existence of pore-size distribution.

#### **1.2.4. Hybrid Membrane Systems**

Hybrid membrane systems i.e. combination of different membrane processes can improve the separation efficiency and recovery. A NF-RO combination for seawater desalination can reduce specific energy consumption. Value addition is also possible as the concentrate generated by RO process can be treated through NF to make it an efficient feed stock for electrolysis of brine for producing caustic soda as the NF treated stream is devoid of most of the multivalent species. In sea water desalination, conventional unit operations such as clarification, sand filtration etc. are used as pretreatment for making the feed compatible with the membrane. The adoption of UF has simplified the whole pre-treatment procedure, besides giving better performance by RO membranes. Such instances where two or more membrane processes can be used in tandem to improve the separation factor and efficiency can be broadly called as 'hybrid membrane systems'. Extension of this philosophy for the effluent treatment would enable the application of eco-friendly operations as well as to meet the stringent environmental regulations.

Several possibilities exist for hybridising membrane systems, with a large number of membranes in RO, NF and UF with different characteristics such as average pore size, pore-size distribution and surface characteristics. There are number of examples of application of hybrid membrane system in various industries. De Carvalho et.al [27] carried out studies on retention behaviour of sugar (glucose, fructose and sucrose) in the process of clarification of pineapple juice by UF-NF process in sugar industry. Puliot Y. et.al [28] reviewed the application of pressure driven membrane processes in pre-concentration before cheese manufacture and different steps of dairy industry. Wolters,R. et.al [29] carried out studies on combined UF/NF treatment for metal recovery of acidic rinsing water in Steel Industry. Govalvez et.al [30] carried out studies on the treatment of waste water from cotton thread factory by UF-NF combined process in textile industry. Walha et.al [31] investigated treatment of high salinity wash water from sea food conditioning Industry by hybrid pressure driven membrane system. The capabilities of hybrid systems in nearly bringing out absolute separations affording the opportunity of reusing the treated solution depends on the judicious combination of membrane processes in tune with the separation objective.

#### **1.2.5. System configuration**

There are two main flow configurations of membrane processes: cross-flow and dead-end mode [32]. In cross-flow mode, the feed flow is tangential to the surface of membrane and the concentrate stream is removed from the downstream of the membrane. The product permeating through the membrane is collected on the other side. In dead-end filtration the direction of the fluid flow is normal to the membrane surface (shown in Fig 1.5) [32]. Both flow geometries offer some advantages and limitations. The dead-end filtration process is usually a batch-type process, where the filtering solution is loaded (or slowly fed) into membrane device, which then allows passage of some species subject to the driving force.

The main disadvantage of a dead end filtration is the extensive membrane fouling and concentration polarization. The fouling is usually induced faster at higher driving forces. The cross flow/tangential flow devices are less susceptible to fouling due to the sweeping effects and high shear rates of the passing flow.

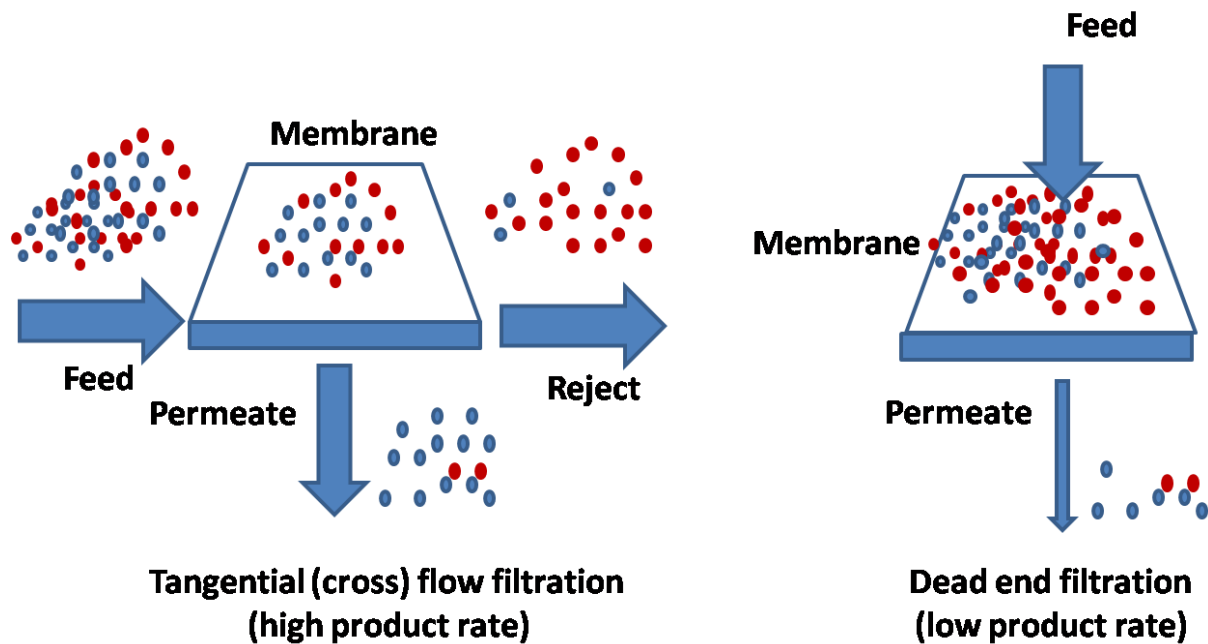


**Fig-1.5 Cross Flow filtration and Dead End filtration**

### **1.3. Mechanisms of Membrane Performance**

A number of mechanisms are proposed for explaining the behaviour membranes in separating the components in a solution. The primary mechanism is the size exclusion philosophy or popularly known as sieve mechanism.

#### **Sieve Mechanism**

The simple concept of “sieve-mechanism” [33] is based on the difference between the molecular sizes of solutes and solvent, with the pore size of the membrane in the intermediate range between the two. Sieve filtration is the basic mechanism for the ultrafiltration process.

When the concentration polarisation is significant, osmotic pressure of the boundary layer reduces the permeation rate. In addition when the gel layer is formed, it offers additional resistance for the flow

### **Wetted Surface Mechanism (Water Clustering) [33]**

In this mechanism, it is recognized that the membrane material is quite wettable, so that the solvent (water) tends to cling to it by means of hydrogen bonding as an absorbed film. This film then obstructs the pores in the membrane and thereby prevents solute ions from entering. The solvent progresses through the membrane by passing from one wetted site to another within the membrane structure.

### **Solution-Diffusion Mechanism [34]**

In "solution-diffusion" mechanism is based on the assumption that both solvent and solute dissolve in the homogeneous nonporous surface layer of the membrane and transported by diffusion in an uncoupled manner. Accordingly it is desirable to have membranes with a completely nonporous surface layer (perfect membrane) which has high solubility and diffusivity for the solvent as compared with those of the solute. In an attempt to improve the "solution-diffusion" model, the "solution-diffusion-imperfection" model has been introduced which accounts for some imperfections on the membrane surface and thus allows pore flow of solute and solvent in an undiluted form; i.e., the pore size is large enough to allow bulk flow. However, when the pore size is small, of the order of molecular size, this assumption is no longer valid and the concentration gradient within the membrane must be taken into account.

### **Preferential Sorption-Capillary Flow Mechanism [34]**

In contrast to the solution-diffusion mechanism, the "preferential sorption-capillary flow" model, assumes that the surface layer of the membrane is microporous and heterogeneous at all levels of solute separation. The mechanism of separation is partly governed by surface phenomena and partly by fluid transport under pressure through capillary pores. Thus the size and number of pores and the chemical nature of the layer constitute the separation mechanism. If the chemical nature of the skin layer in contact with the solution is such that it has a preferential sorption or preferential repulsion for one of the constituents of the mixture, then a steep concentration gradient and hence a preferentially sorbed fluid layer exists at the interface which is enriched by one of the constituents of the bulk solution. Polymeric membranes with low dielectric constant, such as cellulose acetate, repel ions in the close vicinity of the surface which results in preferential sorption of water. This layer of water is then forced through the membrane capillaries under pressure. The dissolved solids which when saturated due to increase in concentration on the brine side of the membrane impose scaling threat on the membranes thus reducing the flux and membrane life.

### **Application of Membrane Systems**

Membrane processes are eco-friendly processes as they do not require large addition or processing of chemicals. Single membrane processes do not mostly lead to absolute separations. The combination of two or more membrane processes with or without additional conventional unit operation can lead to near zero liquid discharge. Moreover, it is generally believed that RO/NF is more suited for the decontamination of multi-valent species such as uranium, cobalt, cadmium etc. it is also believed that scaling components such as calcium and sulphate if present in the feed, limit the recovery and adversely affect the membrane performance. In designing seawater desalination systems, the recovery is limited because of

calcium sulphate scaling be it thermal or membrane desalination. Recent studies have indicated that NF–RO [35] combination can lead to more recovery in membrane desalination by circumventing the scaling of calcium sulphate. Similar studies have also been reported [36] for thermal desalination for raising the top brine temperature. The deeper analysis of the process indicates a slightly charged surface such as NF membranes do not allow the adherence of the species preventing the growth of crystals on the surface. Further the gelation process of calcium sulphate also takes some significant time. Thus, combined with optimal hydrodynamics we felt that the NF/RO hybrid system can be applied to achieve high recoveries.

One of the major problems in industry is to meet the stringent environmental regulations with reference to the heavy metal pollutants such as Cu, Cd, Pb etc. The allowed discharge limits of these metal ions are less than few tenths of ppm while the effluent feeds concentration levels could be a few ppm. In the case of domestic water purification, the removal of heavy ions such as As is required to be below ten of ppb. Use of NF or RO is theoretically a good solution. Given the osmotic pressure limitation due to the dissolved solutes and increasing permeation of solutes with increasing recovery the application of RO or NF is limited. Even if the process is useful the energy cost and the disposal of concentrates pose a major challenge. On the other hand, if complexation UF is used, which makes the size of the complex larger than the pore size of the membrane then the contaminants can be separated into a small volume. Most of the complexes being reversible in nature, it may be possible to reverse the complex say by change in pH and recover the metal ions as value product and complexing agent for recycling. In fact this technique can be extended even to separate two metal ions contaminating the effluents in minor amounts.

#### **1.4. Mathematical model development of membrane based system**

Mathematical modelling is an integral part of any process development in order to effectively design the system for a given objective. M.Soltaneih and W.N. Gill [37] published a comprehensive and detailed review of transport equations and mathematical model of pressure driven membrane processes. Accordingly the most important membrane properties of concern are the transport properties (i.e diffusivities and permeability) of solute and solvent. The equilibrium solubility of solutes and solvents in the membrane phase play an important role in the mechanism of separation.

Permeation is a phenomenological definition which refers to mass transfer through a medium not only by diffusion but by a variety of transport mechanisms under various driving- forces such as the concentration gradient, pressure gradient, electrical potential gradient and temperature gradient. In the reverse osmosis process, the first two driving forces contribute to the permeability of the membrane. Since the actual mechanism of transport through the membrane is not fully known it is both useful and practical to use the term "permeability" for specifying the membrane transport. Authors also commented that in contrast to permeability, the diffusivity in the membrane phase is not easy to use because of the lack of information on concentrations within the membrane matrix. Since the membrane structure is microporous, with pore sizes in the same order of magnitude as that of the solute or solvent molecules, the process of molecular diffusion is hindered by the pore wall effects.

#### **Classification of Membrane Models**

Membrane transport models have been derived from two independent general approaches. First set of the models are based on non-equilibrium or irreversible thermodynamics(I.T.), where the membrane is treated as a black box in which relatively slow processes are taking place close to equilibrium. No information is needed on the mechanism of transport. This

method is useful especially when flow coupling exists between various species which are being transported through the membrane.

In the second approach, some mechanism of transport is assumed and accordingly fluxes are related to the forces that exist in the system. Thus, the physicochemical properties of the membrane and solution are involved in the transport model. For example, the morphological characteristics of the membrane such as porosity, tortuosity and the pore size, membrane physical properties such as solubility of the solute and solvent and their transport properties such as solute and solvent diffusivity, are required to develop an appropriate membrane model. If all of this information is available, one can predict the membrane performance without having experimental data under actual operating conditions. From this view point the second approach is advantageous as compared to irreversible thermodynamic (I.T.) methods.

When structural features are not available, the membrane is normally treated as a "discontinuous" phase separating the two solutions. In this case, all gradients will be replaced by difference quantities and the models-derived are called "discontinuous models." However, if structural features are available, transport equations can be applied on a local level within the membrane. In this case the membrane is treated as a "continuous" phase and the models derived are called "continuous models." It is obvious that if the concentration profile within the membrane is not linear and the phenomenological coefficients are changing with concentration and pressure, then the continuous models are expected to give better results than discontinuous models because they are treated on a differential basis. The continuous models can also be derived when I.T. is used. In this case the linear laws relating fluxes and forces are applied to a differential element within the membrane.

## Irreversible Thermodynamics

When the structure of the membrane is not known and the molecular mechanisms of transport processes within the membrane are not fully understood then the need of irreversible thermodynamics is realised. One of the basic assumptions of the thermodynamics of irreversible processes is that the system can be divided into small subsystems in which "local equilibrium" exists and therefore thermodynamic quantities be written for these subsystems. Thus at least on a local basis, the system should not be too far from equilibrium in order for the methods to be applicable.

### Kedem-Katchalsky Model [38.39]

The first practical model based on irreversible thermodynamics was developed by Kedem and Katchalsky in 1958 for transfer of non-electrolytes through membranes.

For isothermal non-electrolyte systems, and in the absence of chemical reaction,

$$\phi = \sum_{i=1}^n J_i \text{grad}(-\mu_i)$$

Here,  $\phi =$  rate of entropy change with surrounding due to temperature change+ rate of entropy change due to chemical potential change+ rate of entropy change due to chemical reaction

For steady state systems, the flux of component  $i$ ,  $J_i$  remains constant and  $\mu_i$  is chemical potential of  $i$ th component.

$$\int_0^{\Delta x} \phi dx = \phi_m = \int_0^{\Delta x} \sum_{i=1}^n J_i \cdot \text{grad}(-\mu_i) dx$$

Here  $\Delta x$  is membrane thickness.

$$\phi_m = \sum_{i=1}^n J_i \Delta \mu_i$$

Here  $\phi_m$  is the dissipation function of whole membrane.

$$J_{v,i} = L_p (\Delta p - \sigma_i \Delta \pi_i)$$

This is the transport equation of  $i^{\text{th}}$  component. Here  $J_i$  is solvent flux of  $i^{\text{th}}$  component,  $L_p$  is filtration coefficient,  $\Delta P$  is available operating pressure,  $\sigma_i$  is reflection coefficient of  $i^{\text{th}}$  component and  $\Delta \pi_i$  is osmotic pressure gradient of  $i^{\text{th}}$  component.

$$J_{s,i} = (C_{s,i})_{\ln} (1 - \sigma_i) J_v + \omega_i \Delta \pi_i$$

Here  $J_{s,i}$  is solute flux of  $i^{\text{th}}$  component,  $(C_{s,i})_{\ln}$  logarithmic solute concentration of  $i^{\text{th}}$  component and  $\omega_i$  is solute permeability.

### **Spiegler-Kedem Model [40]**

In Kedem-Katchalsky model, the coefficients ' $L_p, \sigma$  and  $\omega$ ' are not too sensitive to concentration. This is true as long as the volume flux and concentration gradients are not too large. When large volume fluxes and high concentration gradients are involved then the changing concentration profile at different flow rates have to be taken into account into Spiegler-Kedem Model.

## 1.5. Objective of present work

Membranes can play a significant role in abating pollution and providing a means to convert waste to wealth. It has also been observed that combination of membrane processes judiciously can lead to eco-friendly and sustainable solutions. In view of this it is thought pertinent to study the treatment of effluents through hybrid membrane systems; one for the recovery of water from bulk scaling contaminants and the other for the removal & separation of trace contaminants and develops mathematical models for their wider applicability. Consequently the studies have been undertaken with specific objectives of

- a. Investigations on hybrid UF systems for the ‘Removal / Separation of trace contaminant/s from effluent stream using complexation–UF system’
  - a. Experimental Investigations on the removal of copper through UF membrane with three different MWCO cut-off characteristics.
  - b. Experimental investigations on the Copper-PEI systems with same set of UF membranes used in (a).
  - c. Developing a mathematical model based on Kedem-Katachlsky equations as the basis.
  - d. Experimental investigations for the estimation of pore-size distribution of the membranes.
  - e. Estimation of molecular weight distribution of the ligand polymer
  - f. Development of the model and validation with experimental data.
  - g. Experimental investigations on iron-Co mixed solute system and optimisation of their separation through hybrid UF membrane system

- b. Studies on the 'Recovery of water from near saturated sparingly soluble effluent stream for reusing NF/RO hybrid Membrane system'.
  - a. Experimental investigations with NF membrane in the removal calcium sulphate from its solution to study the performance characteristics with recovery.
  - b. Identification and analysis of the different resistances and their impact on performance.
  - c. Experimental studies on the physics of  $\text{CaSO}_4$  precipitation phenomenon.
  - d. Simulation model development for the above system.
  - e. Coupling of the above model with RO model

## CHAPTER 2

# **MATHEMATICAL MODEL FOR THE REMOVAL OF TRACE CONTAMINATION**

Stringent environmental standards and increasing realization that ‘waste is wealth’ have made it imperative to direct efforts towards recovering trace constituents from effluent streams as well as seawater. Sorption techniques are being widely investigated for preferential separation of the trace constituents such as uranium [41]. However, the presence of bulk constituents makes the process cumbersome and more often economically unviable. In the last few years, membrane based processes such as liquid membranes (LM), ultra-filtration (UF), nano-filtration(NF), reverse osmosis (RO) etc. are emerging as alternative options for the separation or removal of trace contaminants. Liquid membranes [42] can be highly specific but require the use of costly solvents. Nano-filtration and reverse osmosis are pressure driven processes requiring more energy. Besides, the trace metal concentrations which are normally in the range of a few ppb to ppm are not well rejected as the rejection behaviour of NF and RO are concentration dependent (solution controlled) at extremely low levels of solute concentration. Even if they are rejected, the separation of the species from the bulk constituents becomes difficult. In such cases complexation-ultrafiltration can play an important role. It operates at low pressures and separates the complexed species from the remaining bulk species [43-51]. In most cases, complexation-ultrafiltration utilizes the option of recovering the metal species and ligand by changing the solution properties such as pH [45].In complexation-ultrafiltration, the size of the trace metal species is enhanced specifically to facilitate the separation. Extensive studies have been reported [44-51] with respect to experimental investigations and development of mathematical models to explain the behavioural characteristics of metal ions in the presence of complexing ligands. Most of these studies [43-44] aim at establishing the mechanism of separation and were carried out under laboratory conditions in flat sheets with membrane areas of about a few square centimeters. These studies are useful in developing the basic equations for the designing or modelling but cannot be applied directly for larger systems in practice without modifying

some of the assumptions and model equations. Some of the models proposed in the literature include assumptions such as ‘total rejection of the ligands through UF membranes’[43], the ‘applicability of average experimental rejection data of pure ligand and pure metal, for ligand-metal mixed systems’[50,51] etc. The membrane systems are modular in nature and capacity can be enhanced by adding or multiplying the unit systems. The basic unit of UF is mostly hollow-fibre based (spiral and flat sheet configurations are also available) and is available with a large spectrum of porosity (designated in terms of molecular weight cut off) (MWCO). Even though, they are designated by distinct MWCOs such as 6KD, 20 KD, 100KD etc., the membranes do have a pore-size distribution which can be theoretically estimated [52-54] or determined using different species of known molecular sizes [52]. Commercially available polymeric ligands also have molecular weight distribution. Complexation is an equilibrium phenomenon and consequently free ions, free ligands and complexed species would coexist in the feed stream. Some of these factors which can be ignored under test cell conditions have significant influence on the performance of the system at bench / pilot scale environment. Thus, there is a need to accommodate these factors in the mathematical model to facilitate application of the complexation ultrafiltration in practice. With this objective, attempts have been made to develop a mathematical model by suitably incorporating necessary corrective terms to account for the membrane and ligand characteristics. The relative error improvement with each additional correction term has been compared with the experimental results obtained from copper – Polyethyleneimine (Cu-PEI) system. The validity of the model is further established with experimental systems with aqueous solutions of cobalt and iron. The model has been extended for systems involving fractionation.

## 2.1 Theoretical consideration

All membranes prepared by phase inversion technique have a pore-size distribution and the rejection behaviour of the membrane at very low concentrations of solute species in the feed stream is governed by least resistant route for the solute passage or one can say that it is 'solution controlled'. Generally, as the solute concentration increases from the base level of zero concentration, the solute rejection slowly increases upto a point beyond which there is a marginal decrease. In complexation-UF, it is presumed that the trace metal species is bound to the polymeric ligand and hence gets excluded because of the increased size. Once the complexing polymeric ligand is added to the solution containing the trace metal ions it is expected that some metal ions would be complexed. The extent of complexation would depend on the equilibrium conditions which, in turn would be a function of pH, temperature and relative concentration ratio of metal ion and complexing ligand. Unless the modified size is higher than all the pores present in the membrane surface, there is a probability that the modified-metal species may not be completely rejected by the membrane. The selection of the polymer with appropriate molecular weight, ratio of the polymer/ metal species and the molecular weight cut off (MWCO) of the membrane are important to ensure efficient separation of the desired species.

Several models have been reported with different assumptions depending on the experimental systems. Ruey Shin Juang in 1996 [43] has developed a mathematical model for measurement of binding constants of polyethyleneimine (PEI) with metal ions and metal chelates in aqueous media by ultrafiltration determining the binding properties of metal ions and polymeric ligands on the assumption of total rejection of ligands. Javier Lianos [51] has evaluated the affinity of partially ethoxylated polyethyleneimine (PEPEI) towards industrially valuable metal ions ( $\text{Cu}^{+2}$ ,  $\text{Ni}^{+2}$ ,  $\text{Cd}^{+2}$  and  $\text{Zn}^{+2}$ ) and proposed a model based on the

competitive reaction between polymer functional groups and the cations present in the solution to predict metal rejection coefficients using the complex formation constant data. In the present work, the rejection behaviour of metal and ligand have been predicted by incorporating membrane discretised pore size distribution and ligand size distribution in an irreversible thermodynamic transport model by modifying the ‘reflection coefficient’ and ‘solute permeability constant’ to predict the performance.

## **2.2 Objective**

Hitherto, the most important assumptions of model development of complexation ultrafiltration membrane [43] are ‘rejection of free metal through membrane is zero’ and ‘rejection of pure ligand through membrane is 100%’, resulting in high percentage of error in practical systems where the recoveries are significantly high. In the present study, these two trivial assumptions are eliminated and equations are modified by incorporating discretised pore size distribution and size distribution of ligand in irreversible thermodynamics transport model, to get better predictability of trace element rejection.

## **2.3 Experimental and Theoretical work carried out**

Broadly the work carried out in the present study includes,

- Development of mathematical model for separation of single component (trace metal) system for membrane process.
- Validation of the developed mathematical model for cobalt-PEI and iron-PEI system
- Validation of model for multi-solute (cobalt-iron-PEI) system.
- Validation of model by fractionation experiment with cobalt and iron with 6 KD and 100 KD membranes

- Demonstration of fractionation of multi-solute (cobalt-iron) system through complexation UF.

### **2.3.1 Materials and Methods**

In the present work, hollow fibre ultrafiltration membranes of 6 KD, 20 KD and 100 KD molecular weight cut-off hollow fibre ultrafiltration membranes were selected. The membranes were characterized by standard characterization methods. Selection of membranes has been carried out to exhaust the whole range of ultrafiltration membrane. Low flux, high selectivity 6 KD UF resembles a loose NF and high flux, low selectivity 100 KD UF resembles a tight MF. 20 KD UF would provide the information in between of its two boundary counterparts. In this work, selection of polyethyleneimine as a ligand for binding trace elements over other polymers was endorsed by the high selectivity of polyethyleneimine towards target trace elements (copper, cobalt, iron) and recovery of trace metals from metal-ligand complex by adjusting some physical parameters such as pH. The mathematical model of separation of single component (trace metal) through complexation ultrafiltration is developed, guided by the step by step experiments using copper-polyethyleneimine system. The system has been selected because of the high stability constant of the complex and ease of analytical measurements. In all the experiments carried out in present work; polyethyleneimine concentration has been taken constant 160 ppm suggested by Molinari in his work [45]. Copper concentration has been varied from 1.6 ppm to 160 ppm. The rejection behaviour of copper-polyethyleneimine system has been studied at different operating conditions and the base mathematical model available in literature is modified step by step to reduce the error between the model prediction and actual results. In the process of modification, discretised pore size distribution of membrane and molecular weight distribution of ligand have been incorporated in irreversible transport model. Each discerning

trend is analyzed conceptually and mathematically corrected in the model. After developing mathematical model for single component element guided by the rejection study of copper-polyethyleneimine system, mathematical model has been validated using cobalt-polyethyleneimine system and iron-polyethyleneimine system. Equilibrium constant for cobalt-polyethylene system has been taken from literature [45]. Equilibrium constant for iron-polyethylene system has been calculated mathematically. Later the mathematical model has been modified for multi-solute system and model has been validated with cobalt-iron-polyethyleneimine mixture. This mathematical model has been applied for fractionation of multiple solute mixtures (iron-cobalt). One schematic flow sheet of developmental approach has been given in Fig 2.1.

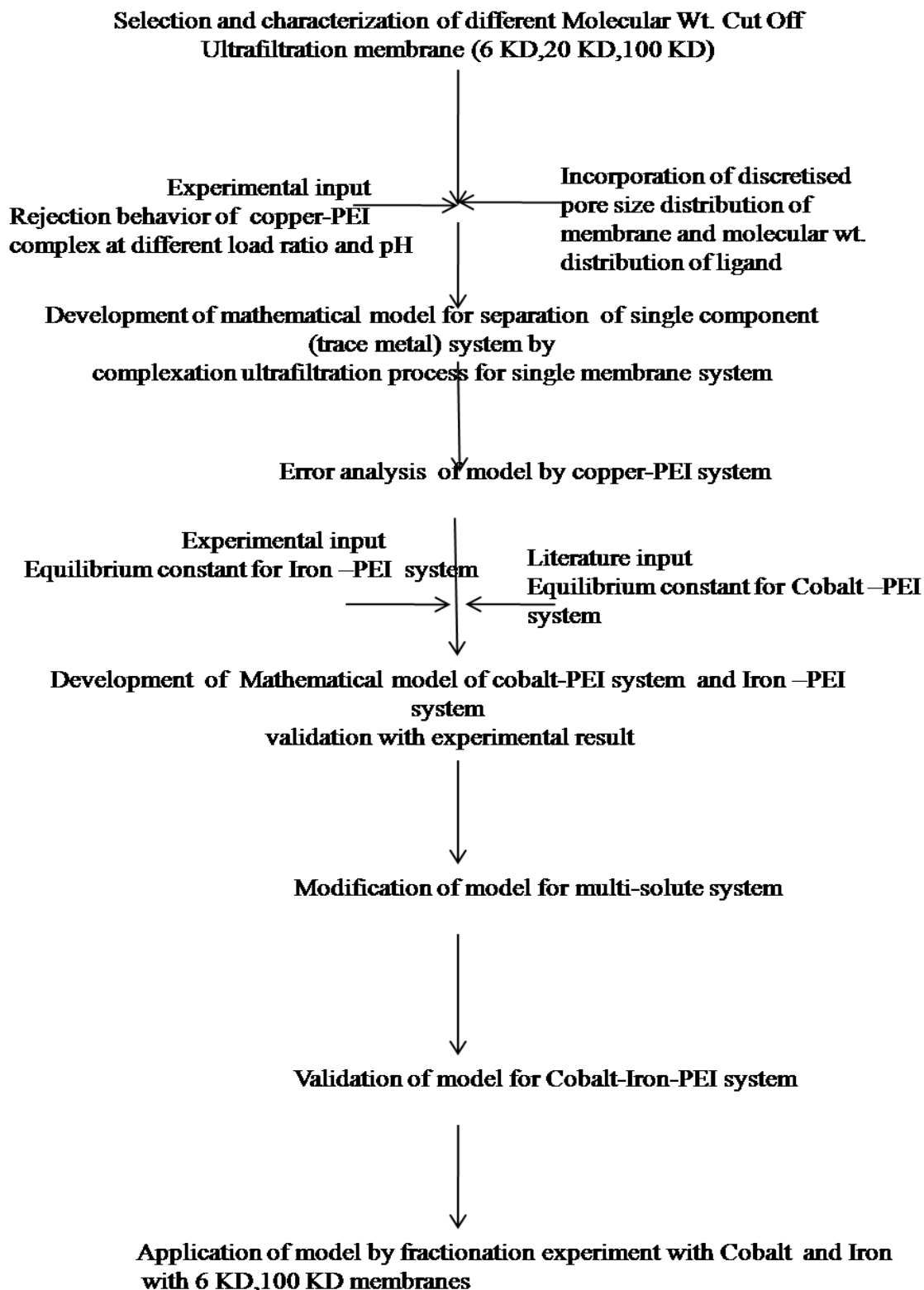


**Fig 2.1 schematic flow sheet of developmental approaches Experimental Methods**

Membrane: Hollow-fibre ultrafiltration membranes supplied by Davey Product having MWCO 6KD, 20 KD and 100 KD have been used in all experiments. All the membranes have been characterized by standard PEG and PEO method [52].Dimensions and available area of these membranes are given in Table 2.1.

**Table-2.1 Ultrafiltration membrane characteristics**

	Dimension (mXm)	Available area(m <sup>2</sup> )
6 KD	0.09X1.1	2.8
20 KD	0.09X1.1	2.8
100 KD	0.09X1.1	7

Pump: Horizontal centrifugal pump (CNP make, model CHL2-40) rated for 33 lpm flow rate and 3 bar pressure was used. The feed flow rate of 35 lpm at 2.2 bar pressure was maintained throughout the experiments by suitably manipulating the valves (concentrate recycle). The fluctuations in flow measurements were about  $\pm 0.25$  lpm and that of pressure was about  $\pm 0.1$  bar.

Preparation of test solutions: Polyethyleneimine (50000D, AR grade) was purchased from Sigma Aldrich. Copper Nitrate (AR grade) was purchased from S.D.Chemicals. All solutions were prepared in distilled water, pH of solutions were adjusted by sodium hypochlorite and hydrochloric acid as required.

Analysis of samples: For Copper, the samples are analyzed with atomic absorption spectroscopy (model no. ICE3000, Thermoscientific make).For polyethyleneimine the samples are analyzed with TOC (model no AnaTOC-2 SGE Australia).

Experimental System:The schematic diagram of the experimental set-up is shown in Fig.2.2.The synthetic feed solution consisting of different load factor ratio of metal and

ligand at constant pH has been prepared in UF feed water tank. The feed is pumped through different molecular weight cut off UF module. To maintain the constant concentration in feed tank, both the reject and product streams are recycled back to feed tank. The tanks are calibrated in terms of volume.

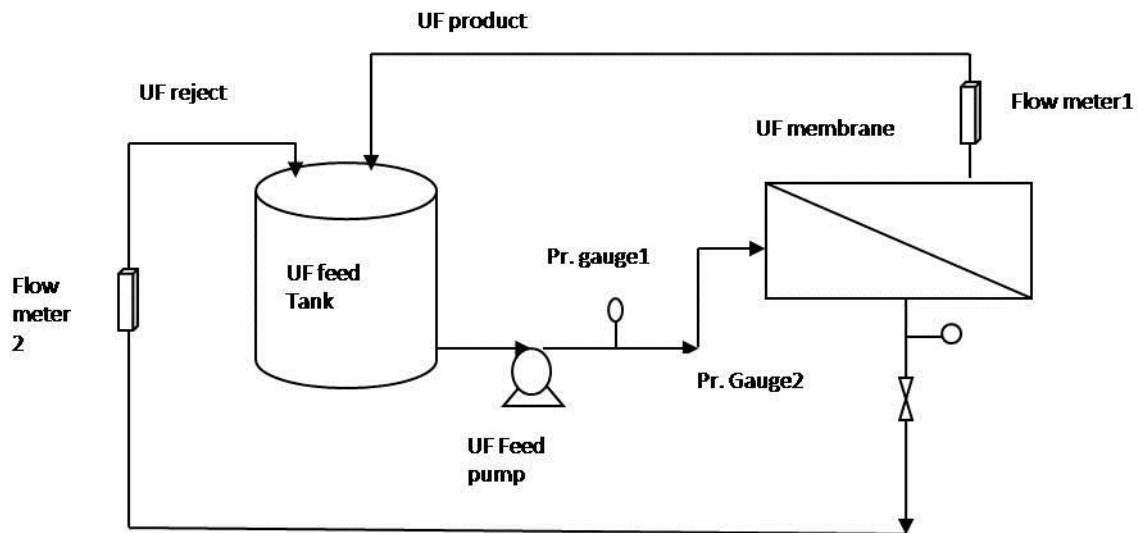


**Fig-2.2 Schematic diagram of Ultrafiltration complexation System**

### 2.3.2 Estimation of mean pore diameter $r_p$ of membranes

There are several methods for the determination of pore size of the membrane both instrumental and physical as described below [52-54]

Instrumental Methods: Electron microscopic techniques viz scanning electron microscopy (SEM) transmission electron microscopy (TEM) and Atomic force microscopy (AFM) are available to view the top or bottom or the cross section of the membrane. AFM is not suitable for our purpose as it can give information on surface charges. In the case of SEM & TEM, there could be change of pore structure during sample preparation stage. Further the resolution is not very good in the ranges of UF membranes.

Experimental Methods: Bubble pressure method is based on measurement of pressure necessary to blow air through a liquid filled porous membrane. It acts on liquid displacement technique. This method is reliable for measurement of largest pore and smallest pore. It does not give precise idea on pore size distribution. Mercury porosimetry is a specific variant of the bubble pressure method wherein mercury is used to fill the pores of the dry membranes. Other methods include thermo-porometry and permoporometry. The former is based on the principle that the solidification point of the vapour condensed in the pores is a function of interface curvature. The principle of the latter process is controlled blocking of pores by condensation of vapour present as a component of a gas mixture.

Solute transport method or solute rejection method is direct method by in which the solute retention of standard molecular weight species is measured. From this information combined with statistics, the pore size distribution is arrived as described. The basic assumption is that pore size distribution follows the normal distribution which is reasonable considering that the pore formation occurs as a natural process when the pore forming agent is leached out during the membrane preparation step. Thus, this method is chosen for the evaluation of mean pore sizes and standard deviation of membranes from where one can estimate the distribution. Solute transport method provides information pertaining to pore sizes throughout the membrane area.

When solute rejection (%) of an UF membrane is plotted vs. the solute diameter on a log normal probability paper, a straight line is formed. In practice, UF membranes are being characterized by taking different molecular weight of polyethylene glycol (PEG) and polyethylene oxide (PEO). The formula for calculation of solute diameter (A) of PEG and PEO with respect to their molecular weights (M) are given below.

For PEG:  $A = 16.73 \times 10^{-10} M^{0.557}$

For PEO:  $A=10.44 \times 10^{-10} M^{0.587}$

From the plot of experimental values of solute rejection (%) of UF membrane against the solute diameter, the solute diameter corresponding to 50% solute rejection is taken as the mean pore diameter of membrane. The geometric standard deviation is obtained by the ratio of solute diameters corresponding to 83.14% and 50% solute rejection, with the assumption that there exist no steric or hydrodynamic interactions.

Estimation of solute diameter  $r_s$  : Solute diameter (Copper and Polyethyleneimine) is obtained from Stoke Einstein equation given below where  $M_w$  is weight average molecular wt. (gm/gmmol),  $[\eta]$  is specific viscosity (cc/gm),  $N_A$  is Avogadro's No.

Based on Einstein equation [52]

$$D_s = 2 \times 10^{10} \left( \frac{3 \times 10^{-3} M_w [\eta]}{10 \pi N_A} \right)^{1/3}$$

### 2.3.3 Mathematical model for separation of single component

#### Complexation model

This model [51] has the following basic assumptions:

The equilibrium is instantaneously attained.

Metal ligand formation will be governed by stoichiometries from 1:1 to 1:n .

pH value is alike in the both sides of the membrane.

No hydroxides are formed within operating pH interval.

Competitive reactions between metal ions (Me), ligand ions (L) and protons (H) have been considered as follows.  $K_a$  is protonation constant and  $K_n$  is equilibrium constant and  $n$  is coordination number of ligand.



Mass balance applied on total concentration of metal ion

$$[Me] = [Me]_{free} + \sum_n [MeL_n] \quad 2.3$$

Mass balance applied on total concentration of ligand ion

$$[L] = [L]_{free} + \frac{[L]_{free} * [H]}{K_a} + \sum_i \sum_n n \cdot K_{i,n} [Me]_{free} \cdot [L]_{free}^n \quad 2.4$$

Inserting the values of equation 2 and equation 3, we get

$$[Me]_{free} = \frac{[Me]}{1 + \sum_n K_{i,n} * [L]_{free}^n} \quad 2.5$$

Inserting the expression of equation 5 into equation 4, we get

$$[L] = [L]_{free} + \frac{[L]_{free} * [H]}{K_a} + \sum_i \frac{[Me] * \sum_n n * K_{i,n} * [L]_{free}^n}{1 + \sum_n K_{i,n} * [L]_{free}^n} \quad 2.6$$

Free ligand concentration is obtained by solving equation 6 while free metal concentration can be found out by solving equation 5.

Rejection of metal is given by

$$R_{Me} = \frac{R_{Mefree} + R_L \sum_n K_n \cdot [L]_{free}^n}{1 + \sum_n K_n \cdot [L]_{free}^n} \quad 2.7$$

Several authors have predicted rejection of metal  $R_{Me}$  (rejection of metal in complexed form) by taking  $R_{Mefree}$  (pure metal rejection) value and  $R_L$  (pure ligand rejection) values from ultrafiltration experimental data [51]. Some authors have also taken  $R_{Mefree}$  value zero and  $R_L$  value 100% for mathematical simplicity [43].  $R_{Mefree}$  is not zero for most of the UF membranes. Hence, for the model development, we have modified the terms  $R_{Mefree}$  and  $R_L$  by incorporation of discretised pore size distribution of membranes and ligand size distribution in Kedem -Katchalsky's transport model.

### 2.3.3.1 Modifications carried out in current studies

Various models based on different approaches are reported [55-58] to describe and predict the solute passage through the membrane. Kedem-Katchalsky's irreversible thermodynamics approach has been considered in the present paper as the molecular mechanisms of transport processes within the membrane are not fully understood. The basic equations for the solute flux and the solvent flux [59] are given as

$$J_v = L_p (\Delta p - \sigma \Delta \pi) \quad 2.8$$

$$J_s = (C_s)_{in} (1 - \sigma) J_v + \omega \Delta \pi \quad 2.9$$

$$(C_s)_{\ln} = \frac{C_m - C_p}{\ln \frac{C_m}{C_p}} \quad 2.10$$

Here  $J_v, J_s$  represent solvent & solute fluxes,  $L_p$  is the filtration coefficient,  $\Delta p$  is pressure drop across the membrane,  $\sigma$  is reflection coefficient,  $\omega$  is the solute permeability and  $\Delta\pi$  is the osmotic pressure difference between the fluid on membrane surface and product stream,  $(C_s)_{\ln}$  is logarithmic concentration,  $C_m$  is concentration of solute on membrane surface and  $C_p$  the concentration of solute in product stream.

In essence,  $\sigma$  indicates the solute rejection property of the membrane and  $\omega$  indicates the solute permeability through the membrane. Since  $\sigma$  is dependent on membrane, there needs to have an appropriate correction factor for  $\sigma$  reflecting the membrane nature. Similarly  $\omega$  requires modification as it refers to the permeability of solute species having a size distribution.

### 2.3.3.2 Incorporation of pore theory in rejection model

Pappenheimer [59] and Verinory [60] incorporated pore theory for trans-capillary transport. According to this theory the membrane structure can be estimated by the parameters  $\sigma$  and  $\omega$  Nakao-Kimura et.al [61] has described the structural implications of the ultrafiltration membrane using the ‘pore theory’. They have assumed that cylindrical membrane pore has a constant radius  $r_p$  and length  $\Delta X$  and that the spherical solutes have a radius  $r_s$ .

$\sigma$  and  $\omega$  can be written in terms of pore theory as

$$\sigma = 1 - g(q) S_F \quad 2.11$$

$$\omega = D.f(q).S_D \left( \frac{A_k}{\Delta X} \right) \quad 2.12$$

$D$  is diffusivity of solute.  $A_k$  is the ratio of total cross sectional pore area to the effective membrane area.  $q$  is ratio of solute radius to pore radius.

$$q = \frac{r_s}{r_p} \quad 2.13$$

$S_D$  and  $S_F$  are the steric hindrance factors for diffusion and filtration flow respectively and are defined as

$$S_D = (1-q)^2 \quad 2.14$$

$$S_F = 2(1-q)^2 - (1-q)^4 \quad 2.15$$

$f(q)$  and  $g(q)$  are the correction factors for the effects of a cylinder wall and are calculated as

$$f(q) = (1 - 2.1q + 2.1q^3 - 1.7q^5 + 0.73q^6) / (1 - 0.76q^5) \quad 2.16$$

$$g(q) = (1 - 0.6667q^2 - 0.2q^5) / (1 - 0.76q^5) \quad 2.17$$

Eq.2.9 can be rewritten

$$J_s = (C_s)_{in} (1-\sigma)(L_p(\Delta P - \sigma\Delta\pi)) + \omega\Delta\pi \quad 2.18$$

$$J_s = (C_s)_{in} (g(q).S_F)(L_p(\Delta P - (1 - g(q).S_F)\Delta\pi)) + D.f(q).S_D \frac{A_k}{\Delta X} \Delta\pi \quad 2.19$$

$$J_w = L_p \cdot \Delta P = \left( \frac{r_p^2}{8\mu} \right) \left( \frac{A_k}{\Delta X} \right) \cdot \Delta P \quad 2.20$$

$$\frac{A_k}{\Delta X} = \frac{L_p \cdot 8\mu}{r_p^2} \quad 2.21$$

$A_k$  is constant for a specific membrane and can be expressed in terms of pure water flux using Hagen Poiseuille equation and  $J_w$  is pure water permeability,  $\mu$  is solvent viscosity.  $J_s$  is the solute flux (free metal as well as free ligand).  $L_p$ ,  $C_m$  and  $\Delta P$  were measured during the experiments. The  $r_p$  was estimated based on experimental studies as described in “estimation of mean pore size” section. Solute fluxes for free metal and free ligand were calculated using eq.19.  $\Delta P$  was taken equal to the operating pressure as the pressure drop along the length of the membrane was negligible. As the experiments were conducted at very low concentrations  $\Delta\pi$  is not significant. However, values could be estimated based on the molar concentration.

$D$ ,  $\mu$  and  $r_s$  were obtained from literature.

## **2.3.4 Results and Discussion**

### **2.3.4.1 Basic Membrane and ligand characteristics**

Before starting actual experimental studies on rejection behaviour of trace element, ultrafiltration membranes and ligand polyethyleneimine were characterized. Membranes were characterized by measuring pure water permeability values and later PEG-PEO method for mean pore size evaluation. Ligands are characterized with respect to their size distribution.

Pure water permeability (PWP) values of all the membranes (Fig-2.3) have been taken at different pressure (operating pressure) with distilled water. PWP values of different membranes increase with increasing pressure. PWP value is highest for 100 KD membranes as it is having larger mean pore diameter, more permeable than other two membranes.  $L_p$  values of all the membranes have been calculated by the slope of the graph which measures PWP values of distilled water through the membrane at different pressures. Although there is

no significant pressure drop during the experiment, (Fig-2.4) in general after every experiment the flushing has been done for 2 min and after 2 sets of experiments backwashing was done for 30 sec.

Pressure drop is measured by the difference of two calibrated pressure gauge readings installed at the entry and exit points of the test module element. The feed did not contain any significant concentration of scaling components and hence pressure drop due to scaling was ruled out. The other possibility was fouling of the membranes due to deposition or concentration of PEI molecules near the membrane surface. As per our observations the pressure drop was negligible ( $< 0.2$  bar i.e. detectable limit) indicating that pressure drop due the hydrodynamics is not significant with reference to the present experimental system.

**Pure water permeability (PWP) and pressure drop of different membranes:**

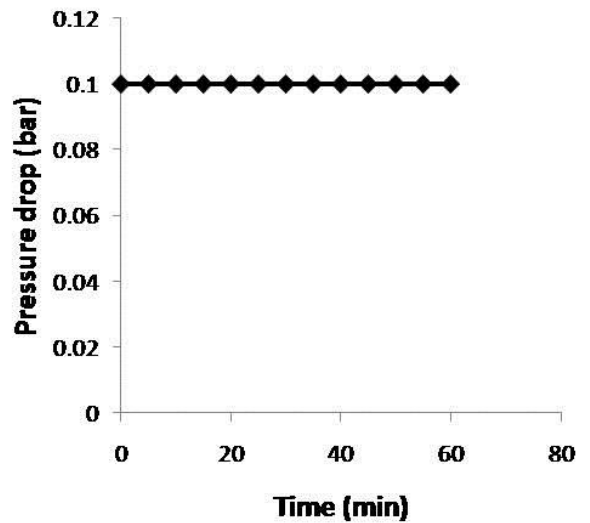
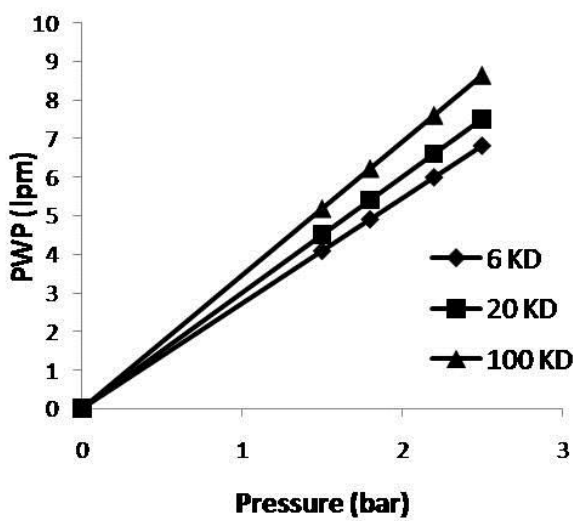


**Fig-2.3 Pure water permeability (PWP)s of different molecular wt. cut off membrane**

**Fig-2.4 variation of pressure drop across UF module during the time of experimentation**

**Membrane characterization and Pore size distribution of membrane**

Molecular weight cut off refers to that molecular weight of solute which gives 90% rejection by that membrane. For confirmation of actual molecular weight cut off of commercially available hollow fibre ultrafiltration membranes standard poly ethylene glycol-polyethylene oxide method has been followed as described in “estimation of mean pore sizes of membranes “section. Standard solution of polyethylene glycol of different molecular weight (upto 35000 Dalton) and polyethylene oxide of different molecular weight (upto 100000 Dalton) have been simulated in feed tank and passed through the different molecular weight cut off membranes (6 KD, 20 KD and 100 KD). Fig 2.5 shows that 6 KD membrane gives 90% rejection of 6000 D (i.e. 6 KD) PEG; 20 KD membrane gives 90% rejection of 20000 D (i.e. 20 KD) PEG and 100 KD membrane gives 90% rejection of 100000 D (i.e. 100 KD) PEO. By this process the molecular weight cut off of commercially available membranes were confirmed.

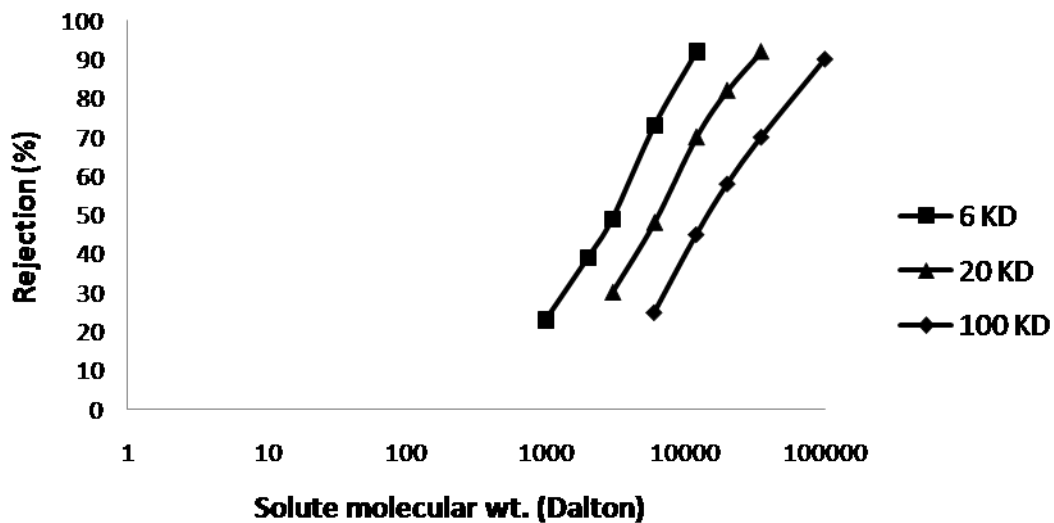


**Fig-2.5 Variation of solute rejection in different membranes with different solute molecular weight**

The solute molecular weight has been converted to solute diameter following equations of size (A) of PEG and PEO vs. Molecular weight (M). Solute size (i.e. solute diameter) has

been plotted in Fig 2.6. Mean pore sizes and standard deviations have been ascertained by the process described in “estimation of mean pore sizes of membranes” section.

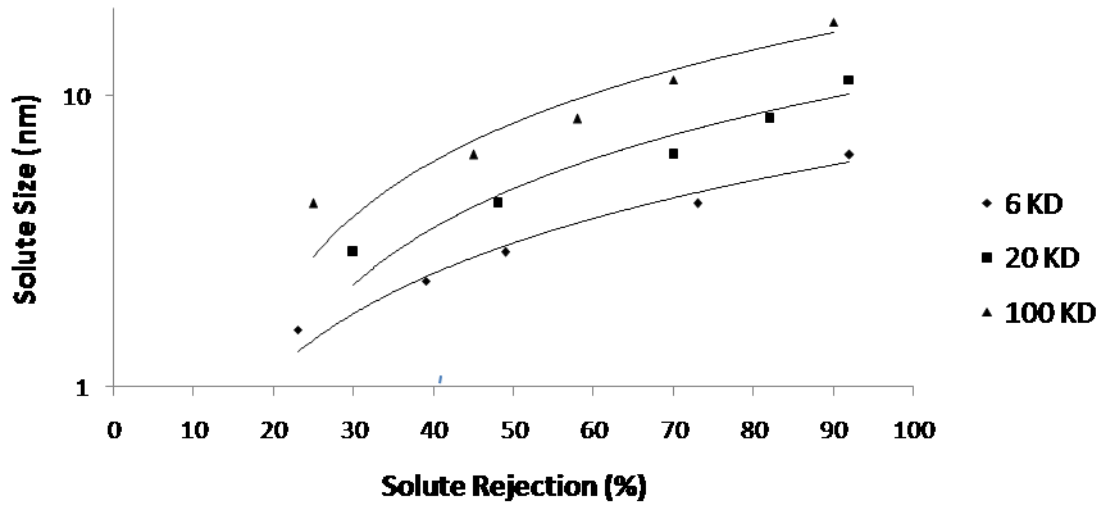


**Fig-2.6 Solute mean size of different molecular wt. cut off membrane**

Mean pore sizes and standard deviations for 6 KD, 20 KD and 100 KD membranes are given in Table-2.2.

**Table-2.2 Mean pore size of Ultrafiltration membrane**

Membrane	6 KD	20 KD	100 KD
Mean pore size(nm)	3.1	4.49	7.20
Standard Deviation	1.82	2.02	2.47

### 2.3.4.2 Discretisation of the pore sizes:

Discretisation in mathematics concerns the process of transferring some continuous function into its discretised (i.e. smaller) counterparts. In this work, physical discretisation of existing membrane pores has been done. Knowing mean pore sizes and standard deviations of three different molecular weight cut off membranes, cumulative pore size distribution of said membranes have been plotted in Fig-2.6. In cumulative pore size distribution of membranes total number of pores of membrane is taken to unity. Each and every fraction of pores has been given a definite specific pore size range.

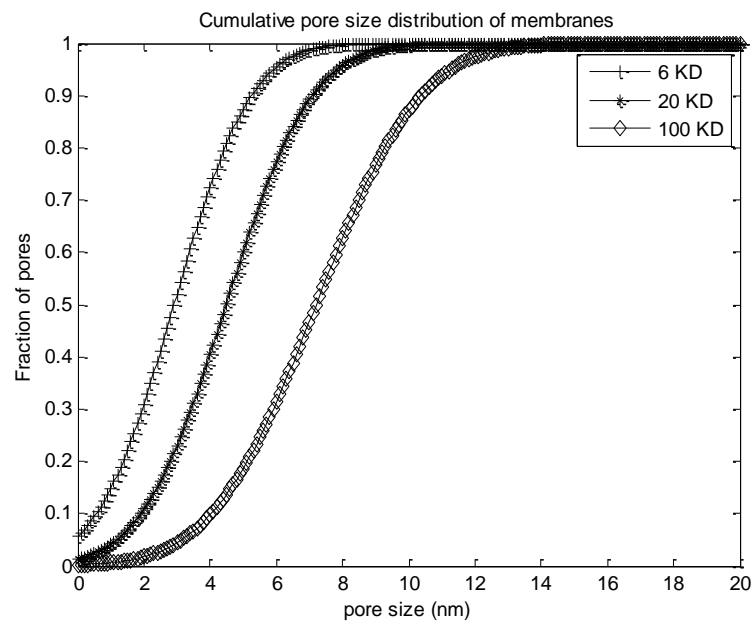


**Fig2.7 Cumulative pore size distribution**

From Fig-2.7 it has been observed that for 6 KD membrane 80-90% of total pores are within 5.5 nm, for 20 KD 80-90% of total pores are within 7.2 nm, for 100 KD 80-90% of total pores are within 11 nm. Here whole domain has been subdivided (discretised) in ten equal sub domains. From this distribution, maximum size of pores in each sub domain has been evaluated as given in Table-2.3.

**Table-2.3 Discretised pore size distribution**

Fraction of pores	0.0-0.1	0.1-0.2	0.2-0.3	0.3-0.4	0.4-0.5	0.5-0.6	0.6-0.7	0.7-0.8	0.8-0.9	0.9-1.0
6 KD	0.7	1.5	2.1	2.5	3	3.5	4.0	4.6	5.4	11.0
20 KD	2	2.9	3.5	4.1	4.6	5.1	5.7	6.3	7.2	12.5
100 KD	4.2	5.3	6.0	6.7	7.3	8.0	8.6	9.4	10.5	17.0

#### **2.3.4.3 Molecular weight distribution of ligand**

Polyethyleneimine (PEI) or polyaziridine is a polymer with repeating unit composed of the amine group and two carbon aliphatic  $\text{CH}_2\text{CH}_2$  spacer. Linear polyethyleneimines contain all secondary amines, in contrast to branched PEIs which contain primary, secondary and tertiary amino PEI is produced on industrial scale and finds many applications because of its affinity towards selective trace metals. The metal-ligand interaction is influenced by many factors including the functionality of the chelating group, the density of chelating groups in the polymer, oxidation state and electronic configuration of the metal, stereochemistry, steric constraints as well as electrostatic interactions groups shown in Fig2.8 .Totally branched, forms are also reported. The chelating functionality usually consists of some type of mono-, bi-, or polydentate moiety of polyethyleneimine. The spacing between the functional groups on the polymer can play an important role for formation of ligand complex. If the donor groups are close together on the polymer chain, or if there is little steric hindrance between chains, several monodentate ligands can act as a polydentate ligand. Thus, the metal ion can induce local folding or crosslinking of

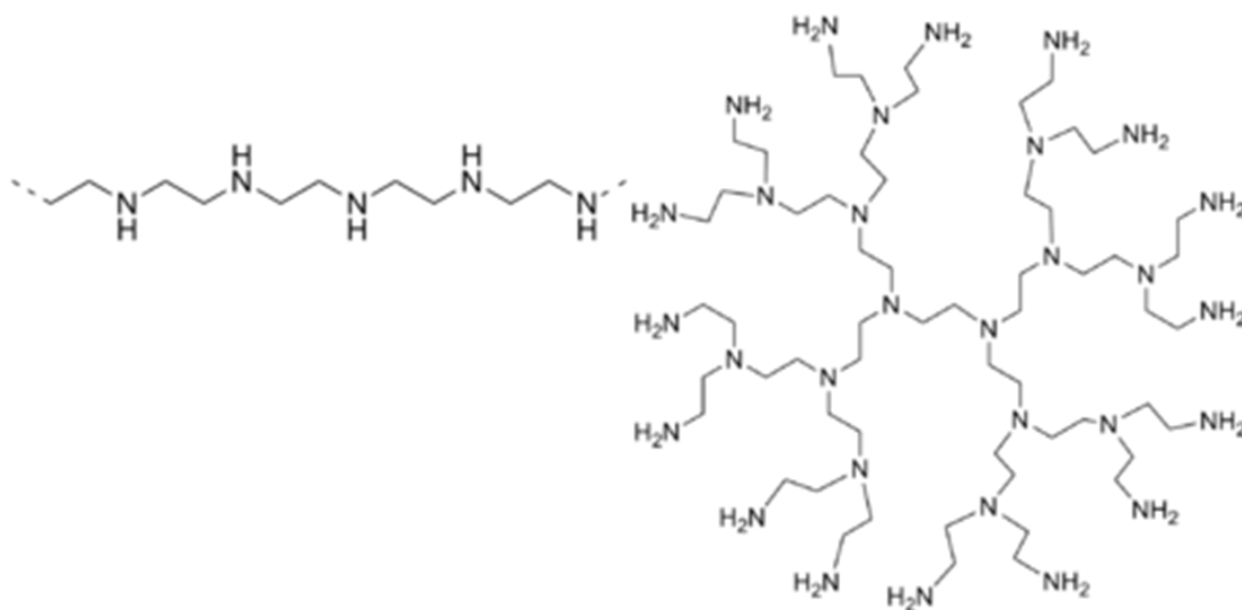


**Fig 2.8 Linear and branched chain polyethylenimine**

the polymer chains. In this present work, branched chain polyethylenimine having 50000 D molecular weight has been taken. The facts that polyethylenimine having lower molecular weight having lower selectivity and higher molecular weight having lower flux and higher scaling threat on membrane surface promotes to select the polyethylenimine in that range. Branched chain polyethylenimine has more active sites compared to its linear or hyperbranched counterpart. Besides, the branched chain polyethylenimine does not cause the conformation change of polymer chains in aqueous solution probably due to highly branched globular structure. Viscosity value of branched chain polyethylenimine remains constant over the pH range of 2-11, whereas viscosity value for linear polyethylenimine decreases with increasing pH.

Average solute size of polyethylene mine evaluated from Stoke Einstein Equation is 39 nm. As earlier discussed that polyethylenimine is a cluster of mono-dentate, bi-dentate and polydentate polymer, so size distribution or molecular weight distribution of this ligand will be very important parameters pertaining to overall rejection.

Size distribution of polyethyleneimine has been obtained from Dynamic Light Scattering (DLS). The basic principle of this instrument is when a monochromatic light beam, such as a laser passes through a solution with spherical particles moving in Brownian motion, it causes a Doppler shift. When the light hits the moving particle, the wave length of incoming light has been changed. This change is related to the size of the particle.

Attached software in the instrument gives the size distribution and molecular weight distribution of given polymer and also the size vs. weight fraction and number fraction data.

The molecular weight distribution plot, size distribution plot and size vs. weight fraction of polymer obtained from DLS experiment are given below.

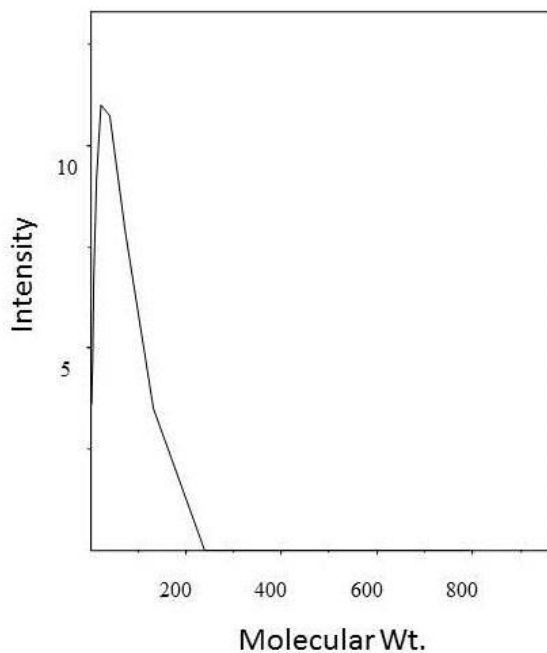


**Fig 2.9 Molecular wt. distribution of PEI**

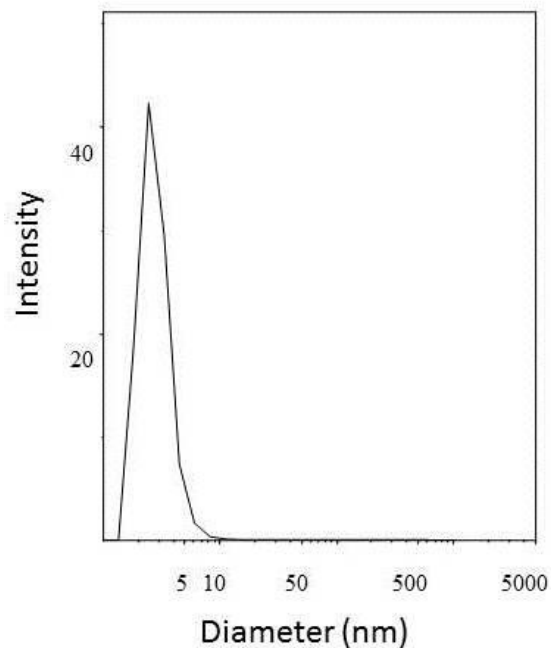


**Fig 2.10 Size distribution of PEI**

Fig 2.9 shows the molecular weight distribution of PEI. This molecular weight distribution is converted to size distribution by software inbuilt in DLS. Fig 2.10 shows that actual size distribution of polyethyleneimine is much less than the size predicted by Stoke Einstein equation (39 nm). The size distribution of polyethyleneimine is given below in table 2.4.

From the size distribution of PEI it has been concluded that almost 66% of PEI weight fraction having diameter less than 3.5 nm.

**Table-2.4 Size distribution of ligand (PEI)**

Wt.fraction	0.107	0.281	0.281	0.166	0.089	0.044	0.02	0.008	0.003	0.001
Diameter (nm)	1.8	2.5	3.3	4.5	6.1	8.2	11.1	14.9	20.2	27.2

### **2.3.5 Experimental rejection data**

#### **2.3.5.1 Rejection information of pure copper and pure ligand**

Fig-2.11 shows pure copper rejection (in red) and pure ligand rejection (in black) in 6 KD membrane. Pure copper rejection is very low due to its small size compare to membrane pore size and this rejection behaviour is independent of copper concentration. As the weight ratio (1:2.5) copper and polyethyleneimine gives most stable complex; rejection of 64 ppm copper has been shown in the graph. Pure ligand rejection is reported quite high. In order to get a satisfactory rejection of copper it has been complexed with ligand and sent through ultrafiltration membrane.

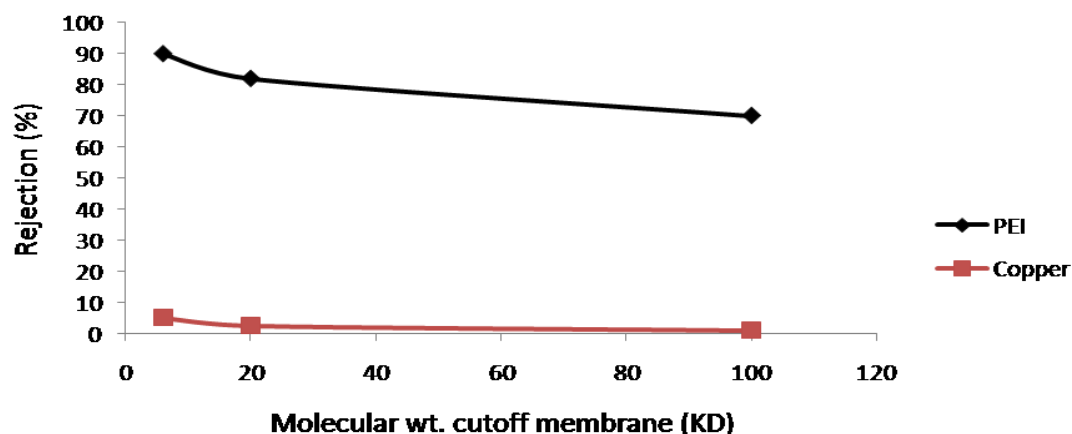


**Fig-2.11 Pure PEI (160 ppm) rejection and pure copper (64 ppm) rejection data**

### 2.3.5.2 Experimental rejection of Copper by complexation with Polyethylene imine (PEI)

The Fig.2.12 refers to the rejection behaviour of copper in the presence of PEI for three different membranes corresponding to three distinct MWCO cut offs namely 6KD, 20KD and 100KD. Because of the different MWCO the membranes exhibit distinct ‘average pore-size’ and ‘pore size distributions’. The fraction of the larger pores as well as the average pore-size is higher for the membranes with MWCO-100KD, less for 20KD and the least for 6KD. Same concentration and same lot of PEI is used for all the three experiments, thereby meaning that the MW distribution is the same. The copper permeation through the membranes now can be due to two reasons i.e. permeation of uncomplexed Cu and permeation of Cu-PEI complex formed with lower MW PEI. The first part of the rejection curves (which is nearly flat) for all the three membranes is the membrane controlled domain, as their pore size distribution is distinct. In this domain all the Cu is in the Cu-PEI complexed form. Therefore the rejection exhibited by copper is due to permeation of low-MW Cu-PEI complex whose percentage is more for 100KD and least for 6KD. On the other hand the

second part of the curve indicates the fall in rejection due to uncomplexed copper (as no more bonding sites with PEI are available) and the slopes are nearly same indicating that the same amount copper is permeating. All the three curves are parallel indicating that other than the pore size distribution no other membrane property is responsible for the behaviour.

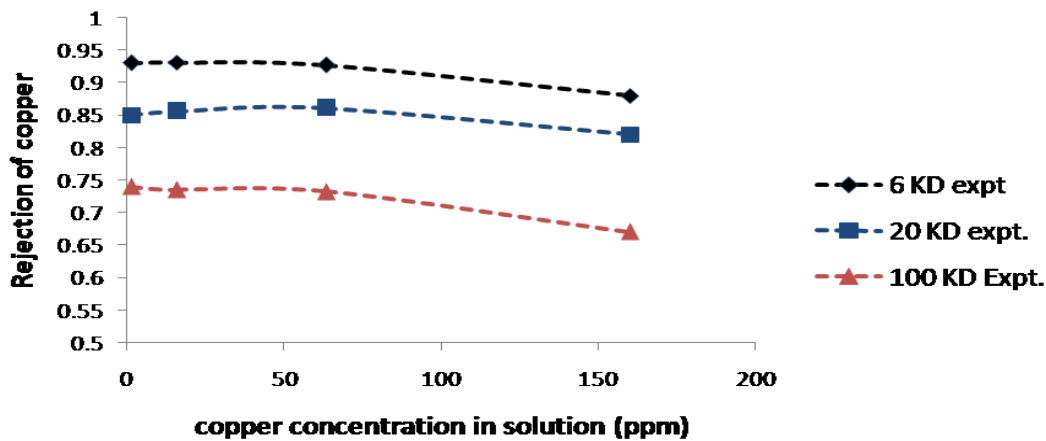


**Fig-2.12 Experimental rejection behaviour of copper as a complexed with PEI ligand, concentration 160 ppm**

## 2.4 Model Validation

The strategy of validation of model is given in Fig 2.13. The model equations have been developed by incorporating modifications to the base model (without corrections for pore size distribution & molecular weight distribution for the complex) and later incorporating the corrections step by step. At every step the model performance is compared with field results and the error margin between the experimental values and model values were worked out. The base model algorithm assumes pure ligand rejection 100% and pure metal rejection 0% as given by [43]. Based on this assumption, the model is used to estimate metal rejection  $R_{Me}$  with the condition  $R_{Me\text{free}} = 0$  and  $R_L = 1$ . Then calculated error margin with respect to experimental value. The ultimate objective is to minimize the error by incorporating

modifications to the base model. In the first modification incorporation of mean pore sizes of membrane has been incorporated and in the second modification discretised pore sizes of membranes and size distribution of ligand has been incorporated. In every step, the error margin has been calculated. Percentage error calculation is given in Table-2.6.

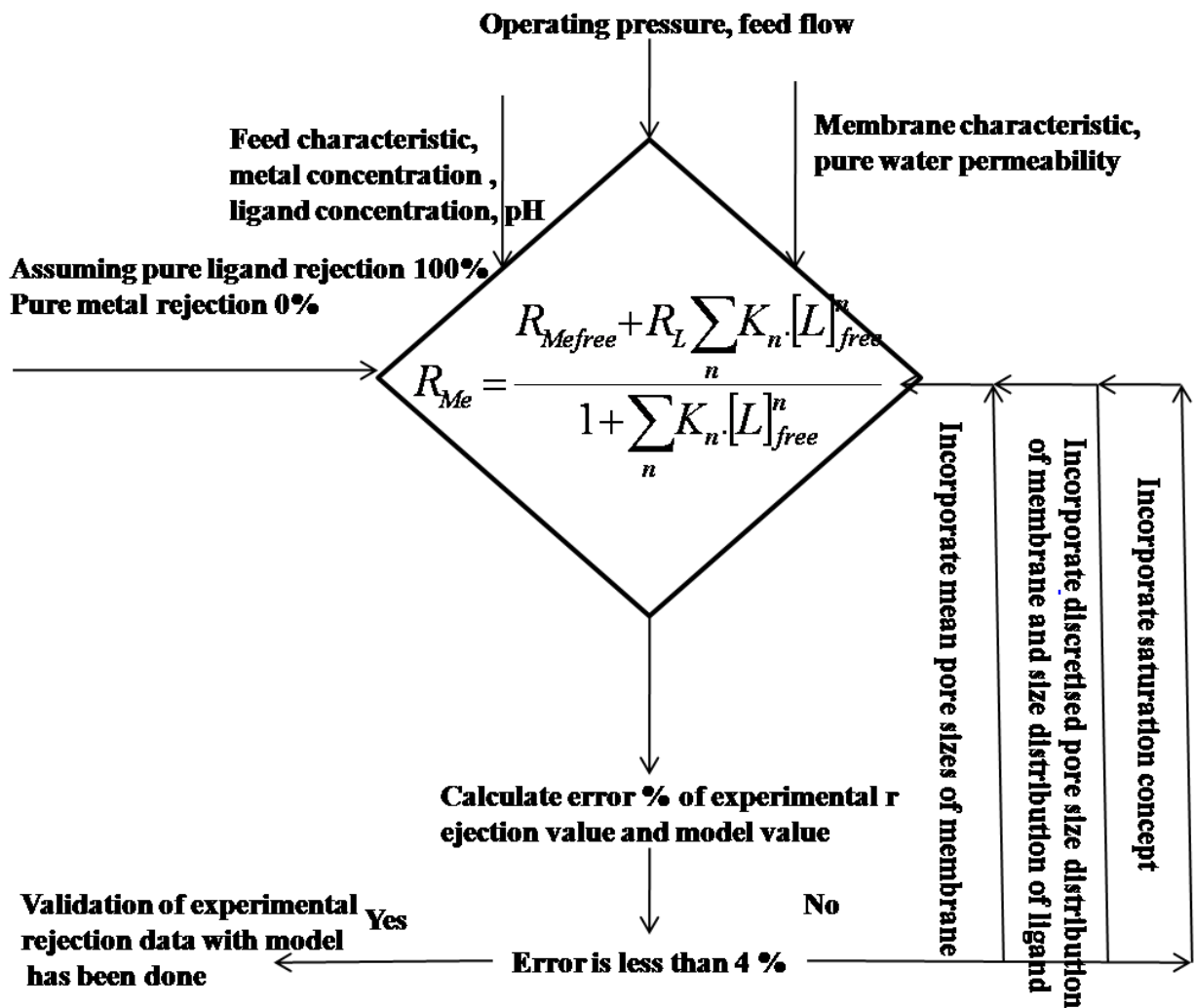
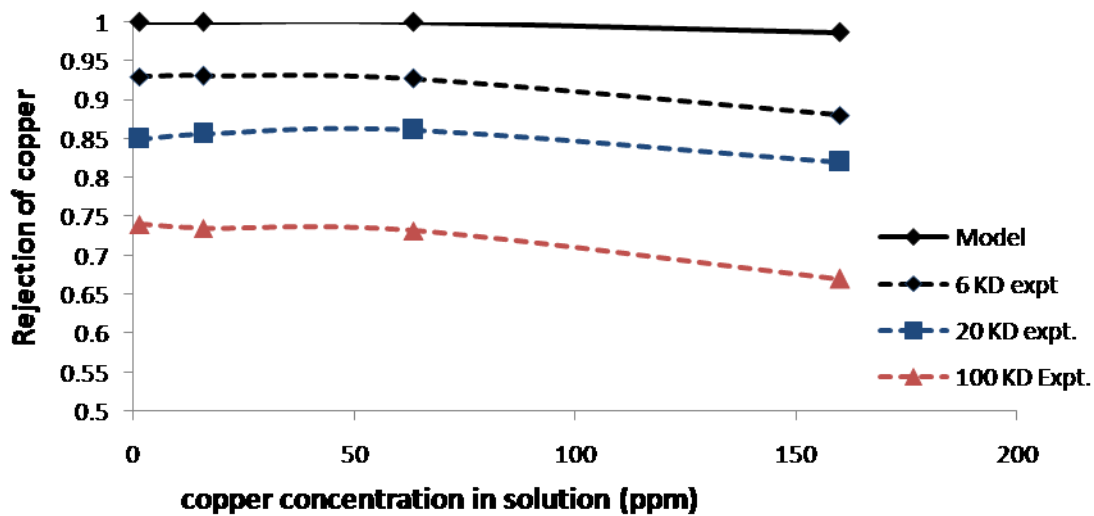


Fig-2.13 Strategy of validation of experimental data with mathematical model

### 2.4.1 Assuming pure ligand rejection 100% and pure metal rejection 0%

Fig 2.14 shows a single mathematical model line far away from actual three numbers of experimental lines fails to validate experimental rejection data. Experimental rejection behaviours of copper are different for three different molecular weight cut off membranes owing to their different pore size distribution. When mathematical model assumes 100% ligand rejection and 0% pure metal rejection for all three membranes it abstains to accept the facts that different molecular weight cut off ultrafiltration membrane has different pore sizes. This primitive assumption in mathematical model leads to a single line instead of three rejection line obtained from actual experimental study. Error margin between experimental study and model has been calculated and reported in Table2.6.



**Fig-2.14 Validation of model with experimental data by assuming pure ligand rejection 100% and pure metal rejection 0%**

## 2.4.2 Validation of experimental rejection data of copper with incorporation of mean pore sizes of membrane

Fig 2.15 shows that with incorporation of mean pore sizes of membranes in mathematical model; three different molecular weight cutoff membranes acquire different characteristic with respect to their pore sizes, consequently single model line splits into three model lines, still they are far away from actual experimental data. Predicted rejection is still higher than actual rejection behaviour of copper.

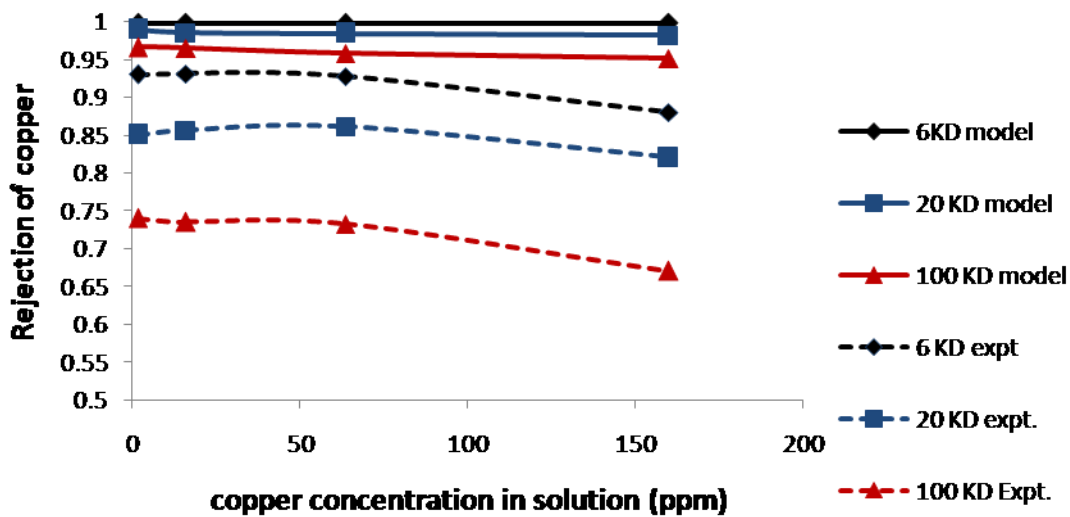


**Fig-2.15 Validation of experimental rejection data by incorporating mean pore sizes of membranes in mathematical model**

Calculation procedure is given below (schematically explained in Fig 2.16):

For incorporation of mean pore sizes of three membranes for each components (copper and Polyethyleneimine) six sets of  $q$  values are obtained. For evaluating steric factors ( $S_D, S_F$ ) and wall correction factors ( $g, f$ ) of diffusion and filtration flow by utilizing six sets of  $q$  values, six sets of steric factors and wall correction factors are obtained for individually diffusion and filtration flow. These factors are incorporated in irreversible thermodynamic

model and six sets of  $\sigma$  and  $\omega$  are obtained. From this irreversible model, six sets of product concentration followed by six sets of rejection values have been obtained. Rejection of metal for a particular membrane  $R_{Me}$  has been predicted by putting rejection value of copper and PEI for this particular membrane obtained from irreversible model. Consequently three graphs from mathematical model are obtained for three individual membranes.

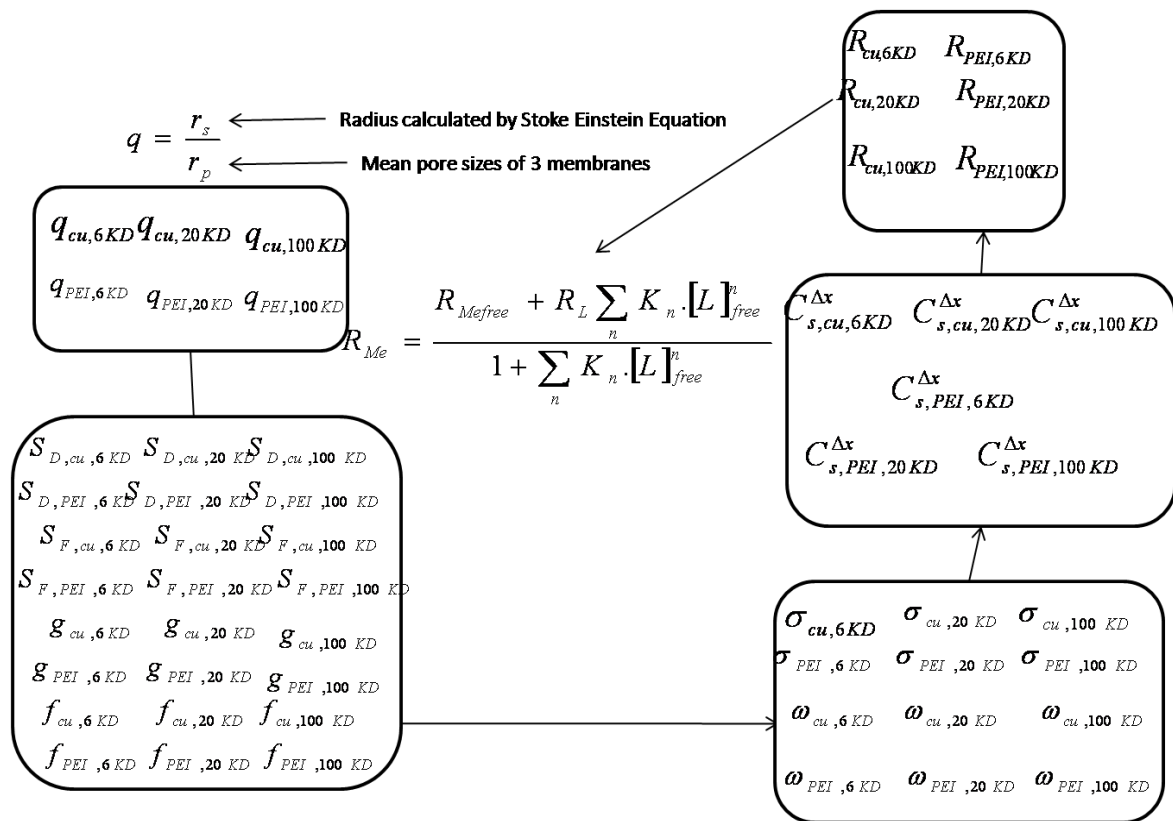


**Fig-2.16 Explanation of Calculation procedure for incorporation of mean pore diameter**

### 2.4.3 Validation of experimental rejection data of copper with incorporation of discretised pore sizes of membrane and size distribution of ligand

Fig 2.17 shows that experimental rejection behaviour of copper is well predicted by modified mathematical model. Final modification of the mathematical model has been done by incorporating discretised pore size distribution of membrane and size distribution of ligand.

By incorporating ligand size distribution in model, it has been realized that 66% of ligand molecule having diameter less than 3.5 nm (less than even mean pore diameter of 6KD) and having a potential escaping tendency through the larger pore diameter of 100 KD, 20 KD and even 6KD. When copper concentration in solution is higher, the model is not good enough for prediction. Model is valid up to 70 ppm copper concentration (saturation limit of metal-ligand complex) in solution, beyond this limit rejection of copper deteriorates. The phenomenon which is prevailed in higher copper concentration region is explained by saturation concept. When all the active sites of ligand get saturated excess copper in solution is reported into product stream which results declining in rejection of copper.

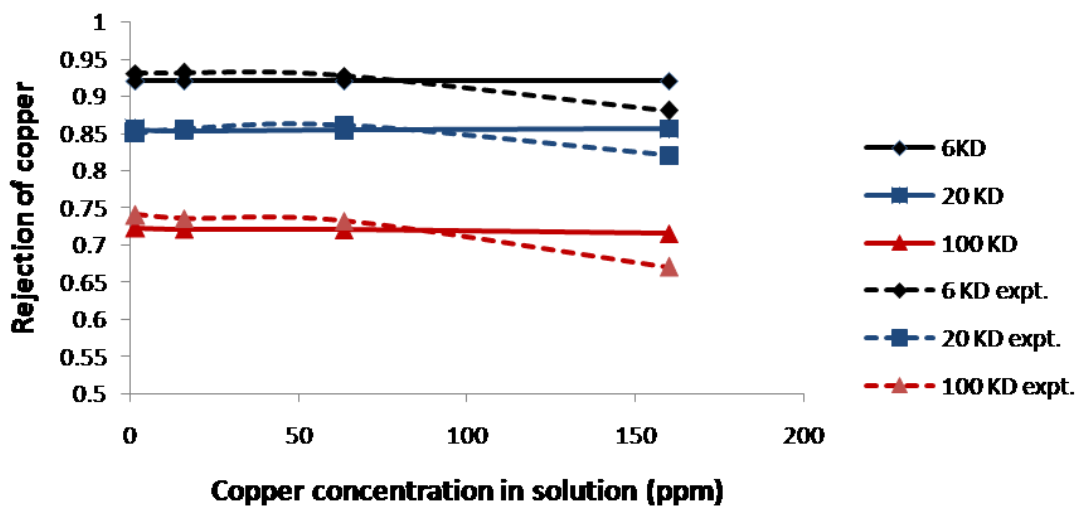


**Fig-2.17 Validation of experimental metal rejection by incorporating poresize distribution of membrane and size distribution of polyethyleneimine**

**Calculation procedure is showing below:**

Calculation of free metal rejection  $R_{Mefree}$  and pure ligand rejection  $R_L$  which are otherwise taken as 0% and 100% respectively has been done by incorporation of discretised pore size distribution of membrane and size distribution of ligand. Three examples of evaluation of

pure ligand rejection at a specific load ratio (1:2.5 copper: PEI) have been shown in Table 2.5A, 2.5b and 2.5C. By following the same procedure, free metal rejection is evaluated at each load ratio. After that, following the equation 1-7, metal rejection is evaluated for this specific load ratio. Hence, for each specific load ratio the error margin has been calculated with respect to actual experimental data.

**Table-2.5a Explanation of calculation procedure for 6 KD 1:2.5 load ratio of copper and PEI**

		PEI fraction	0.107	0.281	0.281	0.166	0.089	0.044	0.02	0.008	0.003	0.0001	1
	Fraction	Dia(nm)	1.8	2.5	3.3	4.5	6.1	8.2	11.1	14.9	20.2	27.2	
6KD	0.1	0.7	100	100	100	100	100	100	100	100	100	100	
	0.1	1.5	100	100	100	100	100	100	100	100	100	100	
	0.1	2.1	99.5	100	100	100	100	100	100	100	100	100	
	0.1	2.5	97	100	100	100	100	100	100	100	100	100	
	0.1	3	91	99.3	100	100	100	100	100	100	100	100	
	0.1	3.5	84	96.9	99.9	100	100	100	100	100	100	100	
	0.1	4	76	92.7	99.2	100	100	100	100	100	100	100	
	0.1	4.6	66	86.9	96.9	100	100	100	100	100	100	100	
	0.1	5.4	56	77.8	91.9	99.3	100	100	100	100	100	100	
	0.1	11	19	34	48.5	69	87.5	97.7	100	100	100	100	
Total rejection			8.43	24.94	26.31	16.07	8.78	4.38	2	0.8	0.3	0.01	92

**Table-2.5 b Explanation of calculation procedure for 20 KD 1:2.5 load ratio of copper and PEI**

		PEI fraction	0.107	0.281	0.281	0.166	0.089	0.044	0.02	0.008	0.003	0.0001	1
	fraction	dia(nm)	1.8	2.5	3.3	4.5	6.1	8.2	11.1	14.9	20.2	27.2	
20KD	0.1	2	99.8	100	100	100	100	100	100	100	100	100	
	0.1	2.9	92.6	99.5	100	100	100	100	100	100	100	100	
	0.1	3.5	83.8	96.9	99.9	100	100	100	100	100	100	100	
	0.1	4.1	74	91.9	98.9	100	100	100	100	100	100	100	
	0.1	4.6	67	86.9	96.9	100	100	100	100	100	100	100	
	0.1	5.1	60	81.1	94	99.7	100	100	100	100	100	100	
	0.1	5.7	52.8	74	89.9	98.7	100	100	100	100	100	100	
	0.1	6.3	46	68.8	84.4	96.9	100	100	100	100	100	100	
	0.1	7.2	39.3	60	77.1	92.9	99.4	100	100	100	100	100	
	0.1	12.5	15.5	27.3	41	60.5	81	94.4	99.7	100	100	100	
Total rejection			6.75	22.1	24.78	15.75	8.72	4.37	1.99	0.8	0.3	0.01	85.6

**Table-2.5 c Explanation of calculation procedure for 100 KD 1:2.5 load ratio of copper and PEI**

		PEI fraction	0.107	0.281	0.281	0.166	0.089	0.044	0.02	0.008	0.003	0.0001	1
	fraction	dia(nm)	1.8	2.5	3.3	4.5	6.1	8.2	11.1	14.9	20.2	27.2	
20KD	0.1	4.2	73.4	91.1	98.6	100	100	100	100	100	100	100	
	0.1	5.3	58	79	92.7	99.4	100	100	100	100	100	100	
	0.1	6	49.4	72	87.4	97.8	100	100	100	100	100	100	
	0.1	6.7	44	64.2	81.6	95.2	99.8	100	100	100	100	100	
	0.1	7.3	38	58	76.4	92.2	99.2	100	100	100	100	100	
	0.1	8	33	51.5	70	88.6	98.1	100	100	100	100	100	
	0.1	8.6	30.8	49	65	84.8	96.6	100	100	100	100	100	
	0.1	9.4	27	42.6	60.3	80.3	94.1	99.6	100	100	100	100	
	0.1	10.5	22	35.7	52.8	73.4	89.8	98.9	100	100	100	100	
	0.1	17	10.3	16.5	27.1	42.5	60.5	97	100	100	100	100	
total rejection			4.13	15.72	20.04	14.2	8.34	4.38	2	0.8	0.3	0.01	70

## 2.5 Percentage error calculation

Percentage error (Table-2.6) has been calculated in order to assess the validity of the model developed.

**Table-2.6 Percentage error calculation**

Load ratio( Cu:P ED)	6 KD			20 KD			100 KD		
	Case-1	Case-2	Case-3	Case-1	Case-2	Case-3	Case-1	Case-2	Case-3
1:100	7.5	7.2	1.0	17.6	16.3	0.56	35.13	30.9	2.3
1:10	7.4	7.1	1.1	16.8	15.0	0.3	36.05	30.17	1.9
1:2.5	7.8	7.6	0.7	16.1	14.2	0.8	36.6	30.03	1.6
1:1	13.6	13.3	4.5	21.9	19.7	4.3	49.2	41.9	6.6

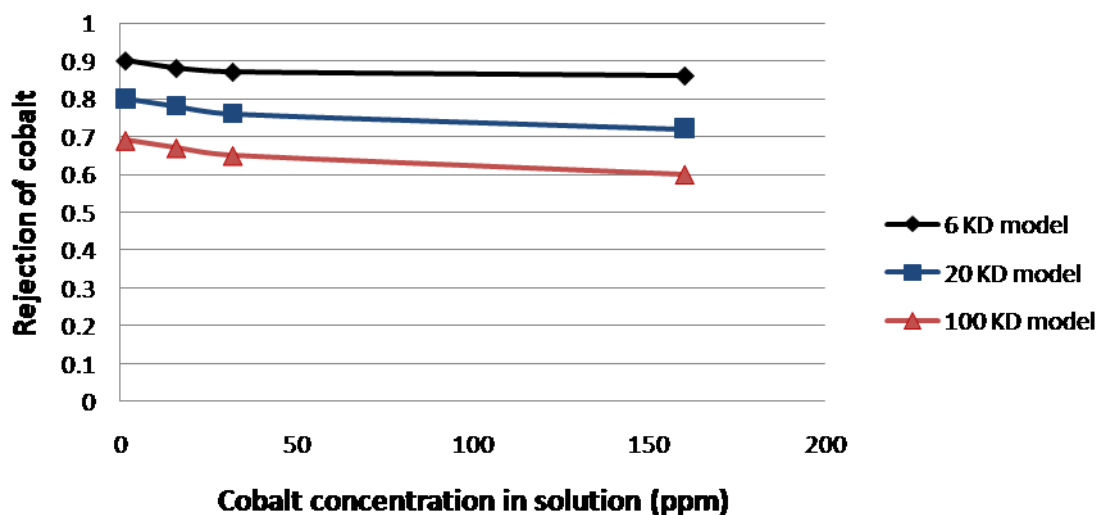
**Note:** Case-1 represents pure ligand rejection 100% and pure metal rejection 0%; Case-2 incorporates of mean pore size of membranes; Case-3 incorporates of discretised pore sizes of membrane and size distribution of ligand.

Table 2.6 shows that each modification in mathematical model helps to bring down error significantly. For 6 KD, two step modifications bring down error from 7.5% to 1.0% at 1:100 load ratio. When load ratio increases with respect to copper (copper concentration increases in solution) error margin depletes from 13.6% to 4.5%. At higher copper concentration, once all coordination sites of ligand gets exhausted; excess metal reports in product stream decreasing rejection significantly. For 100 KD, two step modifications bring down error from 35% to 2.3%. For 100 KD molecular weight cutoff membrane the assumption of 100% ligand rejection is imprudent and hence it gives rise 35% error value.

## 2.6 Prediction of rejection behaviour of single system by mathematical model

### 2.6.1 Prediction of rejection behaviour of cobalt system

Rejection behaviour of cobalt –polyethyleneimine system has been developed in mathematical model by following same mathematical equations. The equilibrium constant of cobalt-polyethyleneimine system has been obtained from literature [43]. Fig 2.18 shows that with increasing cobalt concentration in solution rejection of cobalt decreases. In model equation (equation 7), rejection of metal is directly proportional to free ligand concentration. Higher metal concentration leads to lower free ligand concentration, as coordination sites of ligand get exhausted.



**Fig-2.18 Prediction of rejection behaviour of cobalt in cobalt –PEI complex by mathematical model at PEI concentration 160 ppm**

Validation of mathematical model has been done by experimental rejection data of cobalt when cobalt-PEI complex has been passed through ultrafiltration membrane. Fig 2.19 shows that experimental rejection is highest at (1:5 weight ratio of cobalt and Polyethyleneimine) 32 ppm cobalt concentration. At lower cobalt concentration, for 100 KD molecular weight cutoff

membrane rejection decreases first and then increases. This phenomenon can be illustrated with the fact that at lower concentration rejection through the membrane becomes membrane controlled. Solute prefers least resistance path at lower concentration, hence rejection decreases. Validation of mathematical model with experimental result is fairly good. It is coming below 5% error margin level.

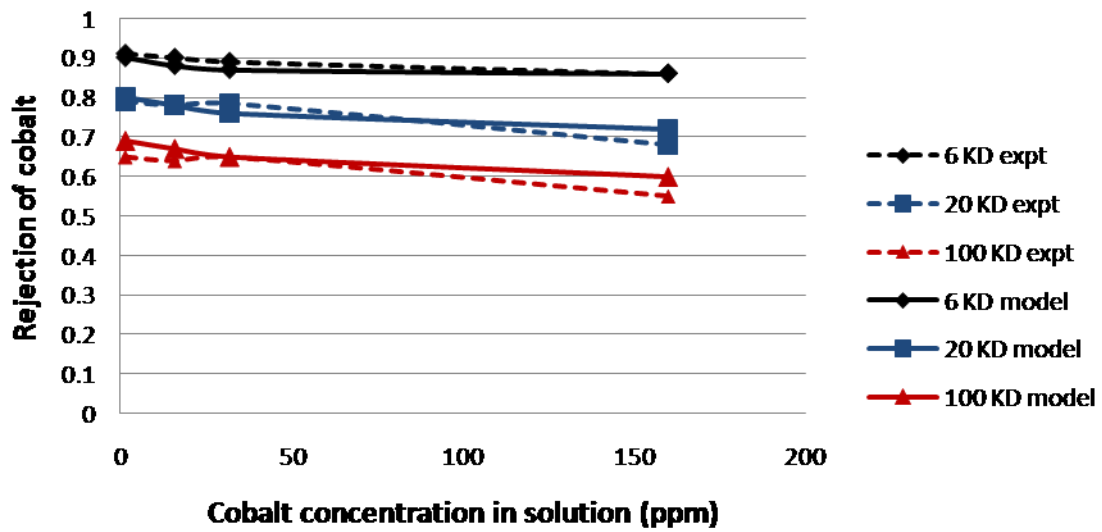


Fig-2.19 Validation of rejection behaviour of cobalt by experiments

### 2.6.2 Prediction of rejection behaviour of Iron system

For development of model for iron-polyethyleneimine system, equilibrium constant has been evaluated from the following equations.

Evaluation of equilibrium constant:[43]

$$R_{Me} = \frac{R_{Mefree} + R_L \sum_n K_n \cdot [L]_{free}^n}{1 + \sum_n K_n \cdot [L]_{free}^n} \quad 2.22$$

Now putting  $R_{Me\text{free}} = 0$ ; and  $R_L = 1$

$$R_{Me} = \frac{\sum_n K_n \cdot [L]_{\text{free}}^n}{1 + \sum_n K_n \cdot [L]_{\text{free}}^n} \quad 2.23$$

For  $n=1$

$$R_{Me} = \frac{K_1 \cdot [L]_{\text{free}}}{1 + K_1 \cdot [L]_{\text{free}}} \quad 2.24$$

$$\frac{R_{Me}}{1 - R_{Me}} = K_1 \cdot [L]_{\text{free}} \quad 2.25$$

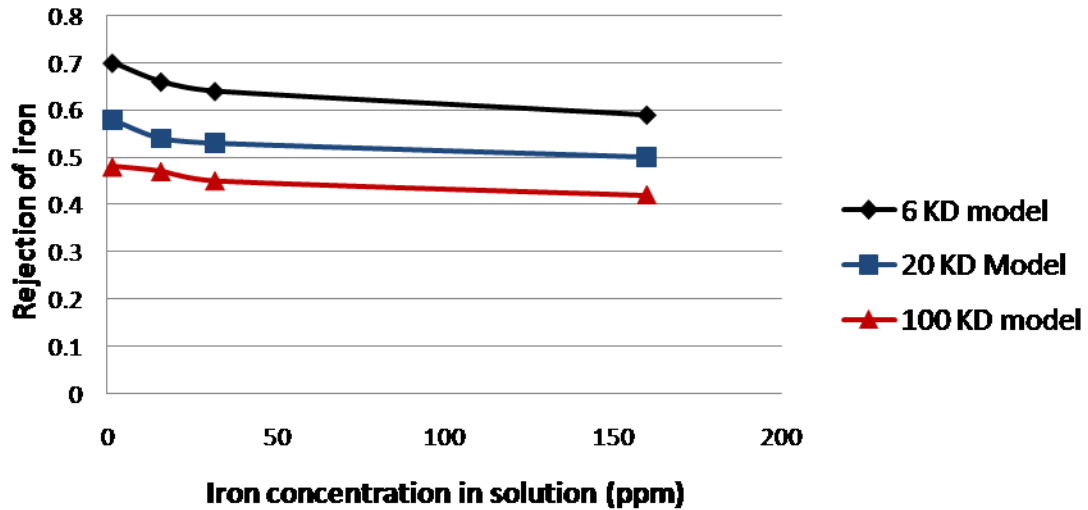
$$K_1 = \frac{R_{Me}}{(1 - R_{Me}) \cdot [L]_{\text{free}}} \quad 2.26$$

$$[L] = [L]_{\text{free}} + \frac{[L]_{\text{free}} \cdot [H]}{K_a} + \frac{n \cdot [Me] \cdot K_1 \cdot [L]_{\text{free}}^n}{1 + K_1 \cdot [L]_{\text{free}}^n} \quad 2.27$$

$$K_1 = \frac{\frac{R_{Me}}{1 - R_{Me}}}{1 + \frac{[H]}{K_a}} \cdot \frac{1}{[Me] \cdot (\beta - nR_{Me})} \quad 2.28$$

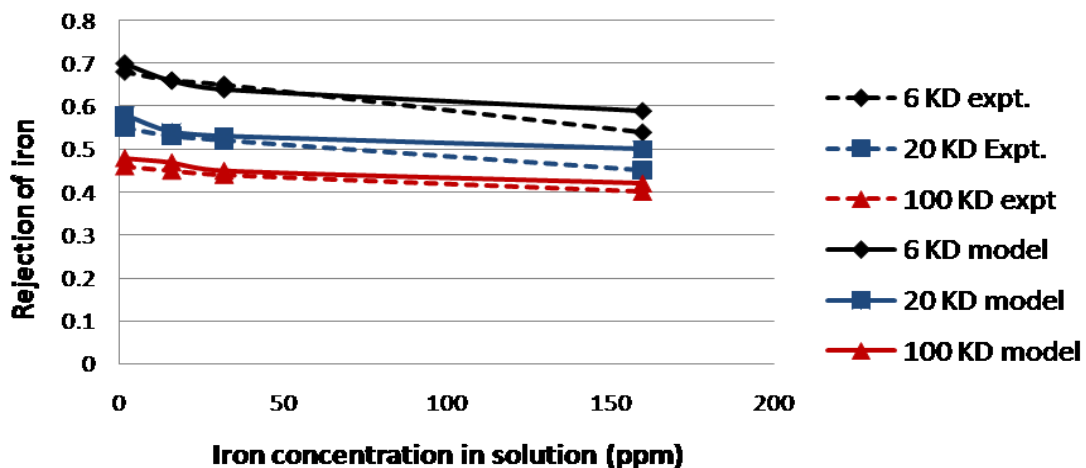
$$\beta \equiv \frac{[L]}{[Me]} \quad 2.29$$

Fig 2.20 shows rejection behaviour of iron in iron-polyethyleneimine complex as predicted by mathematical model. In this figure also, the rejection of iron decreases with increasing iron concentration in solution. This observation ultimately leads to the fact that once saturation of ligand coordination site takes place, feed metal concentration reports into product.



**Fig-2.20 Prediction of rejection behaviour of iron in iron-PEI complex by mathematical model at PEI concentration 160 ppm**

Fig2.21 shows the experimental rejection behaviour of iron and the rejection behaviour predicted by mathematical model is well validated. Error margin is coming below 4% level. The model has been successfully validated by experimental data upto 100 ppm iron concentration, beyond that saturation concept of ligand has to be taken care by mathematical model.



**Fig-2.21 Validation of rejection behaviour of iron by experiments**

## 2.7 Prediction of rejection behaviour of multi-component system

### Modifications of mathematical model for multi component solution [51]

For development of mathematical model for multi-component solute, same equations (1-7) have been rewritten with respect to  $i^{\text{th}}$  no of components. When multi-component present in solution there is a continuous competition observes between two components with respect to binding capability towards ligand.



Here  $i$  is number of components.

Mass balance of each metal ion

$$[Me_i] = [Me_i]_{free} + \sum_n [Me_iL_n] \quad 2.31$$

$$[Me_i]_p = [Me_i]_{free} \cdot (1 - R_{Me_{free}_i}) + (1 - R_L) \sum_n [Me_iL_n] \quad 2.32$$

Mass balance of each ligand ion

$$[L] = [L]_{free} + [HL] + \sum_i \sum_n n \cdot [Me_iL_n] \quad 2.33$$

$$[L] = [L]_{free} + \frac{[L]_{free} \cdot [H]}{K_a} + \sum_i \sum_n n \cdot K_n [Me_i]_{free} \cdot [L]_{free}^n \quad 2.34$$

$$[Me_i]_{free} = \frac{[Me_i]}{1 + \sum_n K_{i,n} \cdot [L]_{free}^n} \quad 2.35$$

$$[L] = [L]_{free} + \frac{[L]_{free} \cdot [H]}{K_a} + \sum_i \frac{[Me_i] \sum_n n \cdot K_{i,n} \cdot [L]_{free}^n}{1 + \sum_n K_{i,n} \cdot [L]_{free}^n} \quad 2.36$$

$$R_{Me,i} = 1 - \frac{[Me_i]_p}{[Me_i]} \quad 2.37$$

$$R_{Me,i} = \frac{R_{Me,free,i} + R_L \sum_n K_{i,n} [L]_{free}^n}{1 + \sum_n K_{i,n} [L]_{free}^n} \quad 2.38$$

### 2.7.1 Rejection of multi-component solute in 100 KD membrane

Fig-2.22 shows that rejection behaviour of multi component system. This system consists of 160 ppm polyethyleneimine, 32 ppm cobalt and iron concentration is varying from 0-160 ppm. Figure shows that the rejection behaviour of cobalt remains unaltered in presence of varying iron concentration although overall rejection of cobalt decreases from its single component counterpart (5% lower) as available free ligand concentration decreases owing to the presence of another co-ion. Rejection behaviour of iron gets drastically deteriorated in presence of cobalt. In 100 KD membrane deterioration of rejection of iron from its single ion counterpart is 55% at low iron concentration and 70% at high iron concentration. This observation corroborates the fact that cobalt forms more stable complex with polyethyleneimine than iron.

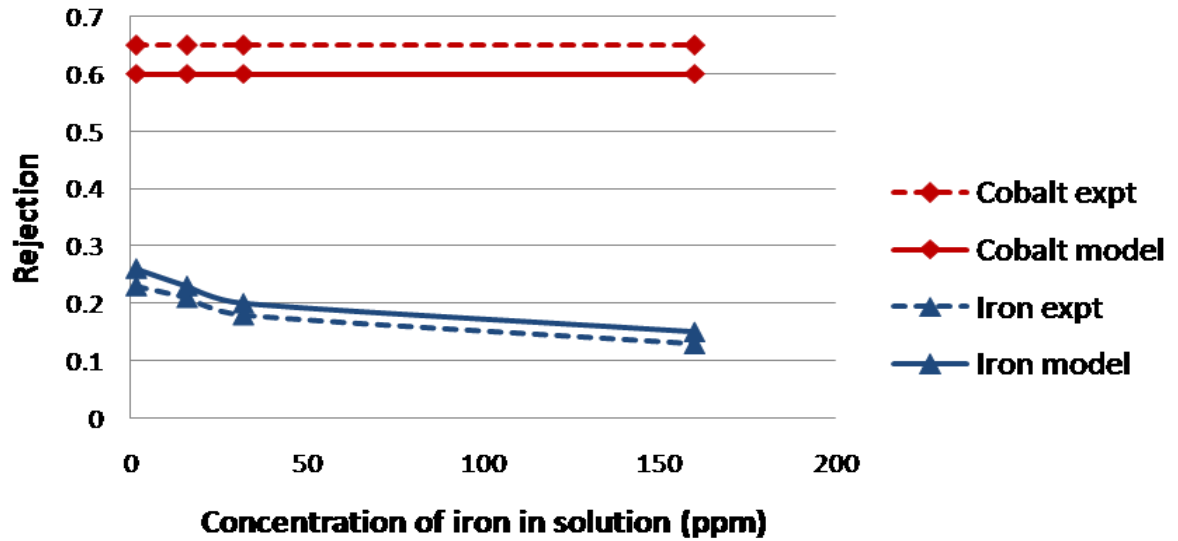


**Fig-2.22** Rejection study of cobalt and iron in mixed solute containing fixed amount of cobalt (32 ppm) and PEI (160 ppm) in 100 KD membrane

### 2.7.2 Rejection of mixed solute in 20 KD membrane

In 20 KD membrane, the same trend of rejection behaviour of iron has been observed in Figure 2.23. Here deterioration of rejection of iron in presence of cobalt is reported 40% lower compare to its single counterpart. Cobalt rejection is unaffected with varying concentration of iron but still it is 3% lower than its single component counterpart.

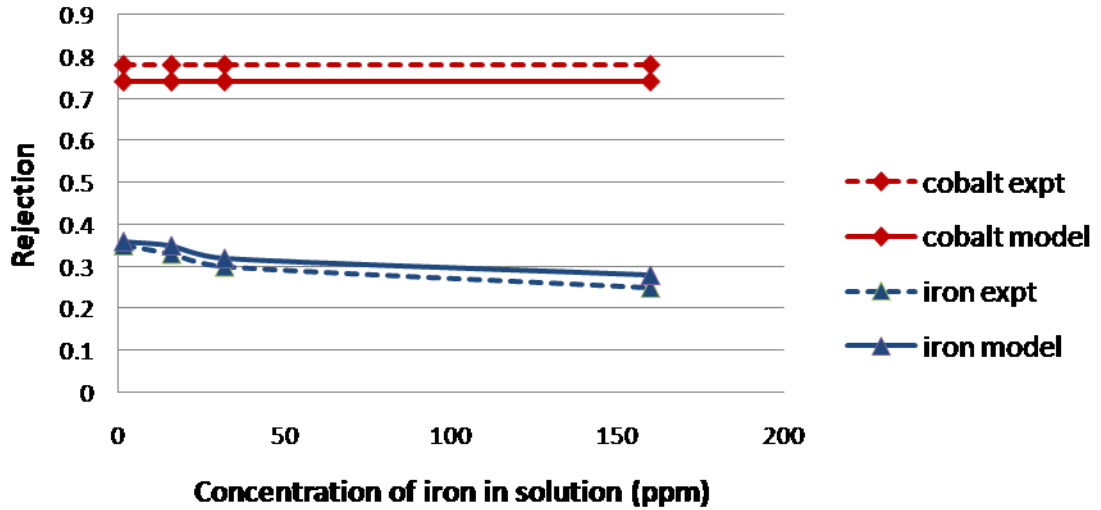


**Fig-2.23 Rejection study of cobalt and iron in mixed solute containing fixed amount of cobalt (32ppm) and PEI (160 ppm) in 20 KD membrane**

### 2.7.3 Rejection of mixed solute in 6 KD membrane

Same trend is being followed in 6 KD membrane showed in Fig 2.24. Here iron rejection deteriorates 30% compare to its single ion counterpart. The variation in rejection behaviour of iron in three different molecular weight cut off membranes is a consequence of different pore size distribution.

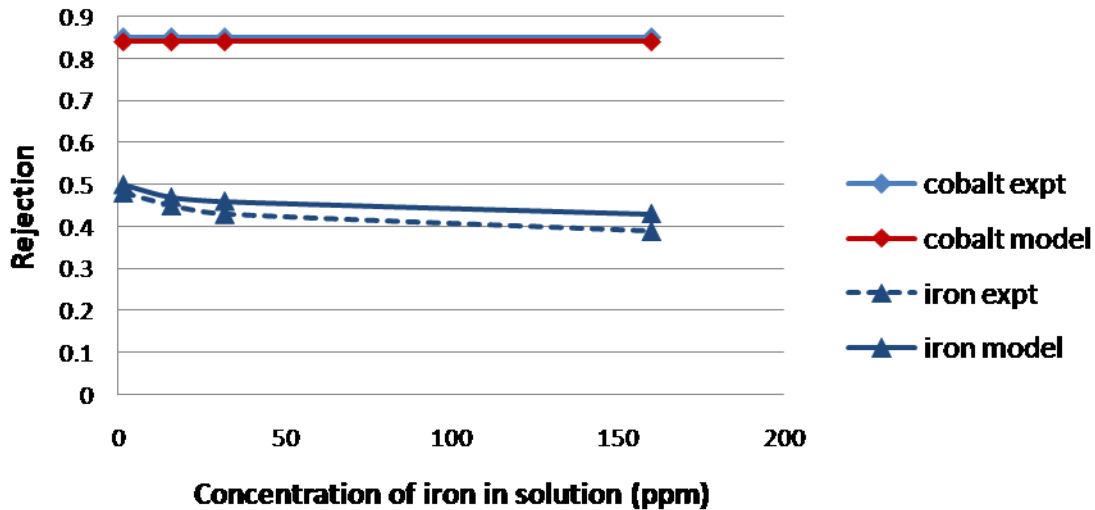


**Fig-2.24 Rejection of mixed solute (cobalt 32 ppm, PEI 160 ppm) in 6 KD membrane**

A vast difference in rejection behaviour of iron in presence of cobalt compares to its single component rejection behaviour leads to study a new arena of separation world i.e. fractionation of multi-solute system.

## 2.8 Fractionation of multi-solute components

Fractionation of multi-solute system is defined as a separation of single component as pure as possible from multi-solute mixtures. Parameter which describes the fractionation performance is defined as separation factor.

Separation factor is defined as the ratio of concentration of target component in final product (may be reject or product) to concentration of non-target component in final product (may be reject or product).

To study the fractionation of multi-component system, a simulated solution with 32 ppm iron, 32 ppm cobalt and 160 ppm PEI has been prepared. Different combination (reject staging, product staging) of 6 KD and 100 KD membranes are selected. The prediction of

fractionation behaviour of cobalt and iron by mathematical model at different combination of 100 KD and 6KD membranes are given below.

### 2.8.1 Reject staging of 100 KD followed by 6 KD membrane

Simulated solution of 32 ppm cobalt, 32 ppm iron and 160 ppm Polyethyleneimine is prepared and sent to 100 KD membrane as shown in Fig 2.25. In presence of multi-component solute 100 KD membrane cobalt rejection is 65% and iron rejection is 18%, whereas 6 KD membrane cobalt rejection is 84% and iron rejection is 43%. Reject stream having 71 ppm cobalt and 43 ppm iron is sent to 6 KD membrane. Final product contains 11.2 ppm cobalt and 26 ppm iron. Reject contains 138 ppm of cobalt and 63 ppm iron. Separation factors of product and reject are given below:

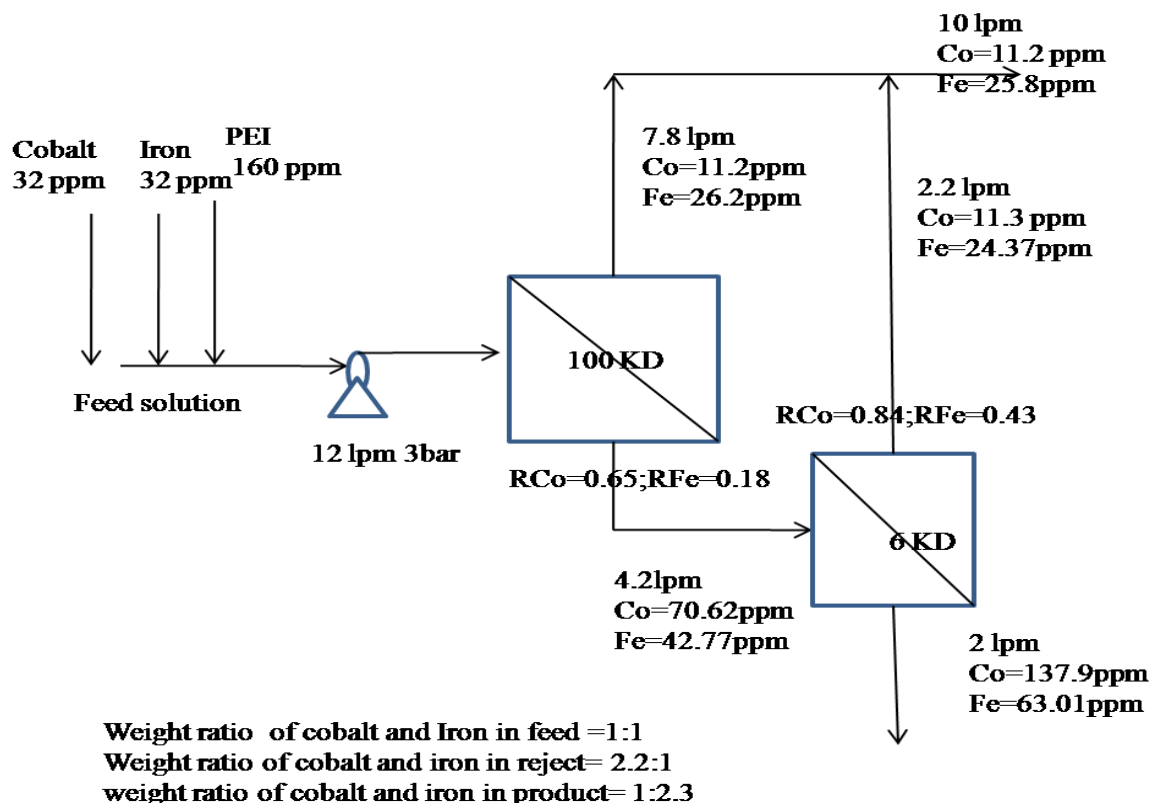


Fig-2.25 Fractionation through 100KD-6KD reject staging

### 2.8.2 Reject staging of 100 KD followed by 100 KD membrane

Simulated solution of 32 ppm cobalt, 32 ppm iron and 160 ppm Polyethyleneimine is prepared and sent to 100 KD membrane as shown in Fig 2.26. In presence of multi-component solute 100 KD membrane cobalt rejection is 65% and iron rejection is 18%, Reject stream having 71 ppm cobalt and 43 ppm iron is sent to 100 KD membrane. Final product contains 15 ppm cobalt and 28.5 ppm iron. Reject contains 153 ppm of cobalt and 57 ppm iron. Separation factors of product and reject are given below:

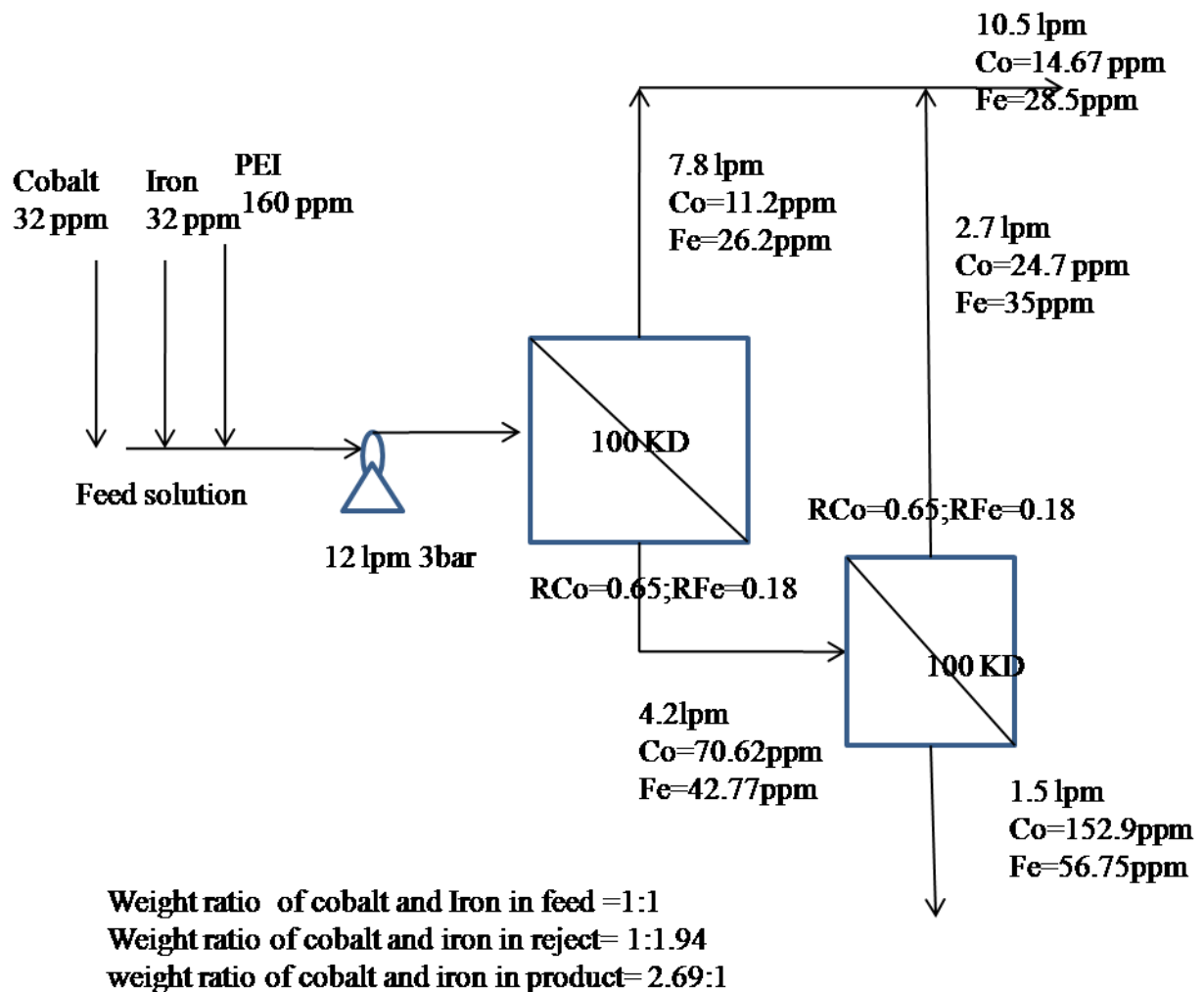


Fig-2.26 Fractionation through 100KD-100KD reject staging

### 2.8.3 Reject staging of 6 KD followed by 6 KD membrane

Simulated solution of 32 ppm cobalt, 32 ppm iron and 160 ppm Polyethyleneimine is prepared and sent to 6 KD membrane as shown in Fig 2.27. In presence of multi-component solute 6 KD membrane cobalt rejection is 84% and iron rejection is 43%. Reject stream having 60 ppm cobalt and 46 ppm iron is sent to 6 KD membrane. Final product contains 7 ppm cobalt and 25 ppm iron. Reject contains 108.5 ppm of cobalt and 54 ppm iron. Separation factors of product and reject are given below:

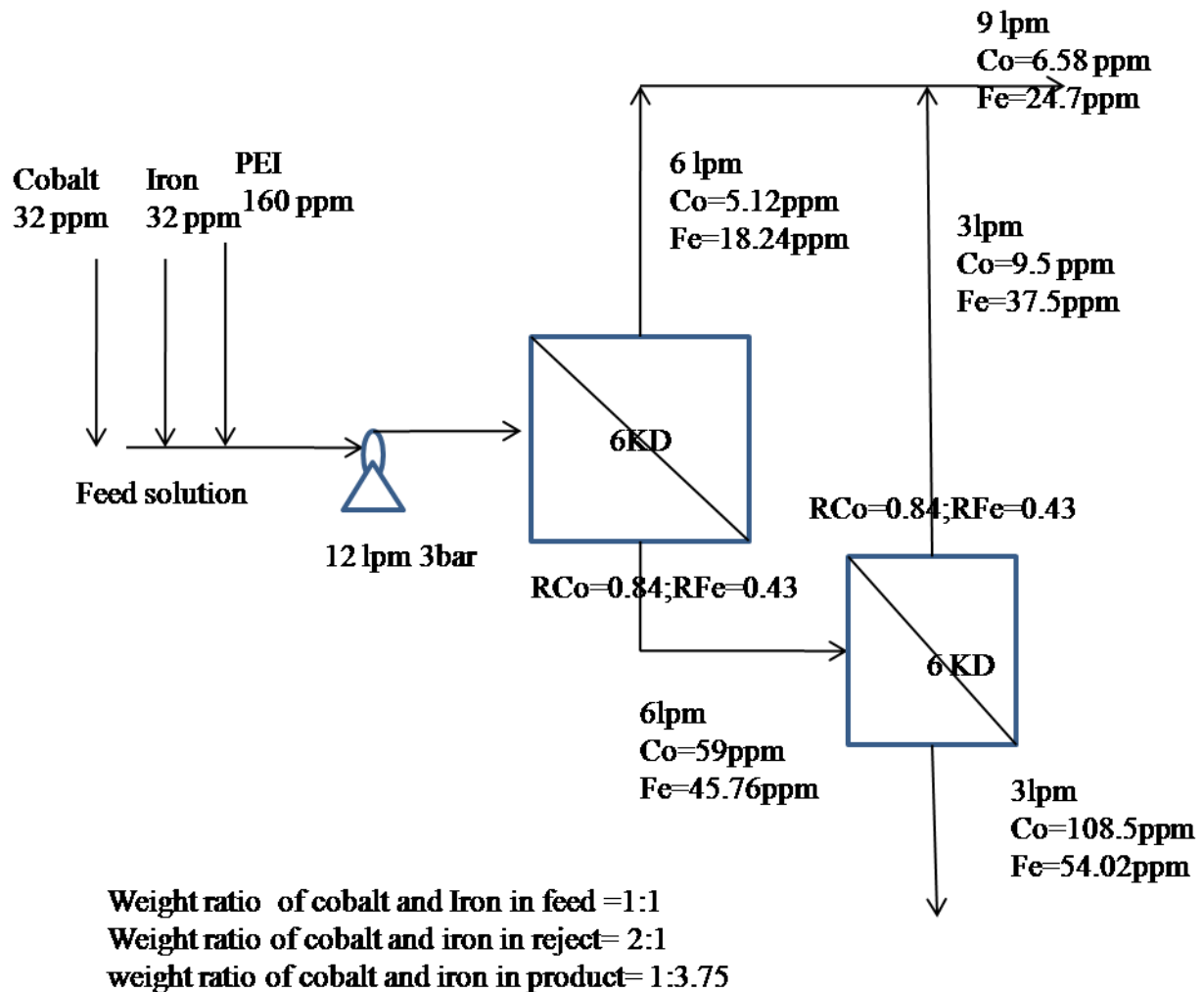


Fig-2.27 Fractionation through 6KD-6KD reject staging

### 2.8.4 Product staging of 6 KD followed by 100 KD membrane

Simulated solution of 32 ppm cobalt, 32 ppm iron and 160 ppm Polyethyleneimine is prepared and sent to 6 KD membrane as shown in Fig 2.28. In presence of multi-component solute 6 KD membrane cobalt rejection is 84% and iron rejection is 43%, whereas 100 KD membrane cobalt rejection is 65% and iron rejection is 18%. Product stream having 5.12 ppm cobalt and 18.24 ppm iron is sent to 6100 KD membrane. Final product contains 1.8 ppm cobalt and 14.6 ppm iron. Reject contains 13847 ppm of cobalt and 41 ppm iron. Separation factors of product and reject are given below:

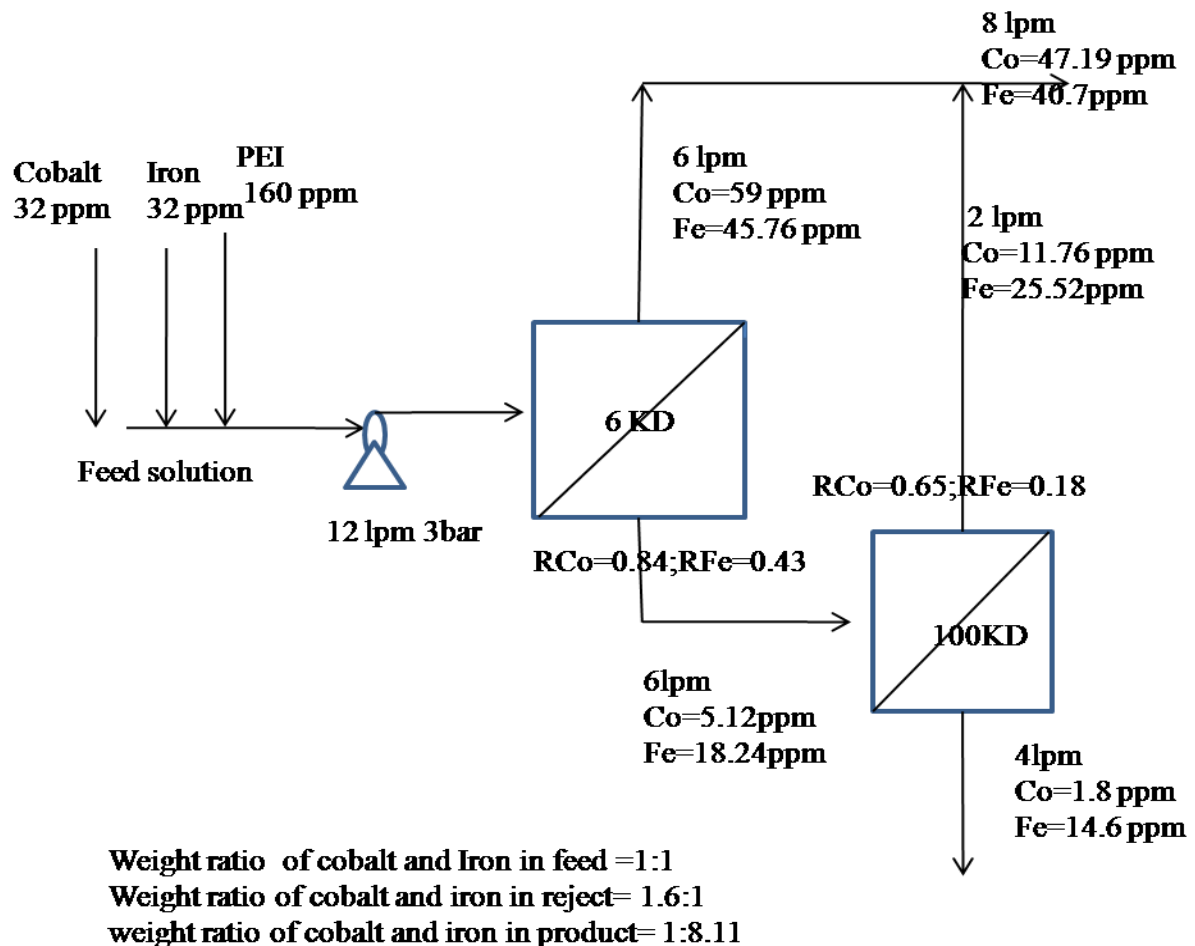


Fig-2.28 Fractionation through 6KD-100KD product staging

### 2.8.5 Product staging of 100 KD followed by 100 KD membrane

Simulated solution of 32 ppm cobalt, 32 ppm iron and 160 ppm Polyethyleneimine is prepared and sent to 100 KD membrane as shown in Fig 2.29. In presence of multi-component solute 100 KD membrane cobalt rejection is 65% and iron rejection is 18%. Product stream having 11.2 ppm cobalt and 26.2 ppm iron is sent to 100 KD membrane. Final product contains 4 ppm cobalt and 21.5 ppm iron. Reject contains 52 ppm of cobalt and 39.5 ppm iron. Separation factors of product and reject are given below:

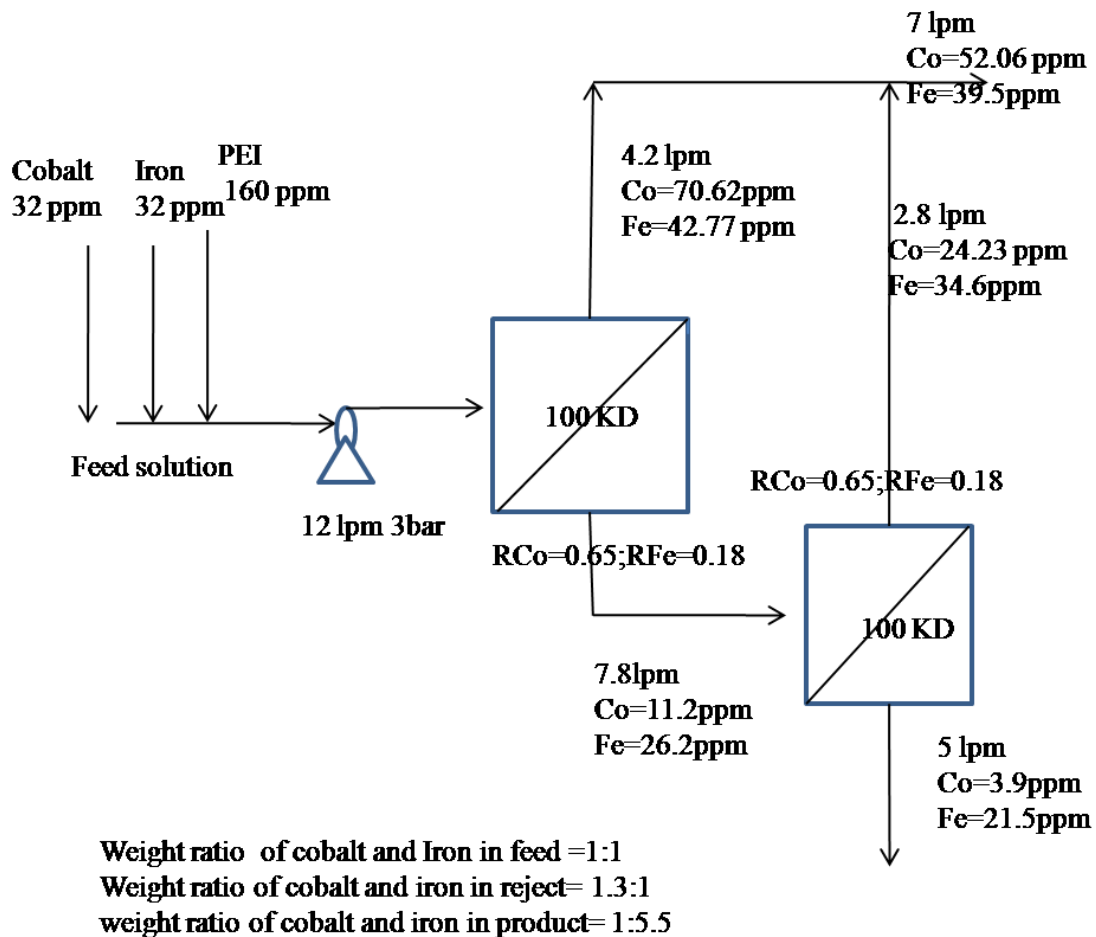


Fig 2.29 Fractionation through 100KD-100KD product staging

### 2.8.6 Product staging of 6 KD followed by 6 KD membrane

Simulated solution of 32 ppm cobalt, 32 ppm iron and 160 ppm Polyethyleneimine is prepared and sent to 6 KD membrane as shown in Fig 2.30. In presence of multi-component solute 6 KD membrane cobalt rejection is 84% and iron rejection is 43%. Product stream having 5.12 ppm cobalt and 18.24 ppm iron is sent to 6 KD membrane. Final product contains 0.82 ppm cobalt and 10.4 ppm iron. Reject contains 42.5 ppm of cobalt and 39.5 ppm iron. Separation factors of product and reject are given below:

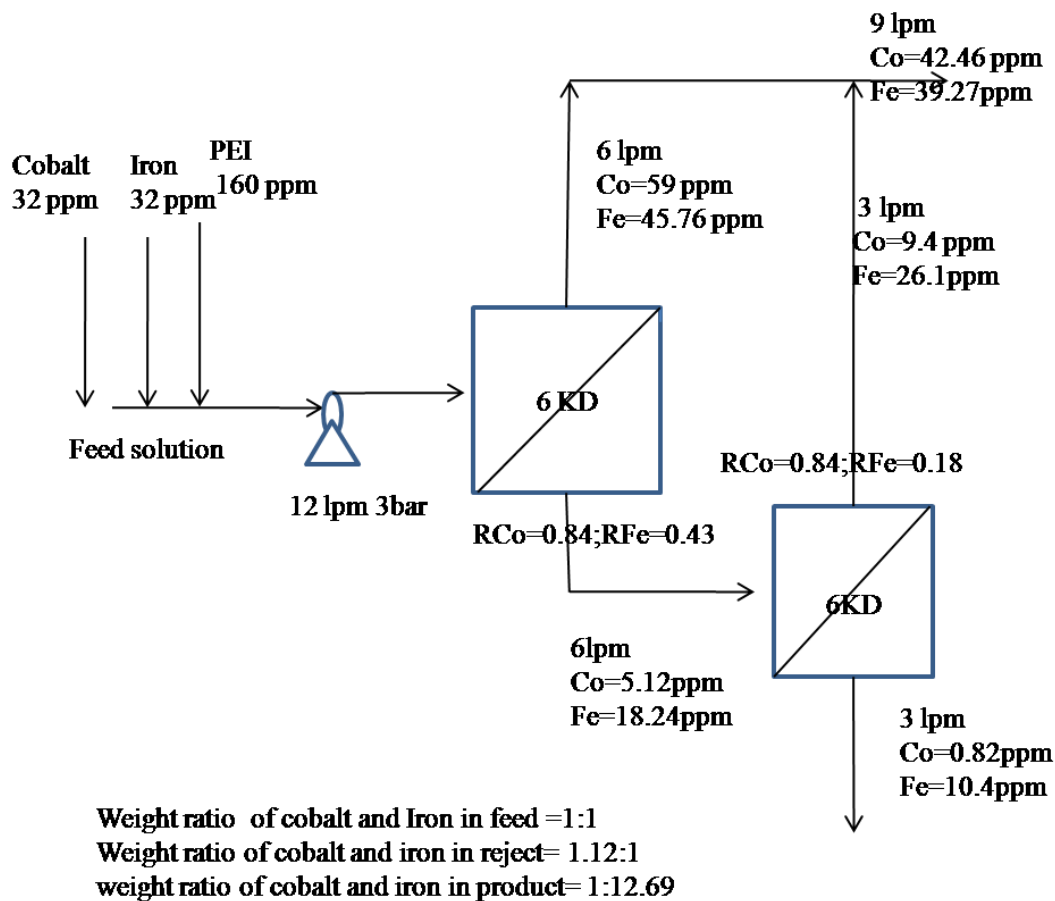


Fig 2.30 Fractionation through 6KD-6KD product staging

### 2.8.7 Experimental validation of fractionation result

In the following table a comparison of prediction of fractionation of iron and cobalt components with different combination of 100 KD and 6 KD membranes is given. Among these six combinations, three combinations (6KD-100 KD product staging, 100 KD-100 KD product staging and 6KD-6 KD product staging) are experimentally validated and their error margin in within 10%. From this table it has been observed product staging provides better separation factor for the sake of sacrificing recovery

**Table-2.7 Fractionation of cobalt-Iron Mixture:**

Combination	Configuration	Separation factor of (Co:Fe)in reject from Model	Separation factor of (Co:Fe) in product from Model	Recovery(%)	Separation factor of (Co:Fe) in reject from experiment	Error	Separation factor of (Co:Fe) in product from experiment	error
6KD-100KD	Product staging	1.16:1	1:8.33	33.3	1.1:1	5%	1:9	7%
100KD-6KD	Reject staging	2.2:1	1:2.3	83.0	-		-	
100KD-100KD	Product staging	1.3:1	1:5.5	41.6	1.4:1	7%	1:5	2%
100KD-100 KD	Reject staging	2.69:1	1:1.94	87.5	-		-	
6KD-6KD	Product staging	1.12:1	1:12.69	25.0	1:1	12%	1:14	9.3%
6KD-6 KD	Reject staging	2:1	1:3.75	75.0	-		-	

The mathematical model which is developed by incorporating both the pore size distribution of membrane and molecular weight distribution of ligand has improved the predictability of actual performance of membrane within the saturation limit of complexation. Validation experiments have indicated that step wise modification of mathematical model has brought down the error significantly. For 6 KD, two step modifications bring down error from 7.5% to 1.0% at 1:100 load ratio. For 100 KD, two step modifications bring down error from 35% to 2.3%. When load ratio increases with respect to copper (copper concentration increases in solution) error margin depletes from 13.6% to 4.5%.

This mathematical model can predict the rejection behaviour of other trace elements (iron, copper) which produces stable complexes with polyethyleneimine. The validation of mathematical model with respect to experimental results is within 10 % error margin.

The mathematical model can explain the rejection behaviour of multi-component solute. In multi-component solute model the rejection of each metal has been expressed in terms of their complexation stability constant. Prediction of multi-component solute rejection has been validated by experimental results. Validation is within 10% error margin.

For fractionation experiment, the prediction of fractionation of multi-component system has been accomplished by multi-component solute model. For three cases it has been validated with experimental results. Validation is within the range of 10% error margin.

## **CHAPTER-3**

# **DEVELOPMENT OF SIMULATION MODEL OF HYBRID MEMBRANE SYSTEM**

Judicious combination of membrane processes based on the chemistry and physics of the solutions can lead to conversion of waste to value. Following the studies on the removal of trace contaminants using membranes, the philosophy is extended to the concept of recovering value from spent streams containing bulk constituents, which otherwise poses an environmental challenge. Removal of water from a saturated solution of bulk component is always a difficult proposition irrespective of achieving the separation goal by means of chemical or physico-chemical processes. Chemical processes involve large amount of chemicals, sludge handling, a large foot print area and high operation time. In the present work, separation studies have been carried out with respect to saturated calcium sulphate solution. Calcium sulphate, a sparingly soluble salt, is often present in neutralised effluent streams. Recommended sulphate level in effluent discharge varies from country to country e.g. it is 500 ppm for effluents in USA whereas it is 1500 ppm for effluents in Canada [64]. Recommended sulphate level in drinking water as per WHO is 250 ppm. The ancient chemical technique for removal of sulphate involves the use of an inorganic source which leads to the formation of a sparingly soluble (or insoluble) surface phase. Formation of gypsum (Calcium Sulphate) and barite (Barium Sulphate) are the two most popular but cost intensive sulphate removal methods. Cleophas [65] noted in his thesis that the degree of sulphate elimination depends on the solubility of the gypsum. According to the International Network for Acid Prevention (INAP, 2003), this process can reduce the sulphate concentration to less than 1200 mg/L, a value which is still significantly higher than the target discharge concentration of 500 mg/L. Sulfate removal through the precipitation of Ettringite (aluminium–calcium sulphate complex) has been proposed by Smit [66] as the SAVMIN process. The three stages of the process successively remove metals as hydroxides through lime addition (pH 12), gypsum through seed crystallization and conversion of sulphates with

aluminum hydroxide to insoluble ettringite. The complications involved in the operation of three steps make the SAVMIN process less popular in industries. Membrane processes appear to be quite attractive as they are predominantly physico-chemical in nature, requiring less chemicals and foot print area compared to conventional operations. The availability of membranes with wide range of pore-sizes, surface charges and chemical matrices, provides the opportunity to synthesize process sequences to achieve the objectives of improving water use efficiency, value recovery and cost reduction. Large quantities of sulphate rich effluents are generated in uranium mining and ore processing operations particularly where acid leaching is practiced. Awadalla and Kumar [67] reviewed the opportunities of the membrane technologies for the treatment of the sulphate enriched mining and mineral processing streams. Reverse osmosis (RO) is extensively practiced for the recovery of water from effluents [68] but its application is limited by the scaling potential of the dissolved species and the osmotic pressure of the concentrate. Anditya [69] proposed an integrated RO desalting followed by accelerated precipitation softening (APS) for achieving high product recovery for brackish water containing gypsum, barite and calcite salts. Efrem Curcio [70] proposed integrated nanofiltration–membrane crystallization (NF–MC) system for the removal of sodium sulfate from aqueous wastes originated by the production process of base raw materials (Ni–H) for special rechargeable batteries. Slurry precipitation and recycle reverse osmosis (SPARRO) [71-73] has been investigated for treating calcium sulphate saturated solution through tubular membrane. Concept of SPARRO involves circulating slurry of seed crystals within the RO system. The seed crystals serve as preferential growth sites for calcium sulphate and other calcium salts and silicates, which begin to precipitate as their solubility products are exceeded during the concentration process within the membrane tubes. The preferential growth of scale on the seed crystals prevents scale formation on the membrane surface. There are enough evidences where appropriate antiscalants[74-77] are

used to protect membrane from scaling by reducing the scaling potential of sparingly soluble salt. Wen-Yi Shih [74] has characterized gypsum crystallization in response to antiscalant treatment. He explained that antiscalants adsorb onto formed crystals or associate/complex with incipient nuclei (or crystals) and thus the scale forming phenomena is inhibited. The use of antiscalant [78] does not allow the gainful processing of the reject stream of RO/NF. Sheikholeslami [79] in her studies on the behaviour of sparingly soluble species has indicated that the scaling potential in reverse osmosis (RO) and nanofiltration (NF) is controlled by a number of factors including kinetics of nucleation, hydrodynamics of the system and the presence of impurities. As the problem of discharges becoming acute and the need to conserve water imminent, it is felt appropriate to revisit the membrane processes to evolve a method to recover water for recycling and approach towards zero-liquid discharge (ZLD). Accordingly, bench scale experiments were carried out initially with saturated solutions of calcium sulphate and later with simulated effluents (uranium mill effluents) containing calcium sulphate to assess the integrated membrane (nanofiltration- reverse osmosis) behaviour under different operating parameters with a view to evolve a scheme for field trials and subsequent implementation. As the sulphate rich acid effluents from mine are normally discharged after neutralization with lime [80] it is considered appropriate to investigate the utility of the lime process for the reject management and the possibility of approaching towards zero liquid discharge (ZLD).

Further it is felt that a mathematical model would help in optimization of parameters under field conditions where the effluent composition could encounter changes very often. Various authors have developed mathematical model on transport of ions in nanofiltration membrane [81-89], but very little information is available on mathematical model which deals with saturated solution. The present model incorporates surface crystal growth kinetics to assess the scale in terms of concentration of calcium sulphate at the membrane surface. The flux

decline phenomenon has been explained more correctly by the model by incorporating cake resistance. In further study, the prediction of operating pressure and operating feed flow for minimum scale threat on membrane surface has been optimized by thermodynamic parameter, 'exergy'.

### **3.1 Theoretical Considerations**

In order to achieve higher recovery, it is necessary to minimize scaling. In RO, all the dissolved solutes are rejected better compared to NF. Consequently, the boundary layer solution of RO would exhibit higher degree of super saturation which would favour scaling and restrict the percent recovery of water. The osmotic pressure of the boundary layer also would be higher requiring higher operating pressure. In NF where the monovalent passage is significant, the boundary layer would contain less solute leading to lower ionic strength and less osmotic pressure under comparable recovery conditions. The existence of residual charge on NF membranes delay the onset of scaling on NF membrane surface compared to RO.

The objective of this study demands prevention or at least minimisation of scaling due to calcium sulphate on the membrane surface enabling higher recovery than permitted by the solubility product considerations. Even though three types of scales are possible viz  $\text{CaSO}_4 \cdot 2\text{H}_2\text{O}$  (gypsum),  $\text{CaSO}_4 \cdot 1/2\text{H}_2\text{O}$  (hemi-hydrate) and  $\text{CaSO}_4$  (anhydrate) in solutions containing calcium and sulphate species, gypsum ( $\text{CaSO}_4 \cdot 2\text{H}_2\text{O}$ ) is predominant at ambient temperatures [78]. As NF process is carried out at ambient temperatures all the discussions pertain only to gypsum scaling. The scaling depends on the ionic product of calcium sulphate in the given chemical environment [90], kinetics of nucleation & hydrodynamics of the process [79]. It is well known that RO membranes preferentially allow water to permeate through, while NF membranes allow monovalents to permeate to some extent, depending on

the membrane. Due to preferential permeation of water, the concentration of the dissolved species in the boundary layer increases leading to the formation of scales (due to precipitation). Antiscalants are extensively used in desalination processes but reports indicate that they may favour fouling of membranes at higher recoveries and is not suggested for gypsum whenever the saturation index is likely to exceed 2.38 [79]. Antiscalants also complicate the reject management issues. So, in this work, usage of antiscalant is avoided. Various studies [91-99] on scaling mechanism of calcium sulphate di-hydrate indicate the formation of mineral scales through three steps: initially the sparingly soluble species becomes supersaturated leading to the formation of crystal nuclei and thence to crystal leading to scale formation[93].Antiscalant affect the growth rate and changes the form or shape of crystals. Crystals are weakened by internal stresses causing them to fracture. It was also indicated that hydrodynamics also influence the formation of crystal nuclei. Growth of crystal nuclei cannot take place further. Uchymiak et.al [91] have studied the kinetics of calcium sulphate dihydrate scaling in detail with reference to RO membranes. Sangho Lee and Chung-Hak Lee [94], and Che-Jen-Lin et al [95, 96] have extensively studied the scaling aspects of calcium sulphate species with reference to NF membranes. The flux decline in NF was considered to follow four stages viz - concentration polarisation, solute nucleation, cake formation and steady state. The rate of deposition at each stage was found to depend on the operating parameters including applied pressure and cross flow velocity. Several researchers [97-99] have opined that nucleation is an important step for crystallisation & hence cake formation. It was also reported that the flux reduction is significant only after the cake formation and the induction period of nucleation stage for calcium sulphate depended on cross flow velocity. Based on these studies, crystal growth appears to be the critical step and its rate is depicted mathematically [94].

$$\frac{dM}{dt} = KS(C_w - C_s)$$

Where, K is the rate constant of crystallisation, S is surface area of active sites,  $C_w$  is wall concentration near membrane surface (for surface crystallisation) and bulk phase concentration (for bulk crystallisation),  $C_s$  is the saturation concentration of calcium sulphate at that temperature.

In view of these observations, it is felt that the scaling could be minimised/ prevented on the membrane surface if we maintain appropriate hydrodynamic conditions (which ensures less residence time on the separation zone, optimal super-saturation) & ensuring a feed nearly free from foulants to achieve higher recovery.

Treatment of the calcium sulphate saturated effluents through NF is only the first step in the overall scheme and would produce a stream containing less calcium & sulphate species and significant amount of chlorides as permeate. Permeate from NF needs to be processed through RO to recover reusable water. The reject stream of NF would contain supersaturated levels of calcium and sulphate and requires to be reduced to unsaturated levels so that the stream can be recycled after bleeding a portion to maintain the dissolved solute levels of the feed for NF. The potentiality of lime column in order to convert supersaturated (calcium sulphate) reject stream of NF to an unsaturated stream has also been investigated in present study.

### **3.2 Objective**

Based on the literature studies and the theoretical considerations, the present work has been undertaken with the specific objective of developing a mathematical model for the

processing of unsaturated solutions (containing calcium and sulphate species) and later to demonstrate the concept on the 'Approach to Zero Liquid Discharge'. Thus the specific objectives on the application of hybrid membrane processes for the management of unsaturated effluent streams containing the calcium and sulphate species are

- a. Experimental studies to understand the scaling philosophy of calcium sulphate solutions and to identify the safe supersaturation levels in tune with hydrodynamics of the feed solution and physical chemistry of the feed particularly with reference to precipitation mechanism of calcium sulphate.
- b. Development of a mathematical model through a series of numerical equations to identify the optimal balance of feed and hydrodynamics for maximum recovery in NF process and to maintain the sustainability of the performance of the membrane besides predicting the membrane behaviour with increasing recovery of water.
- c. Studies on the Integration of NF and RO processes along with lime treatment to identify a scheme for recovering maximum water for reuse and demonstrate an approach to Zero Liquid Discharge as a logical culmination of the present study.

### **3.3 Experimental and Theoretical work carried out**

The studies conducted to achieve the above objectives include

- Experimental studies to observe the critical point of scale formation and other performance characteristics in nanofiltration.
- Development of mathematical model for nanofiltration membrane to evaluate the operating flow and operating pressure at optimized scale safe recovery.
- Resolution of total resistances to permeate flow (intrinsic membrane resistance, osmotic and scale resistances) and their assessment experimentally in nanofiltration membrane.

- Validation of the mathematical model before and after incorporation of resistance term by experimental flux decline data of nanofiltration.
- Optimisation of operating flow and operating pressure of nanofiltration by exergy analysis
- Reject management study of nanofiltration membrane
- Incorporation of an existing mathematical model for reverse osmosis for optimizing the operating pressure for obtaining required product quality and quantity.
- Identification of the overall scheme for the approach to Zero Liquid Discharge

### **3.3.1 Experimental studies to observe the critical point of scale formation and other performance characteristics in nanofiltration**

#### **3.3.1.1 Materials & Methods:**

**Membranes:** Film Tech make nano-filtration membrane element NF-90-4040 was used for NF experiments. At standard conditions (i.e.2000 ppm MgSO<sub>4</sub> at 5 bar pressure) the membranes exhibited 98% percent solute rejection. For sodium chloride the percent solute rejection was found to be 80%, at corresponding conditions (2000ppm NaCl, 5 bar). The membrane area is about 7.6 m<sup>2</sup>. Indigenously developed back-washable spiral polysulphone based 60KD MWCO UF membrane element [100] was used for the filtration of feed solution before using as feed for NF experiments. After each experiment membrane was flushed with RO treated service water (< 5ppm) until the conductance of the discharge stream from NF element indicated constant low conductivity. Depending on the feed flow rates and operating pressure, the water required for flushing varied from 50 to 100 litres. Whenever the original pre-experiment pure water permeability (PWP) was not obtained, the membrane was cleaned with dilute hydrochloric acid at around pH 4 to 5. The experiments were conducted initially with higher flow rates towards and later at lower flow rates. For each flow rate, the data was

collected at three different pressures starting from lower pressure. This sequence was adopted to minimise permanent scaling, if at all formed, that could affect the membrane performance.

**Preparation of test solutions:** Pure calcium sulphate solution was prepared by dissolving excess quantity of calcium sulphate under vigorous stirring, allowed to settle overnight and filtered through UF. The resultant solution is free from turbidity and used in the experiments. For CaSO<sub>4</sub>- NaCl system, the solution has been prepared by dissolving calcium chloride and sodium sulphate in 500 litres water corresponding to a feed composition of 705 ppm calcium, 2000ppm of sulphate, 958 ppm of sodium and 1242 ppm of chloride. The solution was left overnight to allow for any precipitation. Before using in the experiment, the solution was filtered through ultra-filtration element and was collected into the feed tank.

Calcium, chloride and sulphate concentrations were measured by standard analytical methods [101,102]. TDS is determined by evaporation. Sodium is estimated by difference. Conductivity measurements were also made as soon as the samples were taken for initial estimation of the trend.

### **3.3.1.2 Experimental Studies**

#### **Description of Integrated membrane process for treatment of saturated solution:**

The schematic diagram of the experimental set up is shown in Fig.3.1. The synthetically prepared feed was filtered through UF and stored in the feed tank. The feed was then pumped through the NF module through the high pressure pump. Provisions were made for bypassing part of the feed for studying different flow-rates, recycling the concentrate and collection of permeate independently. Higher recoveries were targetted in the NF module by recirculating the reject stream back to the feed tank. The tanks were calibrated in terms of volume. Rotary

Vane pump (Procon make) rated at 15 lpm flow 15 bar pressure was used. By suitably manipulating the valves (by pass valve / concentrate recycle) the requisite pressure and flow were maintained. NF product was collected separately in NF product tank. Product flow of NF membrane was continuously monitored.

Experiments were conducted for lime treatment of the reject stream of NF for the effective removal of calcium & sulphate species from the supersaturation levels to below saturation limits [103]. The supersaturated concentrate of the NF element is recycled back to the feed tank after passing through lime column (where the concentration of calcium and sulphate species would be brought down to less than the saturation levels). NF product water is sent to BWRO module by another rotary vane pump rated at 15 lpm flow and 15 bar pressure. All the experiments were conducted with 500 L feed solution and on a batch-recycle mode. The tanks (both permeate and feed tank) were calibrated and readings of volume can be easily noted at 10 litres interval. Considering the hold up in the membrane element and the associated piping (about 5 litres), the permeate volumes are considered for estimating recoveries. In each experiment, data were collected (permeate rate, product quality) for different recovery points. The product samples were drawn ensuring that its representative nature of the permeate tank solution. The fluctuations in flow measurements were about  $\pm 0.25$  lpm and that of pressure was about  $\pm 0.1$  bar.

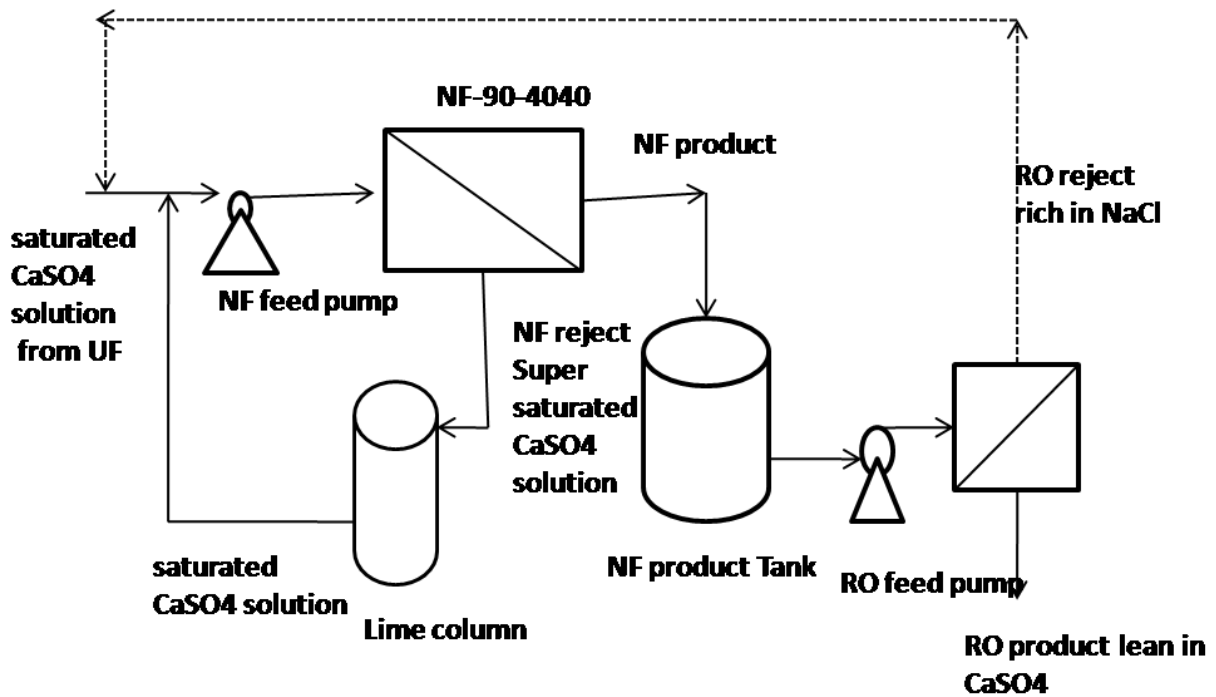


Fig-3.1 Flow sheet of integrated membrane system

### 3.3.1.3 Results & Discussions

The study presented is based on bench scale experiments. The flow characteristics have been represented directly in terms of litres per minute (lpm). We have refrained from designating the flow in terms of Reynolds Number due to the fact that our estimates of the same could not take into account the effect of feed spacers which induces turbulence. However, we have calculated the Reynolds Numbers using the cross sectional area available for flow and thence calculated hydraulic diameter. The estimated values range from 132 for a feed flow of 4.5 lpm to 381 at 13 lpm comparable to the values reported in literature [104]

### 3.3.1.4 Selection criteria of operating pressure and feed flow rates

The objective of the experiment is to minimise surface crystallisation of gypsum ( $\text{CaSO}_4 \cdot 2\text{H}_2\text{O}$ ). At higher operating pressures, the specific recovery (permeate rate /feed rate) would be higher making the environment conducive for surface crystallisation. Considering

that the osmotic pressure of the feed is less than 3 bar, the experimental investigations were carried out from 5 bar onwards, taking into account the estimated concentration at 90% recovery. As per the design guidelines for RO & NF achieving about 90% recovery in single pass, the membrane system would require more elements in series with staggered configuration [105] to maintain minimum required flow rates (as specified by the membrane element manufacturers) and possible only for very large capacities. As our study deals with nearly saturated to supersaturated solutions, the tolerance to the change of feed flow rates would be less. Based on these considerations, it is felt appropriate to opt for a batch system with recirculation to achieve high recovery without compromising on the envisaged basic hydrodynamic parameters albeit at higher energy cost. Accordingly, all the experiments have been carried out at the batch recycle mode at different feed flow rates ranging from 4.5 lpm to 13 lpm with an objective to arrive at a sustainable flow rate and pressure which would minimise surface crystallisation providing the maximum recovery at minimum possible energy cost.

### **3.3.1.5 Parametric studies for the optimisation of operating pressure & feed flow rate**

The experiments are conducted in the range of 5 to 10 bars in four steps and for four flow rates ranging from 4.5 lpm to about 13 lpm. Even though the selection of 4.5 lpm feed flow rate is not apparently justified, the experiments were conducted as the last batch to assess the scaling phenomenon under hostile conditions which is likely when one envisages a series of modules for obtaining higher recovery in one pass.

The permeate rate is function of net driving force as seen from equation below. [106]

$$N_p = A ( P - \pi_b + \pi_p )$$

Where  $N_p$  is the permeate flux ( $\text{m}^3/\text{sec}.\text{m}^2$ ),  $A$  is the membrane constant ( $\text{m}^3 / \text{sec}.\text{m}^2 \text{ bar}$ ),  $P$  the operating pressure,  $\pi_b$  &  $\pi_p$  are boundary layer & permeate osmotic pressure. Since the membrane element used is the same, the membrane area ( $7.6 \text{ m}^2$ ) is constant in all NF experimental runs. Hence, for the purpose of data analysis permeate rate (PR) is considered in terms of litres per minute (lpm) and the membrane constant ( $A$ ) in terms of (lpm/bar. $\text{m}^2 \times 7.6$ ). Boundary layer concentration can be expressed as

$$N_p = k \ln \left( \frac{C_b}{C_f} \right)$$

Where,  $k$  is the mass transfer coefficient in the boundary layer,  $C_b$  and  $C_f$ , the concentrations at the membrane surface and in the feed solution respectively. The membrane surface concentration is then given by:

$$C_b = C_f \exp \left( \frac{N_p}{k} \right)$$

where the ratio  $\frac{N_p}{k}$  is a function of the pressure difference and the cross flow velocity.

Specifically high flux (at high pressure) will lead to higher membrane concentrations (and hence more rapid crystallisation) while high cross flow velocity leads to high mass transfer coefficients, which leads to lower membrane concentrations.

A typical observation of permeate flow as a function of recovery at different pressures for the NF membrane element with saturated calcium sulphate solution as feed at a flow rate of 9lpm is presented in Fig.3.2.

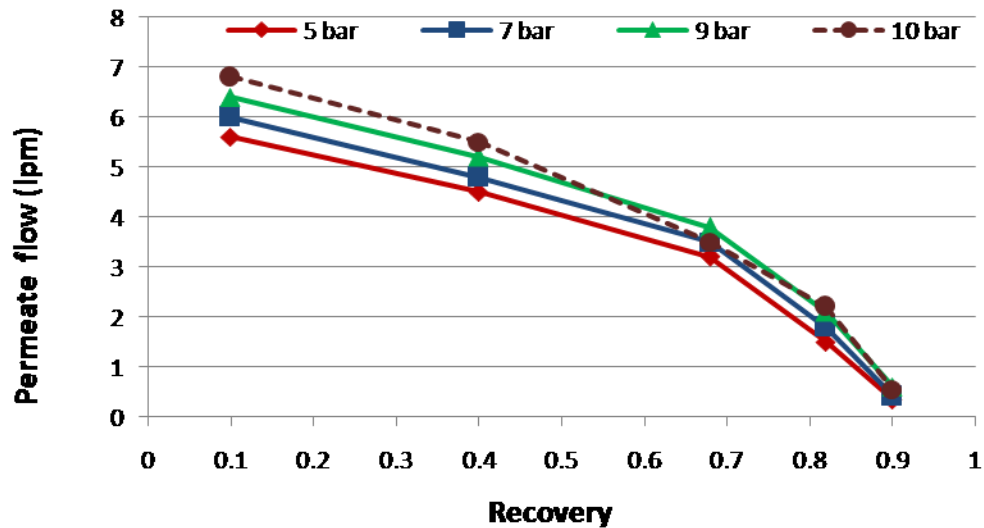


**Fig.3.2. Effect of operating pressure on recovery at 9.0 lpm feed flow rate**

The permeate flow rate decreases with recovery but there are two discernible patterns. In the initial phase, the rate of decrease in the permeate rate is steady. The slopes of all the curves corresponding to different operating pressures are constant up to a particular recovery leading to the inference that permeate flow rate is only a function of osmotic pressure in this region. Since the osmotic pressure of the bulk solution is constant for a given recovery at given feed flow rate, the permeate flow rate is only a function of the operating pressure minus osmotic pressure. The significant fall in permeate rate observed at higher recoveries in the second phase, can be attributed to the additional resistance due to scaling. The onset of scaling can be identified from the point of inflexion. The point of inflexion appears to be a function of the operating pressure.

Fig.3.3 presents a similar observation for the least feed flow rate of 4.5 lpm where the points of inflexions can be seen distinctly suggesting that lower the operating pressures, higher is the recovery at which the inflexion occurs. It has also been observed that the permeate flow rates are higher at lower pressures beyond certain recoveries indicating the predominance of scaling resistance over the loss in permeate rate due to osmotic pressure.

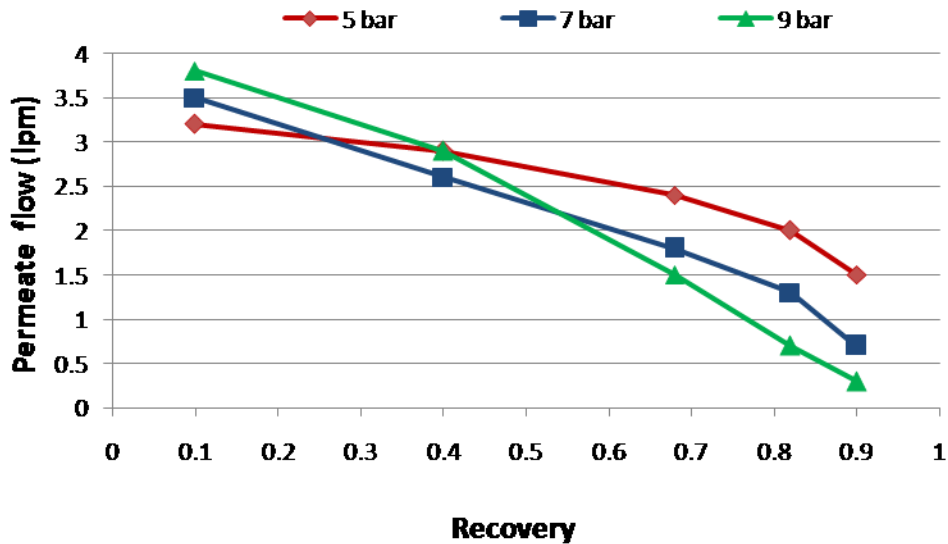


**Fig.3.3 Effect of operating pressure on recovery at 4.5 lpm feed flow rate**

The point of inflexion advances towards lower recovery with increasing pressure indicates scaling effect. As the pressure increases the specific flux of the membrane increases. Consequently the boundary layer concentration would be higher leading to higher degree of supersaturation and hence scaling.

Fig.3.4 clearly indicates that there is a distinct change in the slope corresponding to a recovery of about 0.7. It is evident for all the flow-rates other than at 4.5 lpm flow rate (where the transition is not distinct due to inherently very low values of flow rate). The sharp change in slope leads to the inference that the precipitation occurs at this point and onwards. Considering that it occurs at 0.7 recovery for all the flow rates, the concentration of calcium sulphate in the feed at this point is also the same corresponding to the super-saturation level where calcium sulphate gets precipitated as a scale. The observation leads to the conclusion that scaling point is only a function of concentration (or the level of supersaturation) and is independent of flow rate.

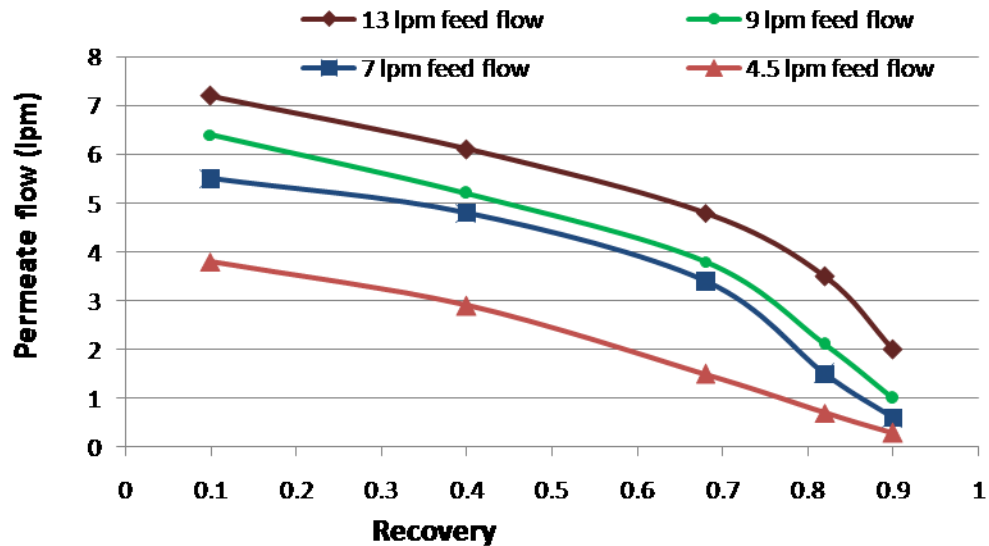


Fig.3.4. Effect of feed flow rate on permeate flow at 9 bar pressure

Based on the study of permeate flow rates as a function of operating pressure and feed flowrate it can be concluded that scaling is a function of both feed flow rate and operating pressure.

Rearranging previous equation, we obtain

$$\pi_b = P - N_p/A + \pi_p$$

Recalling  $\pi$  is  $iCRT$  where  $i$  is the number of species,  $C$  is the molar concentration,  $R$  gas constant and  $T$  temperature,  $\pi_b$  and thence the concentration at the boundary can be estimated.

The degree of supersaturation i.e. the ratio of concentration of the solution to the saturation concentration can be calculated based on the boundary layer concentration, from previous equation knowing measured values of product rate, product concentration and membrane constant. With the length of the membrane being one metre and the velocities vary from 0.069 to 0.277 m/s, the residence time vary from 14.5 to 3.6 seconds. The estimates of the boundary layer concentration at the point of inflexion using the above methodology,

indicates a molar concentration of about 0.07 moles /litre of calcium sulphate in flowrates ranging from 4.5 lpm and above corresponding to a degree of supersaturation around 12.5 (except 5 bar pressure 4.5 lpm) confirming the formation of scale [107].

### **3.3.1.6 Analysis of decline in permeate rate in terms of scaling**

The Normalised Flux (Nflux), a dimensionless number representing the drop in permeate rate due to different factors under various experimental conditions was plotted as a function of operating pressure.  $Nflux_{pr}$  describes the loss in permeation rate due to all possible factors such as osmotic pressure, scaling, feed flow rate, pressure drop etc. It is the ratio of actual permeate rate at specified conditions to the initial fresh membrane performance at the same pressure.  $Nflux_{uf}$  describes loss in permeate rate due to physical factors such as scaling, fouling etc. and includes both soft & hard scales and is calculated as a ratio of PWP before flushing (with least disturbance to the membrane environment to the extent possible) to the initial PWP.  $Nflux_f$  describes the loss in flux due to hard scales which can not be removed by simple flushing and is calculated as the ratio of PWP after flushing to the initial PWP.  $Nflux_f$  is an indicator of hard scale .It is the condition which one would like to avoid in operating a membrane based system. Figs.3.5a to 3.5d describe respectively the behaviour of Nfluxs as a function of operating pressures at flow rates of 4.5lpm,7 lpm,9 lpm and 13 lpm. All the permeate rates (PR),  $PWP_f$  and  $PWP_{uf}$  correspond to the recovery of 0.7, the terminal point of our experimental run in all the cases. Perusal of the plots of Nflux versus pressure for different flowrates allows us to observe that original flux ( $Nflux_f$ ) is restored for the cases 5bar,7bar and 9 bar operating pressures for 13 lpm feedflow rate and for the cases of 5bar and 7 bar operating pressures for 9 lpm feed flow rates. In the case of 7 lpm feed flow rate, the permeate rate could be nearly restored at 5 bar operating pressure but not restorable for 4.5 lpm under all experimental conditions.

The difference between  $N_{flux_{uf}}$  and  $N_{flux_f}$  describes the loss in permeate rate due to scaling. The difference is higher at higher pressures and lower flow rates.

The slope of the  $N_{flux_{pr}}$  lines decreases with increasing flow rates.

The difference between  $N_{flux_{pr}}$  and  $N_{flux_{uf}}$  is nearly constant for all the operating pressures.

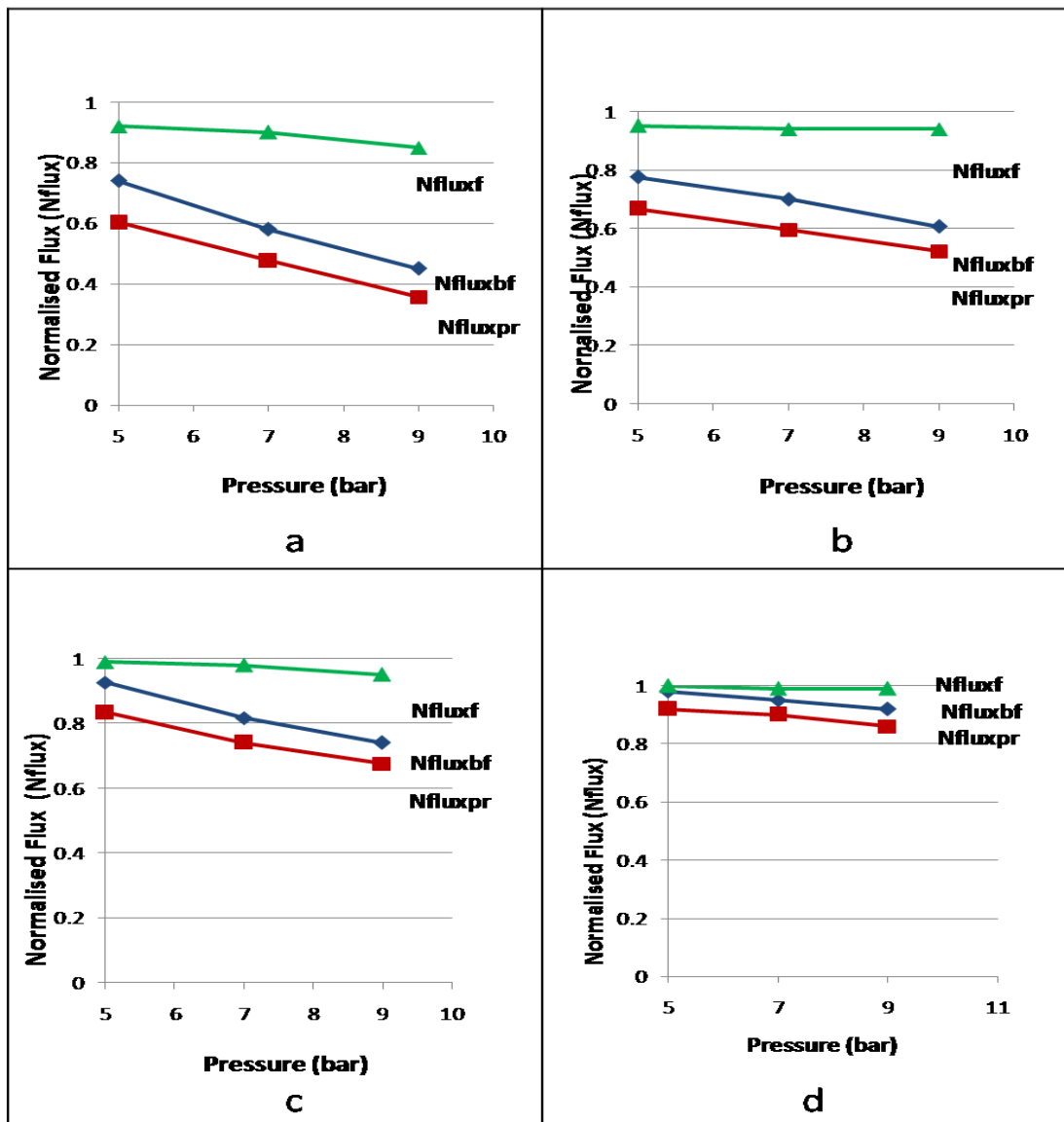


**Fig.3.5 Normalised Flux as a function of operating pressure at 0.7 recovery for different feed flowrates a) 4.5 lpm b) 7.0 lpm c) 9.0 lpm d.)13.0 lpm [corresponding to apparent Reynold's Number 132, 205, 264 ,381 respectively]**

The above observations lead us to infer that scale formation does occur at all operating pressures and flow rates studied but manageable at higher flowrates and moderate pressures.

### 3.3.1.7 Permeate Quality :

The permeate quality in terms of sulphate has been shown Fig.3.6 as a function of different flowrates at constant pressure and different pressures at constant flowrate.

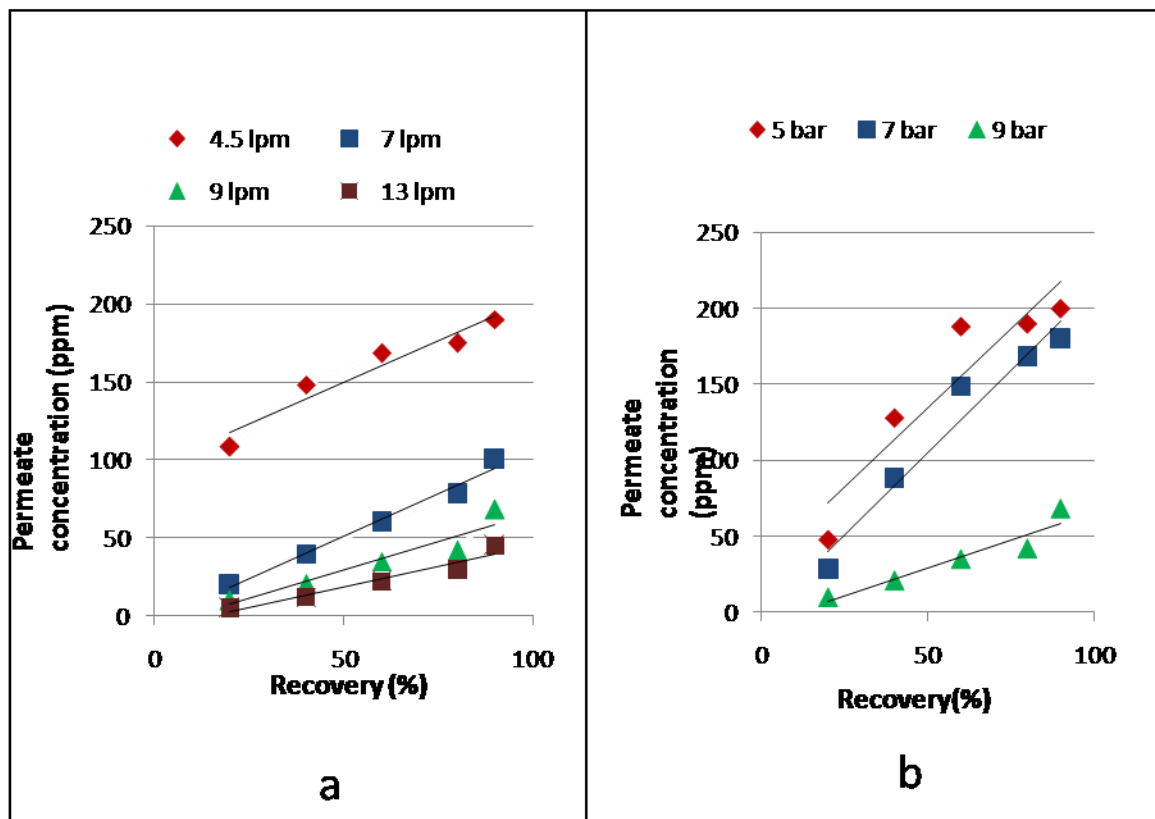


**Fig-3.6 Permeate quality with recovery at (a) constant pressure (9bar) and (b) constant flow rate (9lpm)**

As expected the quality shows improvement with flowrate and operating pressure. The observations indicate that product quality is best at 13 lpm flow rate and 9 bar pressure, the quality is acceptable at around 50 ppm for 9 lpm feed flowrate and 9 bar pressure at 0.9 recovery.

The solute rejection increases with increasing flow rate resulting in less concentration of calcium & sulphate species in the permeate due to more efficient back diffusion of the solute species from the boundary layer. Deposition of calcium sulphates at lower flow rates further reduces the reject concentration. Mass balance based on volume and concentration of feed, permeate and reject streams indicate more deposition at lower flow rates. Based on the conductivity of flushed water we could get a nearly total mass balance within an error of less than 5%. However reject stream on standing reveal more deposition in case of higher flow rate.

#### **3.3.1.8 Experimental study with simulated solution**

In order to extend the results to realtime applications simulated effluents containing a mixture of sodium sulphate and calcium chloride has been prepared and sent to nanofiltration membrane. The trace chemical species have not been added for the present studies as field experiments have been planned. Moreover, with prior ultrafiltration treatment no trace species which can foul the membranes is expected to be present such as manganese and iron. Heavy elements, if at all present would report only in the concentrate which can be either recycled or disposed off suitably in conformity with environmental regulations. As our focus specifically is to assess the recovery of water from saturated calcium sulphate streams, it is felt appropriate to restrict the study to mixed systems containing the major solute species. The experimental observations based on the simulated effluents with respect to recovery is presented in Fig.3.7.

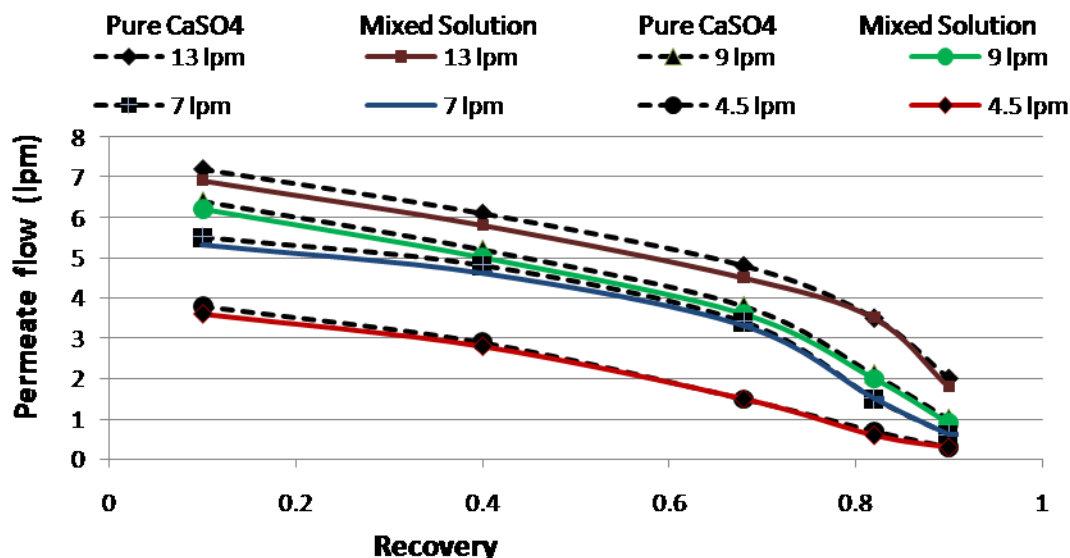


**Fig.3.7 Permeateflow as a function of recovery at 9 bar pressure at different flowrates.**

Fig-3.7 shows that the nature of product flow decline with increasing recovery is same for pure calcium sulphate as well as mixed solution. As the osmotic pressure of mixed solution is higher than pure calcium sulphate solution, the product flow is lower for mixed solution than pure calcium sulphate.

### 3.3.2 Development of mathematical model

#### 3.3.2.1 Development of model algorithm

A schematic flow sheet of developmental approach of mathematical model of integrated NF-RO (Nanofiltration followed by Reverse Osmosis) is presented in Fig 3.8 for treatment of saturated calcium sulphate solution. For nanofiltration system recovery is achieved by recirculating reject on NF feed tank. Product was collected separately (batch process, explained in Fig 3.1). Fig 3.8 explains for a given range of operating feed flow and feed pressure physical model of NF membrane system can predict optimized feed flow and feed pressure at minimum surface scale threat with maximum recovery, provided feed characteristic data, membrane characteristic data and product quality requirement are known.

The product of NF membrane is sent to RO membrane system to achieve required product quality at an optimized pressure.

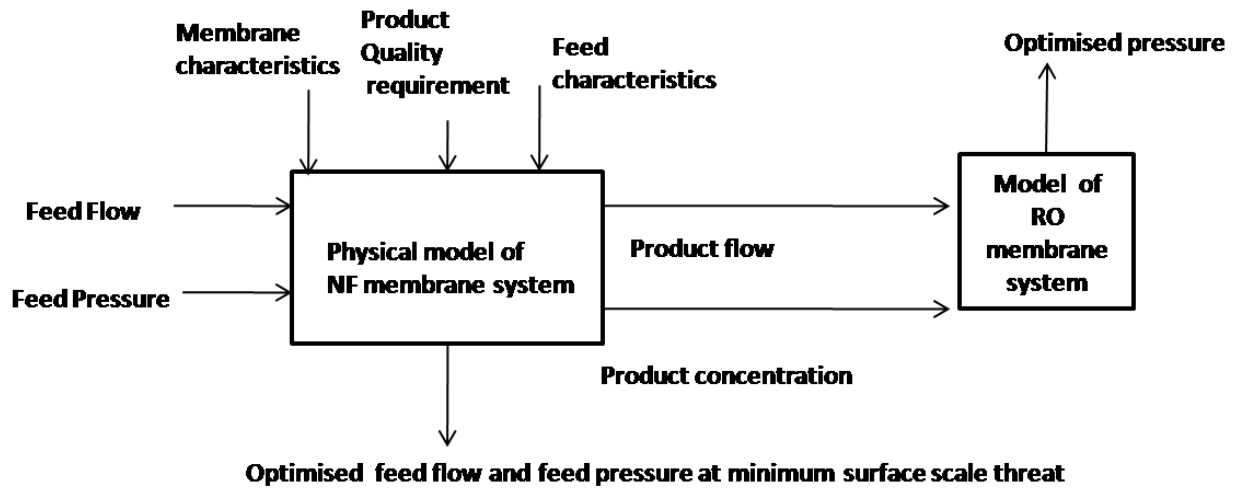


**Fig-3.8 Schematic flow sheet of development of mathematical model**

Fig-3.9 explains schematically the physical model of nanofiltration batch process. For a given feed flow and feed pressure, the extent of scaling on membrane surface is evaluated by surface crystal growth rate model. In this model, wall concentration on membrane surface has been evaluated as a function of bulk concentration. Bulk concentration is expressed as a function of time and it has been evaluated by Euler's forward formulae by solving mass balance and component balance equations for batch process. It has been ascertained that when wall concentration or boundary concentration achieves 0.07 moles/L  $\text{CaSO}_4$  concentration (which is a concentration evaluated experimentally at a point of inflexion) the recovery which has been achieved at this particular time will be the optimized recovery for this feed flow and feed pressure. Time required to achieve this particular recovery is called induction time. The development of mathematical model for reject management through lime column is out of the scope of present work.

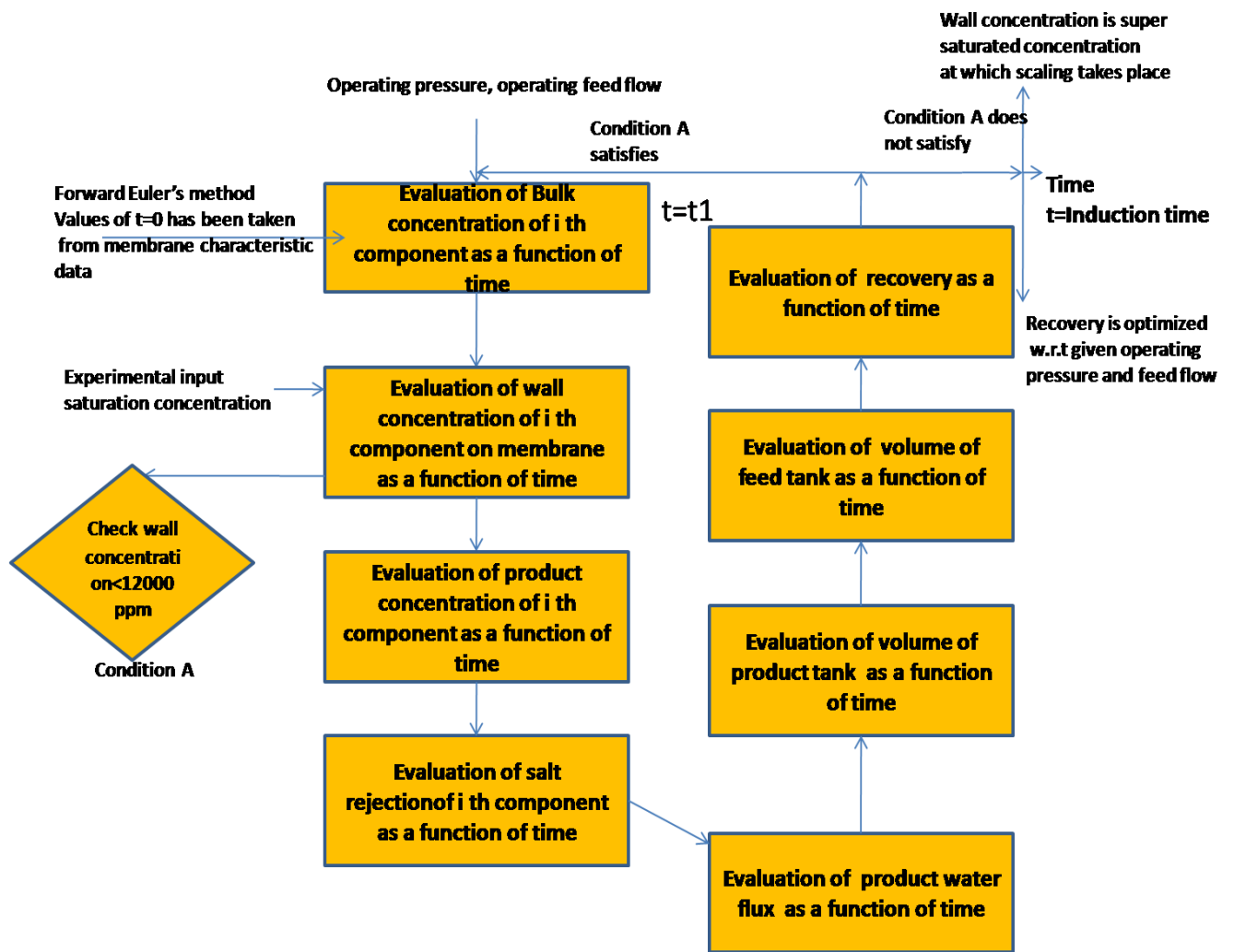


Fig-3.9 Physical model of Nanofiltration system

### 3.3.2.2 Development of model equations:

Surface Crystal Growth model [95-99 ]

The surface crystal growth rate of Calcium sulphate is described by the following equation:

$$\frac{dm_s}{dt} = K_s (C_w - C_s) \quad 3.1$$

Here  $m_s$  is the weight of scale formed directly on membrane surface.  $K_s$  is the rate constant of surface crystallization,  $C_w$  is the wall concentration near the membrane surface,  $C_s$  is the saturation concentration.

Weight of scale formed on membrane surface ( $m_s$ ) can be evaluated as

$$m_s = \frac{A_t}{\beta} \left( 1 - \frac{J_b}{J_w} \right) \quad 3.2$$

Here  $A_t$  is total membrane area,  $\beta$  is area occupied per unit mass,  $J_b$  is product flux,  $J_w$  is pure water permeability.

Estimation of wall concentration:

As the solute flux is negligible in NF, the ratio of membrane wall concentration to the bulk concentration can be estimated as follows: [96]

$$\frac{C_w}{C_b} = \exp\left(\frac{J_b}{k}\right) \quad 3.3$$

Here  $C_b$  is bulk concentration and  $k$  is mass transfer coefficient.

Empirical correlation of mass transfer coefficient is defined as:

$$k = 1.86 \left( \frac{uD^2}{d_h L} \right)^{0.33} \quad 3.4$$

$u$  is flow velocity,  $D$  is diffusion coefficient of salt,  $d_h$  is hydraulic diameter  $L$  is channel length .

Pure water permeability can be defined,

$$J_w = A_w \Delta P \quad 3.5$$

$J_w$  is pure water permeability,  $A_w$  is solvent permeability constant,  $\Delta P$  is operating pressure

By combining equation 1,2,3,4 and express the parameters as a function of time, the equation becomes:

$$\frac{d}{dt} \ln \left( \frac{C_w(t)}{C_b(t)} \right) = \frac{-K_s A_w \Delta P \beta}{A_s \cdot 1.86 \left( \frac{uD^2}{d_h L} \right)^{0.33}} (C_w(t) - C_s) \quad 3.6$$

This is the final operating equation of surface crystal growth model. From this equation it can be established that surface crystal growth model cannot predict the situation (flux decline) beyond scaling condition.

From this equation it is evident that

As  $C_w(t) > C_b(t)$  in left hand side

$C_w(t) < C_s$  in right hand side

Which ultimately concludes

$$C_b(t) < C_w(t) < C_s$$

Above condition does not lead to scale. In this work, validation of experimental flux decline with mathematical model has been restricted upto the point beyond which scaling takes place.

Surface crystal growth rate model does not acknowledge the fact that flow through the membrane experiences some resistance. Section 3.3 has been devoted for discussion pertaining to different resistances.

### 3.3.2.3 Flow balance equation for batch Nanofiltration process

In this integrated membrane processes, nanofiltration operates in batch mode. Nanofiltration product is collected in separate tank. Nanofiltration reject is recycled back to NF feed tank [108-109].

Rate of change of product flow

$$\frac{d(V_p(t))}{dt} = J_b(t).A \quad 3.7$$

Change in volume in feed tank

$$-\frac{dV_b(t)}{dt} = \frac{dV_p(t)}{dt} \quad 3.8$$

Component balance

$$-\frac{d(V_b(t).C_{i,f}(t))}{dt} = \frac{d(V_p(t).C_{i,p}(t))}{dt} = J_{i,b}(t).A.C_{p,i}(t) \quad 3.9$$

Salt rejection

$$SR_i(t) = 1 - \frac{C_{i,p}(t)}{C_{i,b}(t)} \quad 3.10$$

$$V_b(t) \frac{dC_{i,b}(t)}{dt} = -J_{i,b}(t).A.(1 - SR_i(t)).C_{i,b}(t) \quad 3.11$$

Equation 11 can be solved by Forward Euler's method at time  $t=0$  is taken characterization data of membrane

Recollecting equation 6 for component i

$$C_{i,w}(t) = C_{i,b}(t) \cdot \exp\left(\frac{J_{i,b}(t)_o}{k_i}\right) \quad 3.12$$

$$J_{i,b}(t) = k_i \ln \frac{C_{i,w}(t)}{C_{i,b}(t)} \quad 3.13$$

$$C_{i,p}(t) = \frac{B_{i,s} \cdot C_{i,w}(t) \cdot C_{water}}{J_{i,b}(t) + B_{i,s} \cdot C_{water}} \quad 3.14$$

$$SR_i(t) = 1 - \frac{C_{i,p}(t)}{C_{i,w}(t)} \quad 3.15$$

$$V_{i,p}(t) = J_{i,b}(t) \cdot A. \quad 3.16$$

$$V_{i,b}(t) = V_b(t)_o - V_p(t)_o \quad 3.17$$

$$R_i(t) = \frac{V_{i,p}(t) \cdot t \cdot 100}{V_{i,b}} + R_i(t)_o \quad 3.18$$

Calculation Tool:

### Forward Euler's method [110]

Let's denote the time at the  $n$ th time-step by  $t_n$  and the computed solution at the  $n$ th time-step by  $y_n$ , i.e.,  $y_n = y(t = t_n)$ . The step size  $h$  (assumed to be constant for the sake of simplicity) is then given by  $h = t_n - t_{n-1}$ . Given  $(t_n, y_n)$ , the forward Euler method (FE) computes  $y_{n+1}$  as

$$y_{n+1} = y_n + hf(y_n, t_n)$$

### 3.3.3 Modification of flux term incorporating cake resistance

$$J_w = \frac{\Delta P - \Delta \pi}{\eta \cdot R_m} \quad 3.19$$

$$J_c = \frac{\Delta P - \Delta \pi}{\eta(R_m + R_c)} \quad 3.20$$

$R_m$  and  $R_c$  are intrinsic membrane resistance and scale resistance respectively:

In the following section, resolution of membrane resistance from experimental flux decline data and then the conversion of information into model equations have been discussed in detail.

#### 3.3.3.1 Evaluation of individual resistance term from flux decline data:

Experimental flux decline data reveals the fact that membrane has been experienced different extent of resistance to flow at different operating conditions. When a membrane is dealing with a saturated solution; membrane can experience three series of resistance to flow. Membrane intrinsic resistance is defined as the resistance due to the membrane morphology, pore size distribution. It depends on the operating pressure. Osmotic pressure resistance is defined as the resistance experienced by the membrane owing to the nature (concentration) of the solution handled. Osmotic pressure resistance is not a membrane property but it is solution property. Scaling resistance is experienced by the membrane when the scale is formed physically on the membrane top surface. Table-3.1 gives the detail resistance calculation on the membrane surface based on equation 19 and 20.

In previous section, the normalised flux (Nflux), a dimensionless number representing the drop in permeate rate due to different factors under various experimental conditions has been

discussed. These three dimensionless number (shown in Fig 3.5)  $N_{flux_{pr}}$ ,  $N_{flux_f}$ ,  $N_{flux_{uf}}$  actually represents the flux at 70% recovery, pure water permeability before flushing after 70 % recovery and pure water permeability after flushing respectively.

Table 3.1, the resistances have been evaluated corresponding to their fluxes. PWP denotes pure water permeability for clean membrane, PR denotes product flow rate at 70% recovery,  $PWP_f$  denotes pure water permeability before flushing,  $PWP_{uf}$  denotes pure water permeability after flushing.

**Table-3.1 Evaluation of individual resistance term from flux decline data**

<b>Flux decline</b>	<b>Pressure (bar)</b>	<b>Reject TDS(ppm)</b>	<b>PWP (lpm)</b>	<b>PR(lpm)</b>	<b>PWP<sub>f</sub>(lpm)</b>	<b>PWP<sub>ur</sub>(lpm)</b>	<b>Viscosity (Pa.S)</b>	<b>ΔP (Pa)</b>	<b>ΔH (Pa)</b>	<b>ΔP-ΔH (Pa)</b>	<b>Resistance of PWP(m<sup>-1</sup>)</b>	<b>Resisom+scaling(m<sup>-1</sup>)</b>	<b>Resis scale(m<sup>-1</sup>)</b>	<b>Resis hard scale(m<sup>-1</sup>)</b>	<b>Res due osm(m<sup>-1</sup>)</b>
9.5	5	10868	7.8	6.5	7.2	7.72	0.001	500000	308808	191191	1.03E+13	1.2E+13	1.11E+13	1.04E+13	1.2E+12
	7	13128	8.5	6.1	6.96	8.35	0.001	700000	373024	326975	1.6E+13	2.2E+13	1.97E+13	1.64E+13	2.03E+12
	9	12763	8.8	5.9	6.5	8.36	0.001	900000	362652	537347	2.5E+13	3.8E+13	3.46E+13	2.7E+13	3.34E+12
7	5	12595	6	4	4.6	5.7	0.001	500000	357873	142126	9.9E+12	1.5E+13	1.28E+13	1.05E+13	2.1E+12
	7	10803	6.7	3.98	4.7	6.3	0.001	700000	306955	393044	2.5E+13	4.14E+13	3.52E+13	2.62E+13	6.16E+12
	9	11921	6.9	3.6	4.2	6.5	0.001	900000	338722	561277	3.42E+13	6.56E+13	5.64E+13	3.63E+13	9.22E+12
4.5	5	13688	3.8	2.3	2.8	3.5	0.001	500000	388935	111064	1.23E+13	2.03E+13	1.66E+13	1.33E+13	3.8E+12
	7	12748	4	1.9	2.67	3.6	0.001	700000	362226	337773	3.5E+13	7.45E+13	5.32E+13	3.9E+13	2.1E+13
	9	10248	4.2	1.5	2.3	3.57	0.001	900000	291191	608808	6.1E+13	1.70E+14	1.1E+14	7.16E+13	6.1E+13

### 3.3.3.2 Analysis of Resistances for Flow through Membranes:

Basically the water flow through the membrane has to overcome three resistance at the maximum namely membrane intrinsic resistance, osmotic resistance and the scaling / fouling resistance. The first is the characteristic of any membrane and is always present. Osmotic pressure resistance depends on the solution concentration in terms of total dissolved solids used as a feed and the last one depends on the nature of species present.

#### Membrane intrinsic resistance:

The membrane intrinsic resistance (clean membrane resistance) is measured by pure water permeability data by passing distilled water through membrane. Intrinsic membrane resistance reveals the internal characteristics of membrane like pore size distribution, surface tension, hydrophilicity etc. Fig-3.10 shows that the resistance is directly proportional to operating pressure. With increasing pressure, compaction effect of pore sizes leads to higher resistance. For higher feed flow lower friction instigates lower membrane resistance. In lower feed flow, the product flux will be also small which increases the overall resistance of membrane.

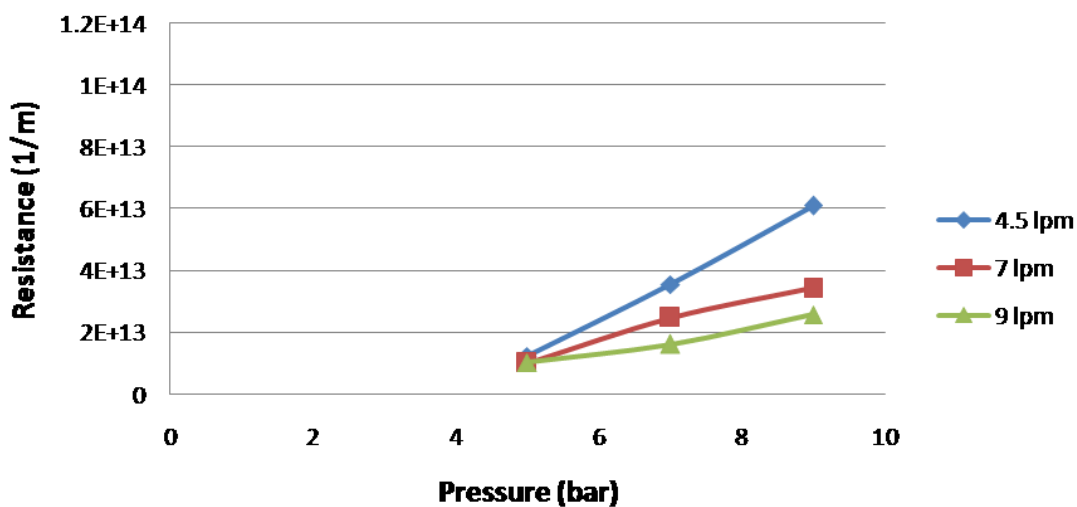


Fig-3.10 Change of membrane intrinsic resistance with pressure

### Osmotic pressure resistance:

The osmotic pressure resistance is the solution property. When the solvent (water) permeates through the membrane, it has to overcome the osmotic pressure, what we term here as osmotic resistance. The resistance would be dictated by the concentration of solution in contact with the membrane surface which we call as 'boundary layer'. At lower feed flow rates and higher pressures the boundary layer concentration and hence the resistance would be higher. In Fig-3.11 the resistance experienced by the membrane at lowest flow rate (4.5 lpm) and highest pressure (9 bar) is maximum due to low back diffusion rate of the solute from concentrate stream to bulk stream. At higher feed flow (7 lpm, 9 lpm) membrane intrinsic resistance is higher compared to osmotic pressure resistance.

This phenomenon can be explained by the introduction of osmotic pressure factor ( $\Delta\pi$ ) into equation 3.20. Introduction of osmotic pressure factor decreases the driving force which is responsible for compaction in pores. Consequently, osmotic pressure resistance is lower compare to membrane intrinsic resistance.

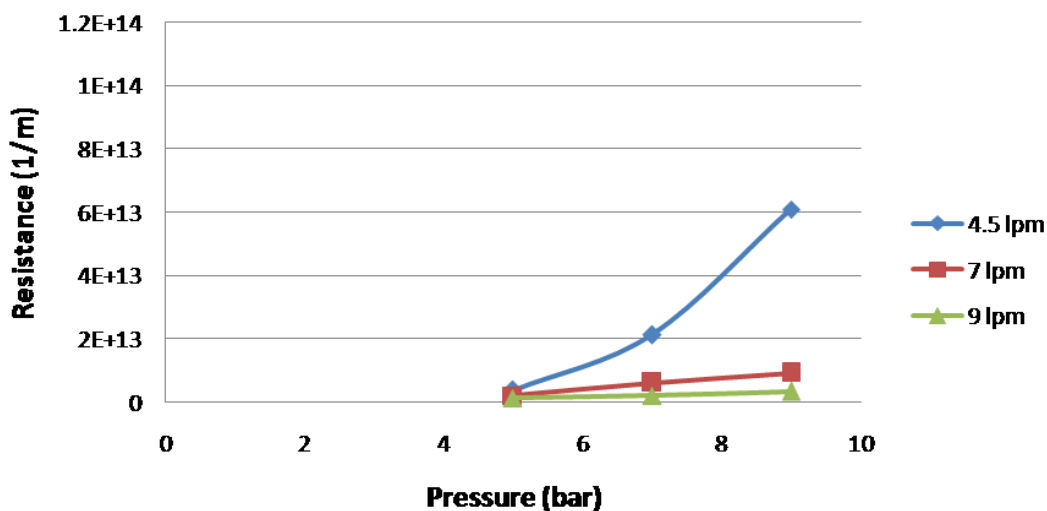
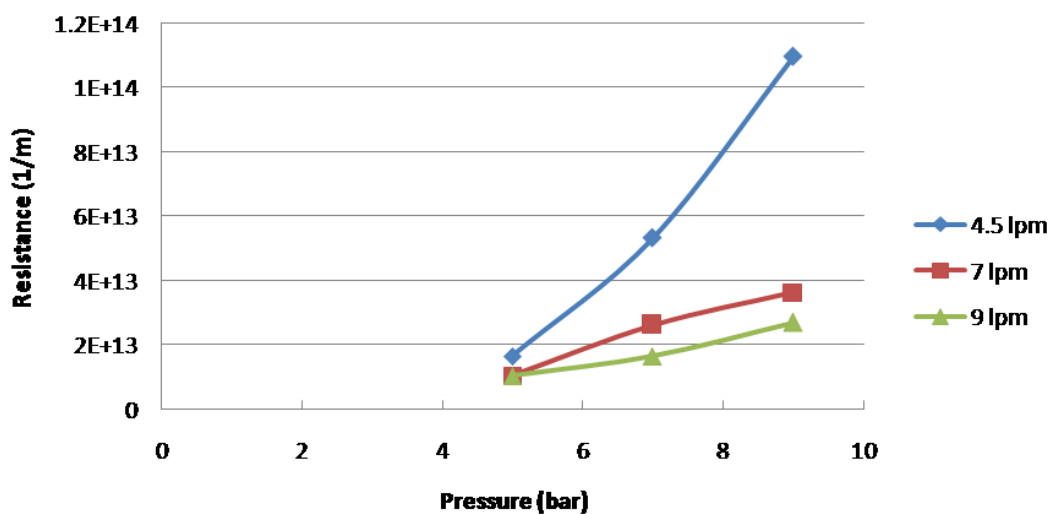


Fig-3.11 change of osmotic resistance with pressure

### Scale resistance

Fig-3.12 shows the behavior of scale resistance experienced by the membrane at different operating conditions. Scale resistance is minimum for higher flow rate and lower pressure. The turbulence which has been created by high feed velocity on membrane surface hinders the promotion of the growth of nucleation crystal, consequently scaling is inhibited. At low feed velocity and high pressure rate of back diffusion gets slower making top surface of the more prone to scaling.



**Fig 3.12 Change of scale resistance with pressure**

#### 3.3.3.3 Incorporation of resistances in mathematical model:

Resistances evaluated by experimental results are incorporated in mathematical model for getting better prediction in flux decline data.

Resistance (Y) can be denoted as dependent variable and Feed flow rate (X1), operating pressure (X2), reject concentration (X3) and product flux (X4) are independent variables, then Y can be expressed as

$$Y=B1X1+B2X2+B3X3+B4X4$$

Where, B1,B2, B3 and B4 are the corresponding parameters.

These parameters are evaluated by multiple linear regression least square method. Parameters are given in the Table3.2:

**Table:3.2 Dependence of resistances on parameters**

Parameters	ScaleResistance ( $10^{13}$ )	(Osmotic +scale ) Resistance ( $10^{13}$ )
B1 (feed flow)	-1.94	-3.59
B2 (operating pressure)	1.69	1.18
B3(Reject concentration)	-0.0001	-0.0005
B4(product flux)	-1.50	-5.46

The above four parameters depict the alliances between resistances and process / system parameters. Among these process parameters feed flow and feed pressure are input system parameters and reject concentration and product flux are output system parameters. These input system parameters are originator of resistance and output system parameters are offsuit of resistance. When feed flow increases, resistance decreases. This relation has been interpreted by negative sign. When operating pressure increases, resistance also increases. This association can be illustrated by positive sign. If resistance increases reject concentration decreases and product flux also decreases, because scaling on the membrane surface takes place. This relation also can be explained by negative sign.

### 3.3.4 Validation of nanofiltration model

Validation of experimental flux decline behavior of nanofiltration model has been shown in Fig 3.13 and Fig 3.14. In Fig 3.13 experimental flux decline has been plotted against model

prediction of surface crystal growth rate model. As surface crystal growth model does not consider resistances error margin of experimental result and model prediction is very high at higher recovery.

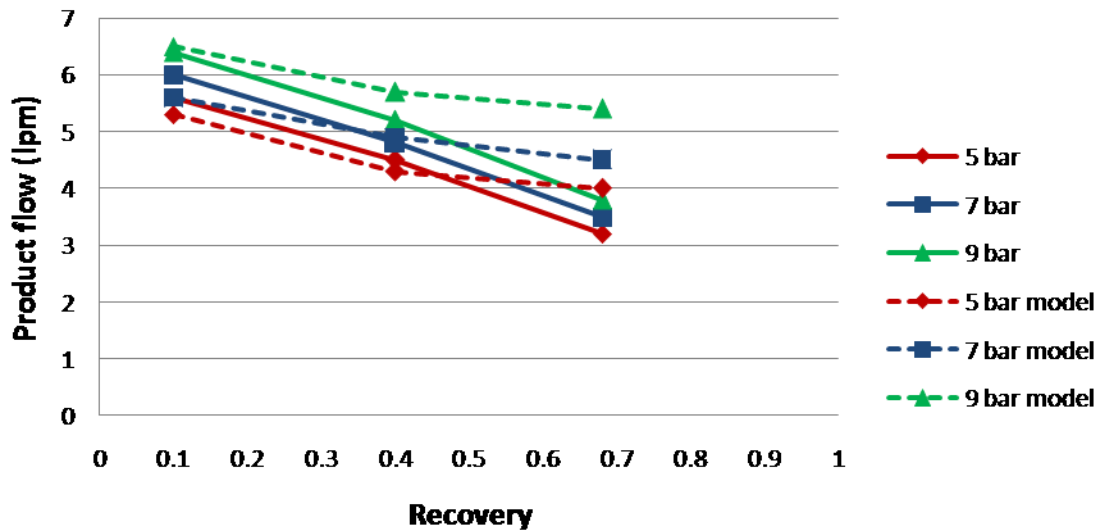


**Fig-3.13 Validation of experimental flux decline of nanofiltration by surface crystal growth model**

Fig-3.14 shows that experimental flux decline of nanofiltration membrane can be well predicted by incorporation of different resistance terms in mathematical model. In higher recovery region error margin has been brought down from 30% ( shows in Fig-3.13) to 5%. In higher recovery region , osmotic resistance and scale resistance both play prominent role to decline the flux.

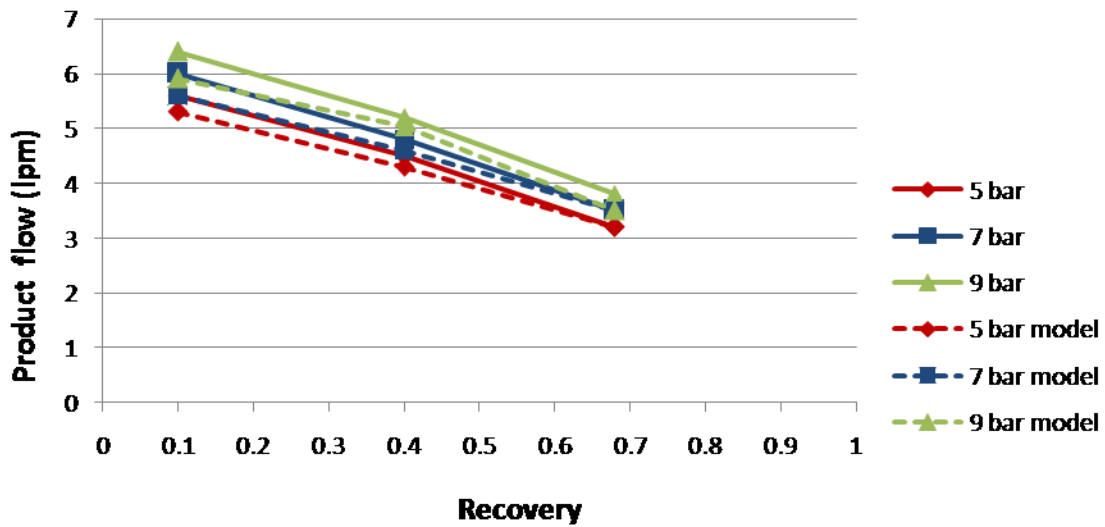


**Fig-3.14 Validation of experimental flux decline of nanofiltration by resistance incorporated surface crystal growth model**

### 3.3.5 Optimised feed flow and feed pressure

From the physical model of nanofiltration optimum feed flow and optimum feed pressure at minimum scaling threat has been evaluated at 9 lpm feed flow and 9 bar pressure. Scaling threat increases if feed flow on membrane surface reduces and feed pressure increases. Increasing feed pressure promotes membrane to produce more pure water, decreasing feed flow reduces the turbulence creation on membrane surface. Consequently a layer of concentration polarisation and cake resistance is formed and flux decline commences. The dependence of scaling threat on hydrodynamics (i.e. feed flow and feed pressure) has been shown schematically in Fig-3.15. From Fig 3.15, it is ascertained that with increasing feed

flow and decreasing feed pressure scaling phenomenon could be averted.

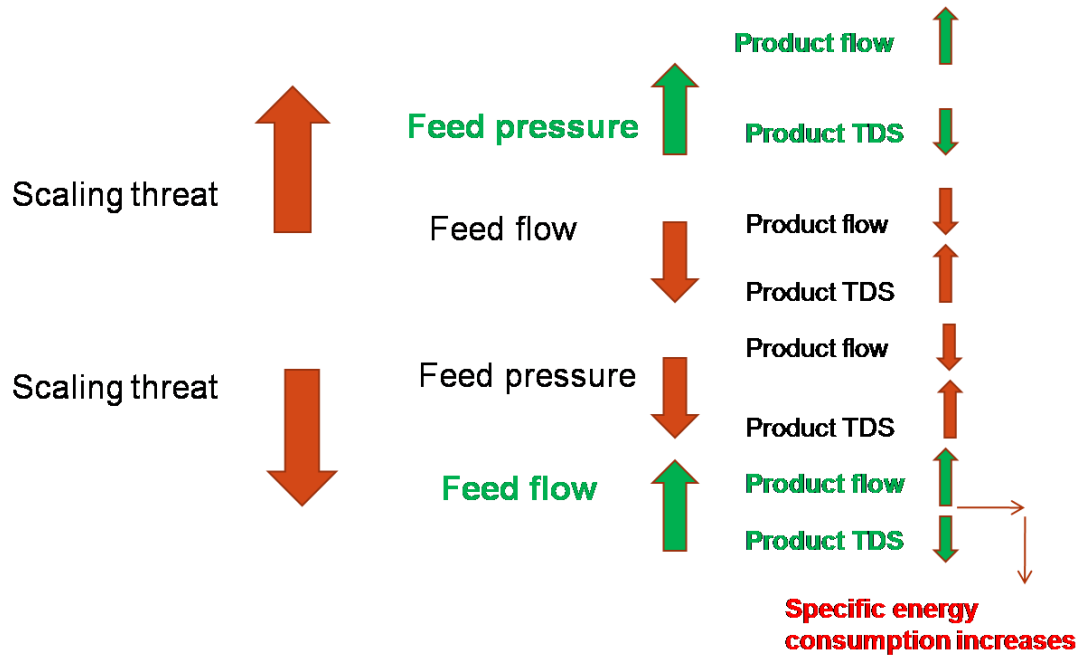


**Fig-3.15 Dependence of scaling threat on hydrodynamics**

From Fig 3.16 it is clear that at 10 bar pressure, flux decline commences at lower recovery (40%) compare to (60%) at 9 bar pressure. When feed flow increases from 9 lpm to 13 lpm product flow also increases (6.2 lpm to 7.2 lpm). But to increase 1 lpm product flow specific energy requirement increases 24%.

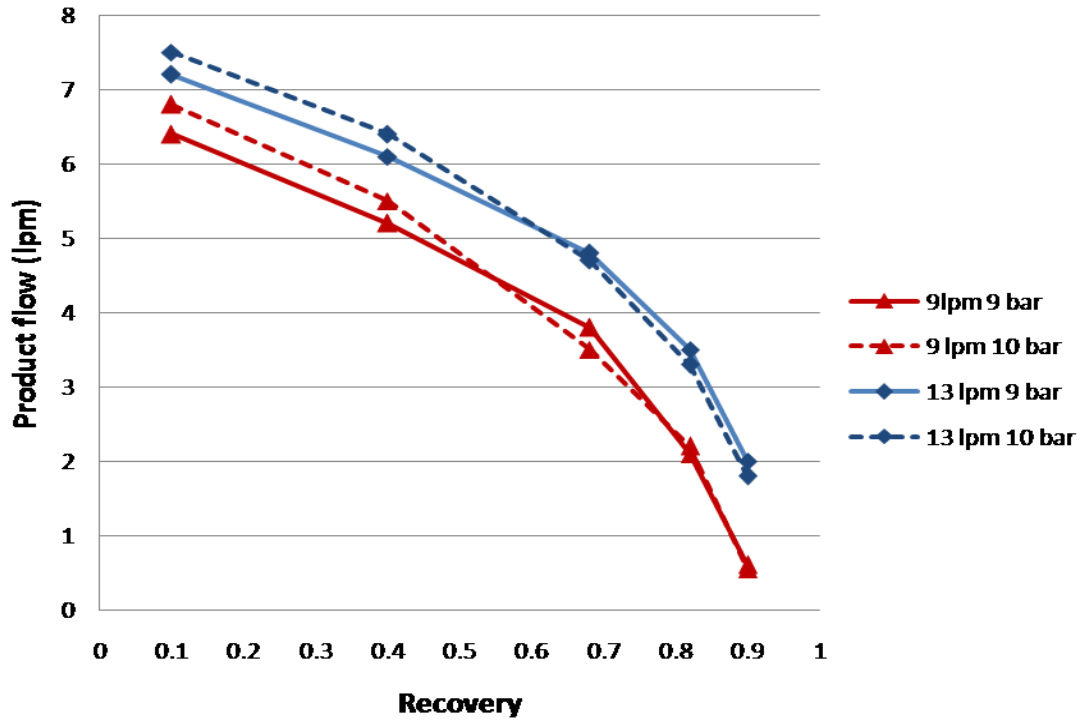


**Fig-3.16** Variation of product flow at different feed flow and different feed pressure

Fig 3.16 shows product quality at different flow rate at 9 bar pressure. From this figure it is ascertained that at feed flow 9 lpm and feed pressure 9 bar, sulphate product concentration is below 70 ppm at 70 % recovery. Safe environmental limit of surface discharge is 200 ppm.

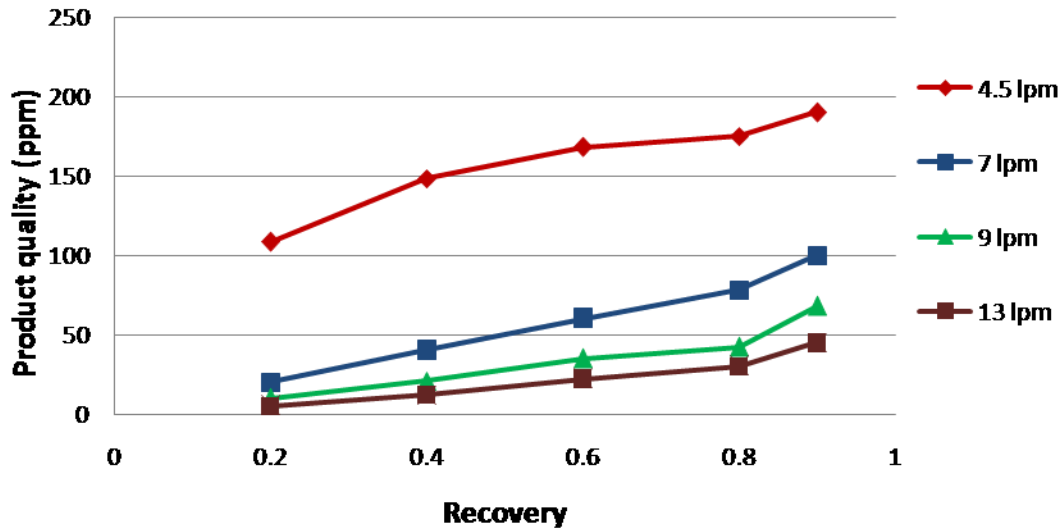


**Fig 3.17** Variation of product quality with feed flow rate at 9 bar pressure

From these two figures (Fig 3.16 and Fig 3.17) it has been confirmed that with increasing feed flow and decreasing feed pressure, occurrence of scaling can be avoided. With increasing feed flow, turbulence on membrane top surface increases and nucleation cannot take place. Though with increasing feed flow, product flow increases and product quality improves; increasing specific energy takes toll on the operating cost. With decreasing feed pressure, product quality deteriorates. So, product quality can not be sacrificed indefinitely in the name of minimal scaling threat. So, a optimisation study should be conducted to verify the optimised feed flow and feed pressure (9 lpm, 9 bar) obtained from resistance incorporated surface crystal growth model. In this work, a thermodynamic parameter ‘exergy’ has been attempted for carrying out the optimisation study.

### **3.3.6 Optimization of operating parameters nanofiltration membrane by thermodynamic efficiency analysis (exergy)**

Objective of this analysis is to evaluate thermodynamic efficiency through exergy analysis of twenty sets of experimental condition (operating feed flow range; 4.5 lpm, 7 lpm, 9 lpm,

11lpm, 13 lpm; operating feed pressure range; 5 bar, 7 bar, 9 bar and 10 bar). For every sets of experimental condition, exergy has been calculated at that particular recovery beyond that scaling is going to take place (flux decline more than 20 %). From the experimental data, we come to know that lower feed flow and higher feed pressure make the top surface of membrane more conducive for scaling.

### **What is exergy?**

Exergy is defined as the potential-work measure of the departure from equilibrium, which may be said to drive all physical processes. It is the availability to perform useful work from a given energy source, Exergy is that part of energy that is convertible into all other forms of energy. Exergy represents the useful part of energy for a system in its environment, i.e., the maximum quantity of work that the system can execute in its environment [111-116]. The exergy destruction represents the wasted work potential i.e. the work that could have been produced but was not.

The basic difference between energy and exergy concept is energy input and output will always balance according to the first law of thermodynamics or the energy conservation principle. Exergy output will not balance the exergy input for real processes since a part of the exergy input is always destroyed according to the second law of thermodynamics for real processes. An energy efficiency or first law efficiency will determine the most efficient process based on wasting as little energy as possible relative to energy inputs. An exergy efficiency or second law efficiency will determine the most efficient process based on wasting and destroying as little available work as possible from a given input of available work.

### Calculation of Exergy:

Exergy for a flow stream consists of three parts, namely temperature, pressure, and concentration contributions [86]:

$$E_x = E_x^T + E_x^P + E_x^C$$

Where the  $E_x^T$  temperature,  $E_x^P$  pressure, and  $E_x^C$  concentration terms are defined as:

$$E_x^T = G[(h - h_o) - T_o(s - s_o)]$$

$$E_x^P = G \left[ \frac{P - P_o}{\rho} \right]$$

$$E_x^C = R * T_o * \sum X_i * \ln \left( \frac{X_i}{X_{io}} \right)$$

The subscript  $o$  stands for reference state,  $G$  is mass flow rate,  $h$  is enthalpy,  $T$  is temperature,  $s$  is entropy,  $P$  is pressure,  $\rho$  is density and  $X_i$  fraction of species  $i$  in a mixture;  $X_{io}$  fraction in a dead state composition,  $R$  is gas constant. Membrane process is a constant temperature process. So, in the present work, discussion has been restricted to pressure exergy and concentration exergy only.

### Thermodynamic efficiency:

$$\eta = \frac{\text{Exergy input} - \text{Exergy loss due to work done}}{\text{Exergy input}}$$

$$\eta = 1 - \frac{\text{Exergy loss due to work done}}{\text{Exergy input}}$$

So, from the definition of efficiency, if exergy input increases and exergy loss due to work done decreases, efficiency will increase.

In Fig-3.18 the nanofiltration process is illustrated in terms of state for optimization study of its hydrodynamic parameters. It is a batch recycle process. State 0 has been depicted to feed condition. This has been taken as reference state. All the calculations of exergy have been done with respect to state 0. State 1 has been put after pressurization of feed. State 2 has been depicted to reject stream and state 3 has been depicted to product stream. In a batch recycle process, two different recovery terms are used.

Specific recovery is defined by the ratio of product flow which is coming out of the membrane and feed flow which is going to the membrane. This is membrane property.

Overall recovery is defined by the ratio of volume of total product collected and initial volume of feed. This is system property.

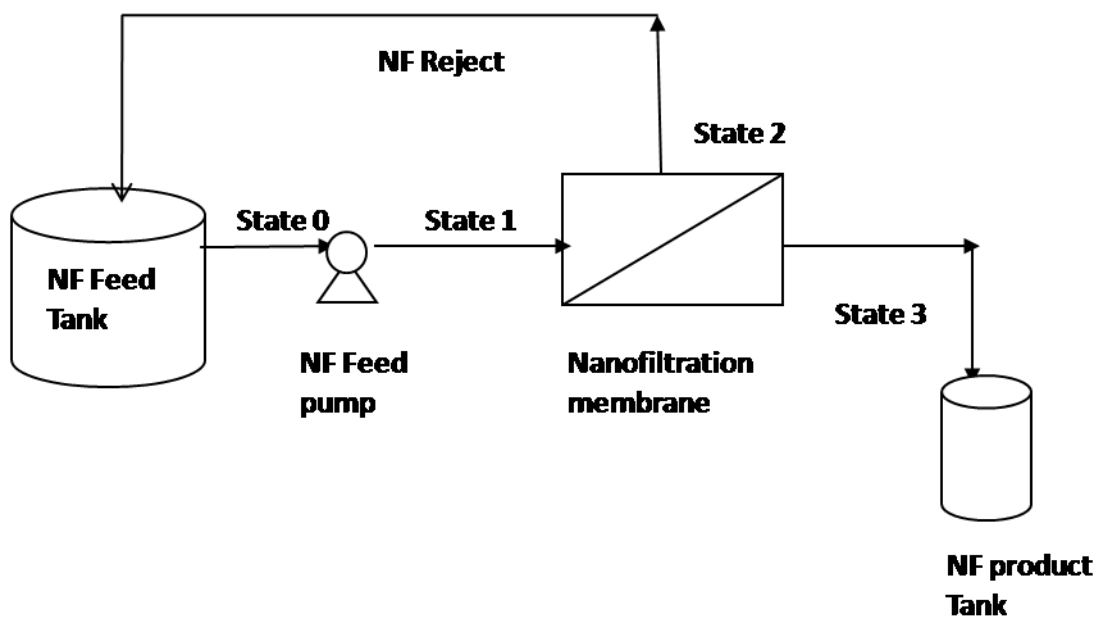


**Fig-3.18**Nanofiltration process

### **Calculation of process parameters in nanofiltration process:**

Calculation of process parameters given in Table-3.3 is required for exergy calculation. Here, final product volume (i.e. overall recovery) signifies that product volume which has been achieved at that particular point beyond this scaling starts progressing (i.e.20% flux decline).

**Table-3.3 Evaluation of process parameters for exergy analysis**

Specific recovery	Flow(lpm)	Pressure(bar)	Final prdt. Volume(l)	Final prdt. Conc.(ppm)	Final reject volume(l)	Final reject conc.(ppm)	Time required(min)	Av prdt flow (lpm)
91	13	10	45	15	55	3624	3.8	11.8
65	13	9	75	57	25	7829	8.8	8.5
56	13	7	72	70	28	6962	9.8	7.3
47	13	5	68	130	32	5973	11	6.2
56	9	10	40	20	60	3320	7.5	5.3
38	9	9	70	60	30	6526	19.2	3.64
33	9	7	65	85	35	5556	20.6	3.15
30	9	5	60	150	40	4775	20.8	2.9
67	7	10	37	24	63	3160	7.8	4.7
53	7	9	60	120	40	4820	16	3.7
47	7	7	62	150	38	5018	19	3.3
39	7	5	58	160	42	4540	21	2.76
78	4.5	10	35	5	65	3074	10	3.5
62	4.5	9	56	80	44	4443	20	2.8
55	4.5	7	57	100	43	4518	23	2.5
51	4.5	5	58	170	42	4527	25	2.3
91	11	10	42	17	58	3435	4.2	10
61	11	9	73	58	27	7250	10.8	6.7
52	11	7	68	78	32	6084	11.8	5.7
47	11	5	65	140	35	5454	12.5	5.2

Tables 3.4, 3.5 and 3.6 provide detailed exergy evaluation for different streams.

**Table-3.4 Evaluation of exergy input at state 1 (after pressurization of feed)**

Flow (lpm)	Pressure(kpa)	Salinity(ppm)	Total volume of feed(m <sup>3</sup> )	Total mass of feed (kg)	Specific exergy(Kj/kg)	Total exergy input(KJ)
13	101.3	2000	0.1	100	0.911	45.04
13	912	2000	0.1	100	0.81	92.72
13	709	2000	0.1	100	0.60	77.45
13	506	2000	0.1	100	0.40	57.95
9	101.3	2000	0.1	100	0.91	64.97
9	912	2000	0.1	100	0.81	147.84
9	709	2000	0.1	100	0.60	118.96
9	506	2000	0.1	100	0.40	80.08
7	101.3	2000	0.1	100	0.91	49.78
7	912	2000	0.1	100	0.81	90.78
7	709	2000	0.1	100	0.60	80.85
7	506	2000	0.1	100	0.40	59.57
4.5	101.3	2000	0.1	100	0.91	41.03
4.5	912	2000	0.1	100	0.81	72.95
4.5	709	2000	0.1	100	0.60	62.91
4.5	506	2000	0.1	100	0.40	45.59
11	101.3	2000	0.1	100	0.91	42.12
11	912	2000	0.1	100	0.81	96.29
11	709	2000	0.1	100	0.60	78.90
11	506	2000	0.1	100	0.40	55.72

**Table-3.5 Evaluation of exergy at state 2 (reject stream)**

Flow (lpm)	Pressure(kpa)	Salinity(ppm)	Total volume of reject(m <sup>3</sup> )	Total mass of reject (kg)	Specific exergy(Kj/kg)	Total Exergy (kJ)
13	101.3	3624	0.055	55	0.07	4.02
13	101.3	7829	0.025	25	0.67	16.76
13	101.3	6962	0.028	28	0.51	14.39
13	101.3	5973	0.032	32	0.35	11.32
9	101.3	3320	0.06	60	0.05	3.00
9	101.3	6526	0.03	30	0.44	13.22
9	101.3	5556	0.035	35	0.29	10.24
9	101.3	4775	0.04	40	0.19	7.62
7	101.3	3160	0.063	63	0.04	2.48
7	101.3	4820	0.04	40	0.19	7.83
7	101.3	5018	0.038	38	0.22	8.38
7	101.3	4540	0.042	42	0.16	6.85
4.5	101.3	3074	0.065	65	0.03	2.22
4.5	101.3	4443	0.044	44	0.15	6.70
4.5	101.3	4518	0.043	43	0.17	6.91
4.5	101.3	4527	0.042	42	0.16	6.78
11	101.3	3435	0.058	58	0.06	3.38
11	101.3	7250	0.027	27	0.56	15.24
11	101.3	6084	0.032	32	0.37	11.86
11	101.3	5454	0.035	35	0.28	9.75

**Table-3.6 Evaluation of exergy at state 3 (product stream)**

Flow (lpm)	Pressure(kpa)	Salinity(ppm)	Total volume of product (m3)	Total mass of product (kg)	Specific exergy(Kj/kg)	Total exergy (kJ)	efficiency	Exergy loss
13	101.3	15	0.045	45	0.263	11.85	0.65	15.88
13	101.3	57	0.075	75	0.24	17.98	0.62	34.75
13	101.3	70	0.072	72	0.23	16.82	0.6	31.21
13	101.3	130	0.068	68	0.21	14.19	0.56	25.51
9	101.3	20	0.04	40	0.26	10.40	0.79	13.41
9	101.3	60	0.07	70	0.24	16.68	0.8	29.90
9	101.3	85	0.065	65	0.23	14.75	0.8	25
9	101.3	150	0.06	60	0.20	12.08	0.75	19.70
7	101.3	24	0.037	37	0.26	9.53	0.76	12.01
7	101.3	120	0.06	60	0.21	12.75	0.77	20.59
7	101.3	150	0.062	62	0.20	12.48	0.74	20.87
7	101.3	160	0.058	58	0.2	11.48	0.69	18.33
4.5	101.3	5	0.035	35	0.27	9.48	0.71	11.69
4.5	101.3	80	0.056	56	0.23	12.83	0.73	19.53
4.5	101.3	100	0.057	57	0.22	12.57	0.69	19.48
4.5	101.3	170	0.058	58	0.19	11.28	0.60	18.07
11	101.3	17	0.042	42	0.26	11.00	0.66	14.39
11	101.3	58	0.073	73	0.24	17.47	0.66	32.71
11	101.3	78	0.068	68	0.23	15.64	0.65	27.50
11	101.3	140	0.065	65	0.20	13.32	0.58	23.07

Fig-3.19 shows two discernible trends for 4.5 lpm to 9 lpm and 11 lpm to 13 lpm. For evaluating specific recovery in lower feed flow range (4.5 lpm -9 lpm), denominator (i.e. feed flow to membrane system) predominates. So, as feed flow increases specific recovery decreases. For higher feed flow range (11 lpm, 13 lpm), numerator (i.e. product flow from membrane system) predominates. With increasing operating pressure product flow across the membrane increases, consequently specific recovery increases. This specific recovery has been evaluated upto a particular scaling free overall recovery value. So, flux decline phenomenon is not experienced here.

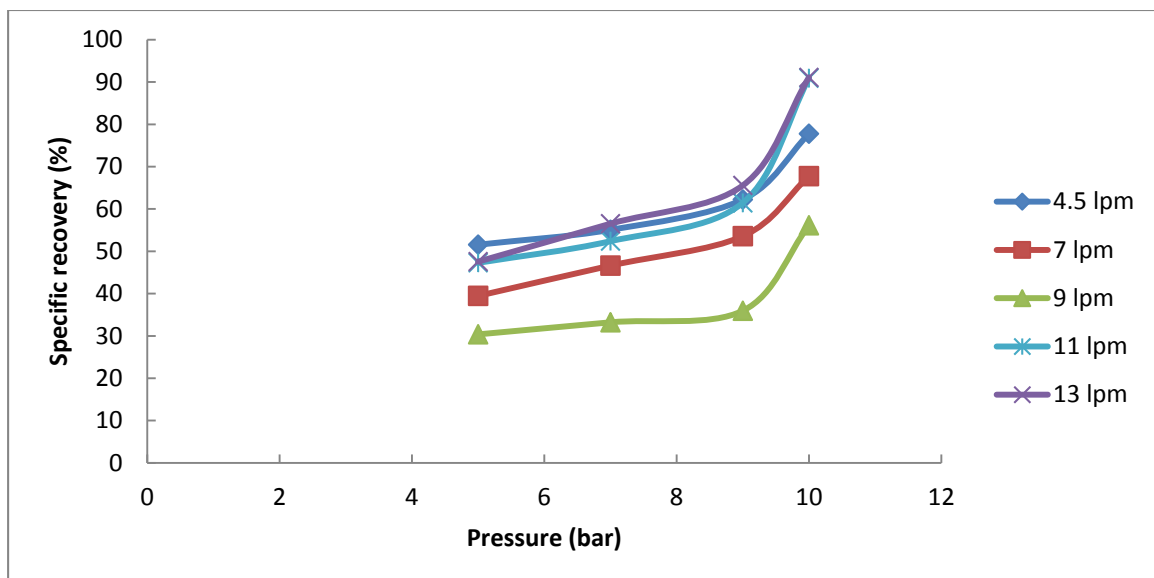


**Fig-3.19 Variation of specific recovery in different flow rate and pressure**

Fig-3.20 shows completely different trends for overall recovery for different flow and different pressure. The basic criteria for selection of overall recovery is the recovery beyond which scaling is going to take place (flux decline greater than 20%). The overall recovery increases with increasing flow rate. With increasing feed flow, by virtue of onset of turbulence on membrane top surface, solid particles could not be settled as a scale on membrane. Consequently, higher recovery can be accomplished with better quality of product

water. With increasing pressure more product water is pushing off through the membrane allowing building up of concentration polarization layer (scaling) on the membrane surface. For higher pressure, recovery is restricted due to scaling constraint.

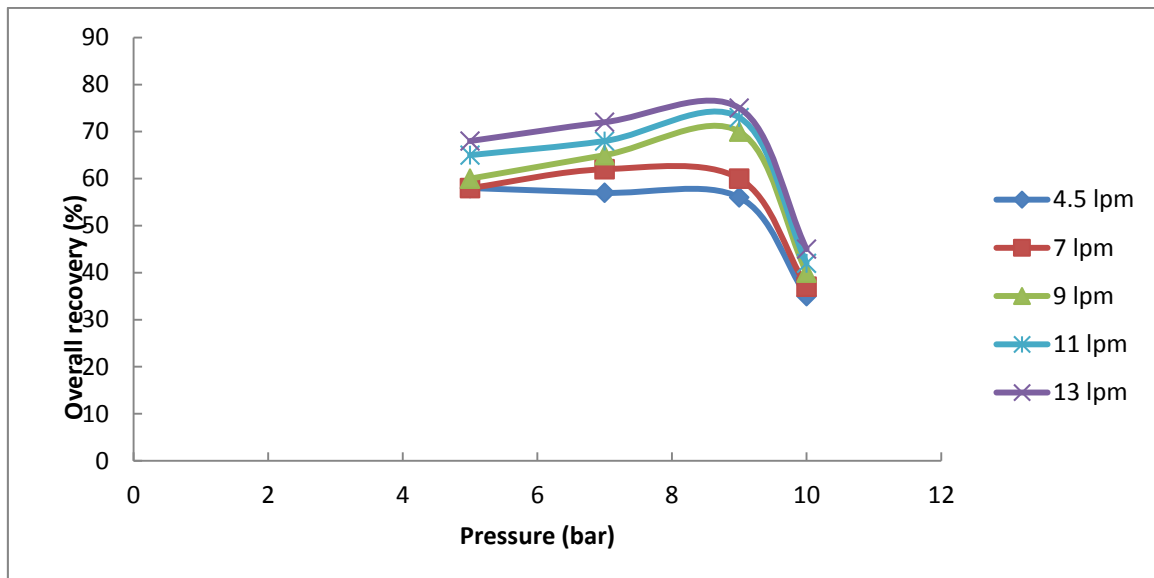


**Fig-3.20 Variation of overall recovery in different flow rate and pressure**

Exergy input is a function of feed flow, feed pressure and duration of experiment to achieve a particular recovery at minimum scale threat. Exergy input is simply evaluated by multiplication of feed flow, feed pressure and duration time. Fig-3.21 reveals two different trends for exergy input as feed flow increases. Initially with increasing feed flow rate, exergy input increases with increasing operating pressure. This trend is observed up to 9 lpm. This process is a batch process, with every time interval reject is losing its energy into atmospheric feed tank, so duration of process to achieve a scale safe recovery is also an important parameter. At higher feed flow rate (11 lpm, 13 lpm) the specific recovery increases which decreases time required to achieve a particular scale safe recovery. At higher pressure also specific recovery increases consequently duration time decreases resulting lower exergy input.

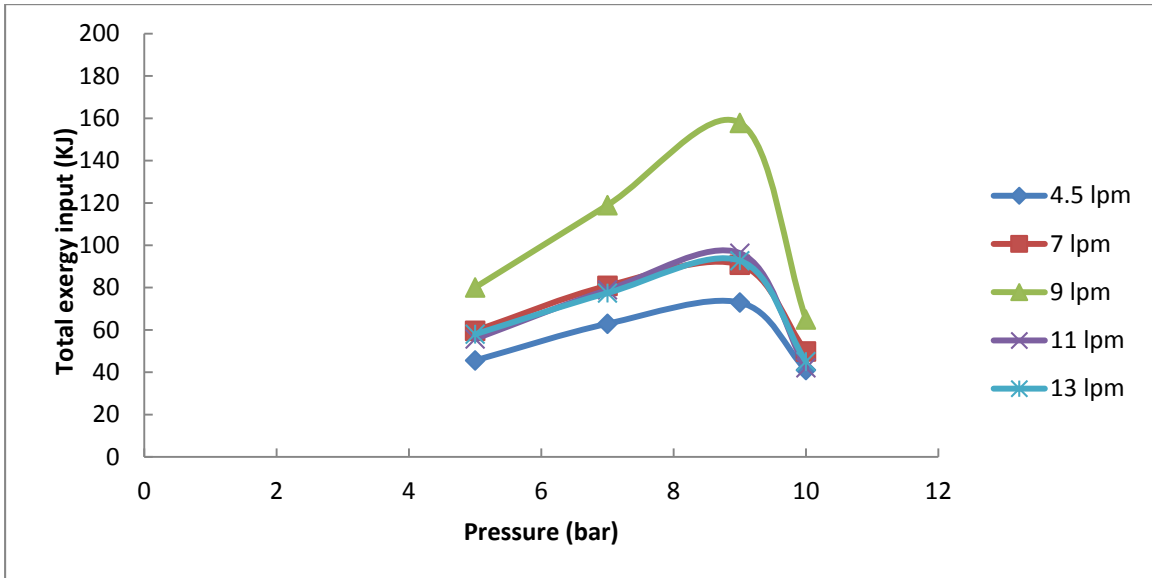


**Fig-3.21 Variation of total exergy input in different flow rate and pressure**

In Fig 3.22 variation of total exergy loss has been at different flow rate has been plotted against pressure. In this particular system, for achieving higher recovery and better quality product exergy loss due to work done will be high which decreases efficiency. Total exergy loss of a system follows the same trend of overall scale safe recovery. Total exergy loss is a function of both overall recovery and also the extent of separation i.e. purity of product. Accordingly Fig-3.22 differs from Fig-3.20

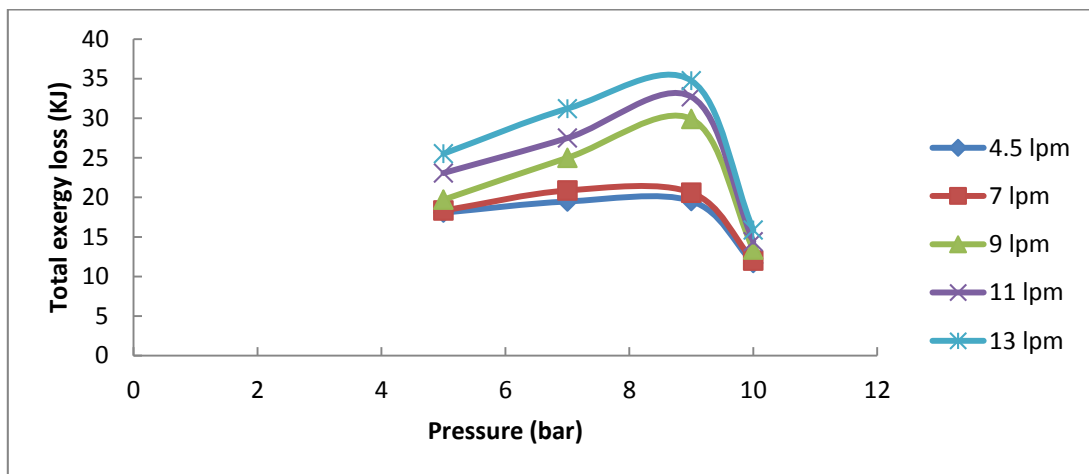


**Fig-3.22 Variation of total exergy loss in different flow rate and pressure**

Fig-3.23 shows that thermodynamic efficiency for a given range of operating pressure and feed flow. It is clear that efficiency is maximum (around 80%) for 9 lpm, 9 bar system. Efficiency decreases for further higher flow rate and higher pressure. For higher flow rate overall scale safe recovery is higher. To achieve this recovery exergy loss will be higher. For higher pressure the product quality is expected to be better. To achieve this extent of separation exergy loss will be higher. For both the cases efficiency decreases.

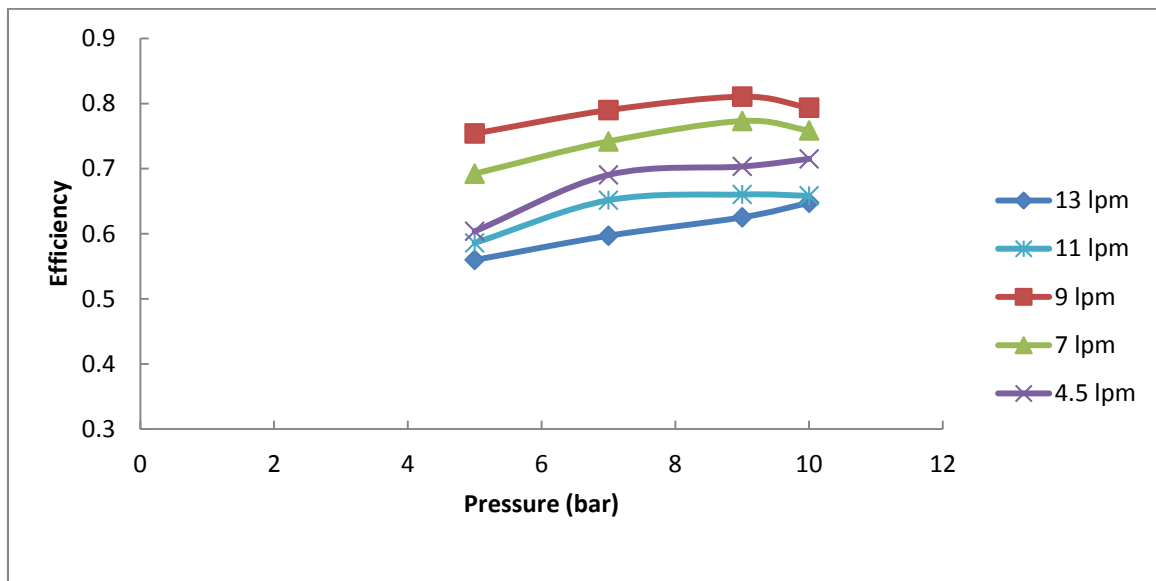


**Fig-3.23 Thermodynamic efficiency of a system for varying pressure and flow rate**

Exergy analysis has given the optimized hydrodynamic parameters (9 lpm feed flow, 9 bar pressure) of nanofiltration process at a minimum scale threat recovery which are the same as evaluated by resistance incorporated surface crystal growth model.

### 3.3.7 Reject Management

Treatment of reject stream with nanofiltration:

Studies were carried out for the concentrates or reject generated from nanofiltration experiments for the removal of excess calcium sulphate present in the supersaturated

solution so as to recycle the solution through NF for further recovery of water. However, this study is confined to the conversion of supersaturated calcium sulphate stream to saturated calcium sulphate stream. The possible methods include free settling, seeding of concentrate & treatment through lime column.

### 3.3.7.1 Free settling:

Concentrates from NF were allowed to settle freely for 120 mins and the concentration of the supernatant solution is monitored with time through the conductance measurement.

Fig.3.24 gives the behaviour of NF concentrates collected from three different flowrates at 9 bar operating pressure. Even though the settling rate appears to be a function of concentration, all the solutions reached the same level of concentration in 120 minutes, which still correspond to supersaturation domain. The experiments reveal that the free settling rate is too slow to recover solid and recycle the concentrate stream.

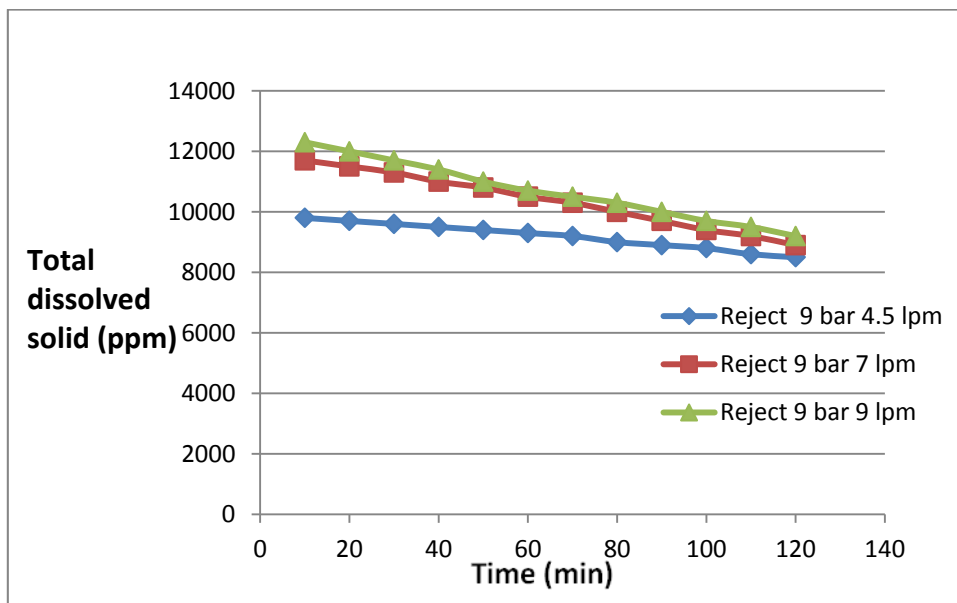


**Fig-3.24 Free settling behaviour of selected reject samples**

### 3.3.7.2 Seeding Studies

Preparation of seed crystals [117]:  $\text{CaSO}_4 \cdot 2\text{H}_2\text{O}$  crystals were prepared by the slow dropwise addition of 500 ml 0.2 M  $\text{CaCl}_2$  solution to 500 ml 0.2 M  $\text{Na}_2\text{SO}_4$  solution at  $70^\circ\text{C}$ . The crystals were washed repeatedly with distilled water until free of chloride ions. In every 200 ml of reject solution 0.75 gm seed has been added.

As seen in the Fig.3.25, seeding with pure calcium sulphate seed crystals only marginally improves the initial settling rate but tends to reach the same levels of concentration akin to settling behaviour without seeding. Increasing the amount of seed for the same amount of solution did not improve either leading to the conclusion that external seeding does not help significantly in the removal of supersaturated calcium sulphate.

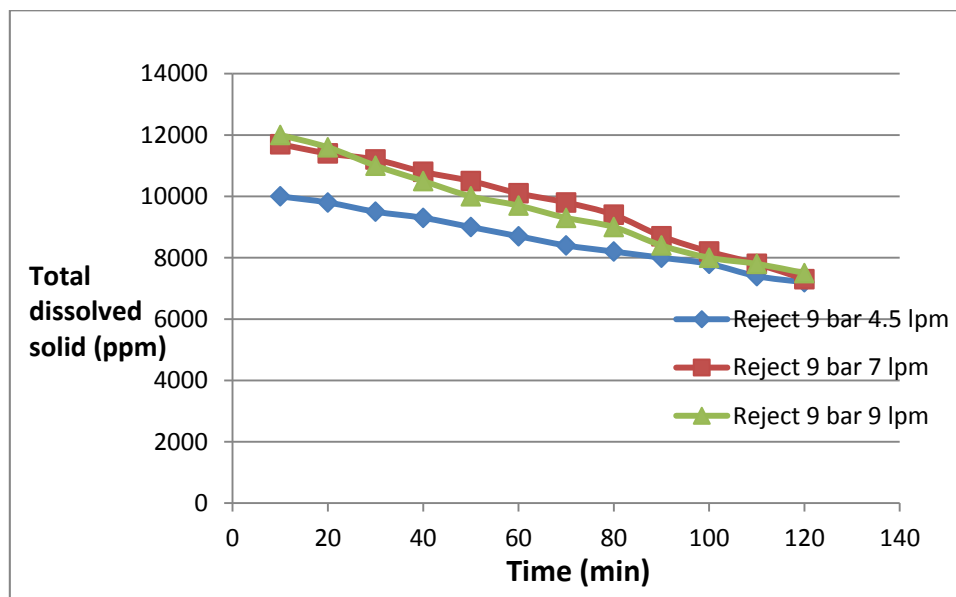


**Fig-3.25 Settling behavior of concentrates with seeding.**

### 3.3.7.3 Treatment through lime column

Lime stone of 1-2 mm size was packed into a glass column of 30 cm dia and the concentrate was passed through at the rate of 3 litres/minute corresponding to a linear

velocity of 0.0007 m/sec by gravity. The concentration of the solution coming out of the column was monitored as a function of time. As can be inferred from Fig.3.26, the passage through lime column appears to be effective in not only in bringing down the concentration of calcium sulphate around saturation level on par with the feed solution but also in a reasonable time.

Following graph shows that lime column is more effective process to decrease the solid content upto saturation limit of calcium sulphate. Here packed lime bed provides the nucleation site which is probably not available in case of external addition of seeding.

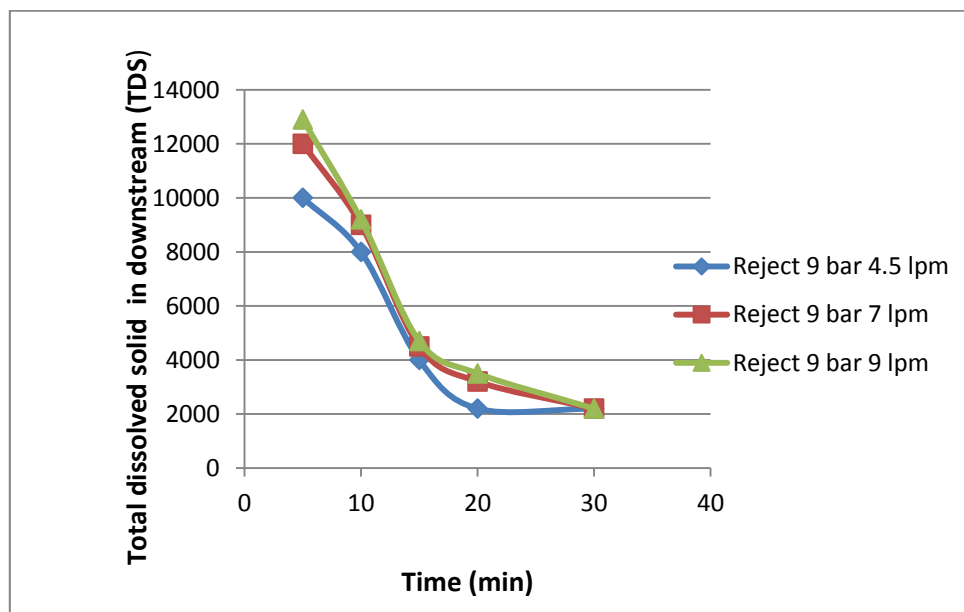


**Fig-3.26 Decrease of solid content of reject samples through lime column**

### 3.3.8 Reverse Osmosis model

Basic objective of this model development is to evaluate the operating pressure at which RO module provides required quality and quantity of product.

By doing mass balance across the membrane

$$J_{w,RO} \cdot C_{p,RO} = J_{s,RO} \quad 3.21$$

$$A_{w,RO} (\Delta P - \Delta \pi) C_{p,RO} = B_{s,RO} \times (C_{f,RO} - C_{p,RO}) \quad 3.22$$

Equation 22 is an iterative equation which evaluate  $\Delta P$  for a given  $C_{p,RO}$

$$J_{w,RO} = A_{w,RO} (\Delta P - \Delta \pi) \quad 3.23$$

Check whether  $J_{w,RO}$  is within the flux range specified by manufacturer.

### **Results from reverse osmosis model**

The optimised pressure for RO is 10 bar

Sulphate concentration obtained from RO is less than 6 ppm

Final product flow obtained from RO is 3.0lpm

(RO feed is taken as 3.8 lpm;the product flow of NF at 9 lpm ,9 bar pressure)

### **3.3.9 Identification of the overall scheme for the approach to Zero Liquid Discharge**

Higher recoveries should be targeted in the NF experiment to reduce the ultimate waste volume. As far as NF experimental run is concerned the operating pressure and feed flow rates have to be chosen to avoid precipitation on the membrane surface. Lime treatment has been found to be effective in removing calcium and sulphate species from the supersaturation levels to below saturation limits as reported [103] and confirmed by our experimental studies. In view of this it is proposed that the concentrate coming out of the NF element be passed through lime column (where the concentration of calcium and sulphate species would be

brought down to less than the saturation levels) and can be mixed with the incoming feed thus leading to higher net recovery of water. It is likely that sodium chloride concentration would go up along with other trace elements. In order to operate the system in a sustainable manner, it must be ensured that the concentrate coming out of the NF membrane and the specific recovery of the module (containing a few membrane elements in series) are well within the limits corresponding to the scaling point at the operating conditions of pressure and feed flow rate. The concentrate then shall be passed through the lime column and circulated back to feed tank. The resultant solution would be rich in sodium chloride but less in calcium sulphate content. When the net recovery is about 90%, the batch can be stopped and the permeate stream can be processed through brackish water RO system for the recovery of water for reuse. The concentrate of RO which is rich in sodium chloride can be used for softener regeneration. A schematic diagram of approach towards zero liquid discharge has been shown in Fig-3.27.

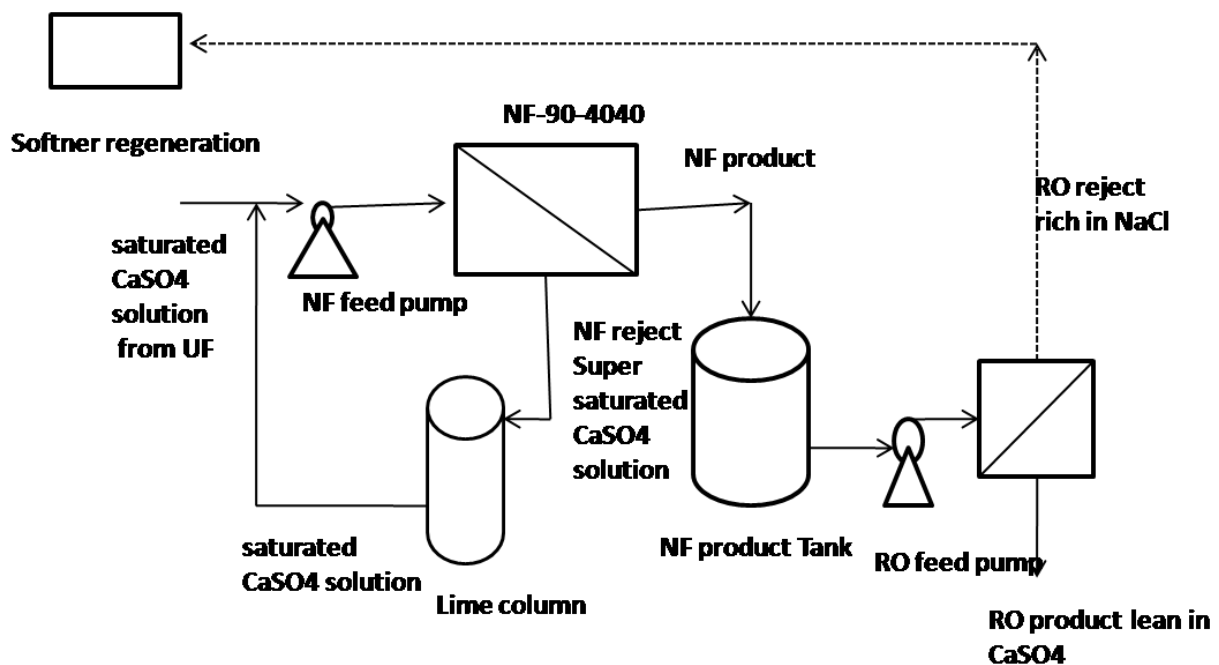


**Fig-3.27 Approach towards zeroliquid discharge**

### 3.4 Conclusion

Our studies have indicated that it is possible to treat saturated calcium sulphate such as those encountered in mining effluents through membrane processes for the recovery of water as well make use of the concentrated salt solution for softener regeneration. The experiments indicated that the scaling of calcium sulphate is a function of degree of supersaturation and the delay time required for the formation of calcium sulphate scales. Our studies indicated that at 12.5 % degree of supersaturation the delay time required was about 400 s. Keeping this fact in mind, if one can decide the operating parameters, it is possible to minimise scaling on the membrane surface. Our detailed experiments have indicated that for the given concentration (similar to mining effluents) at 70% recovery there is a distinct drop in the observed flux for all the flow rates and the pressures employed. Hence, it was concluded that by optimising the operating pressure (which controls the flux) and the flowrate (to ensure that the boundary is not allowed to build up fast), it would be possible to recover water for reuse.

Unlike the case of RO, substantial quantity of monovalents such as sodium chloride permeate through the membrane thus reducing the loss of flux due to osmotic pressure build up. The water through NF therefore has substantial quantities of sodium chloride. This stream when processed through RO yielded concentrated sodium chloride as concentrated stream and water with less total dissolved contents. Hence the product stream can be reused in the process, while the concentrate can be used for the regeneration of softeners. The concentrate of NF system is passed through lime column where the supersaturated levels of calcium sulphate is reduced to unsaturated levels and could be recycled through NF. A small amount requires to be bled in order to maintain the total TDS levels within operable limits.

Thus the membrane based scheme emerged through experimental study consists of NF and RO and a lime column and provides an approach to zero release concept besides allowing the recovery of value through purified water and sodium chloride for reuse in the process.

Mathematical model has been developed not only to predict the behaviour of NF system but also to optimise the operating conditions for a given feed composition to minimise the scale threat for achieving the specific separation objective. Assessment of different resistance terms (intrinsic membrane resistance, osmotic and scale resistance) were carried out experimentally in nanofiltration membrane and by incorporating these resistance terms in mathematical model, experimental flux decline has been predicted for the entire recovery range including post scaling phase. Different operating conditions have been thermodynamically optimised for obtaining maximum recovery at minimum scale threat by thermodynamic parameter 'exergy'. This exercise also concludes that 9 lpm feed flow and 9 bar operating pressure are the optimised condition for the assumed composition of effluents. At these two conditions, thermodynamic efficiency of the system is maximum. Incorporation of an existing mathematical model for reverse osmosis for optimizing the operating pressure for obtaining required product quality and quantity has been carried out. The optimised pressure for reverse osmosis system is obtained as 10 bar for getting sulphate concentration in product water less than 10 ppm.

The reject management of supersaturated stream coming from NF module has been attempted under different conditions including free settling, seeded settling and through lime column. It is observed that the lime column is the best suited as it can bring down the calcium sulphate concentration below the super saturation levels at the minimum possible time and is amenable to integrate with the membrane system for continuous operation. This scheme opens up the possibility of approaching Zero Liquid Discharge for such difficult effluents.

## **CHAPTER-4**

# **SUMMARY AND CONCLUSION**

The present work deals with the applications of membrane processes, particularly the hybrid membrane systems for the treatment / management of effluents. The pressure driven membrane processes involving ultrafiltration (UF), nanofiltration (NF) and reverse osmosis (RO) were chosen in view of their growing potential due to inherent advantages such as simple ambient temperature operation, eco-friendly nature and cost effectiveness. The pressure driven membranes can operate based on size –exclusion philosophy as in UF/MF or combined effect of electrostatic interaction and size exclusion as in RO/NF. It was evident that membrane processes cannot give absolute separation for contaminants owing to its pore size distribution. Removal of trace contaminants or radioactive contaminants from effluent stream demands almost absolute separation of contaminants as the environmentally safe limits of these contaminants are low and stringent. Use of NF or RO for the removal trace contaminants in the presence of benign dissolved solutes may restrict the recovery due to osmotic pressure build up on the feed side. Some of the studies have indicated that complexation ultrafiltration could be useful for the removal of trace contaminants. Hence it was pertinent to look for some other means such as chemical addition or combination of two or more processes- hybrid membrane processes (can be different membrane processes or membrane and conventional processes) to achieve the objectives. The existing models in the literature for complexation UF are essentially based on laboratory studies under near zero recovery conditions and do not represent systems where high recoveries were expected. Mining effluents contain near saturation amounts of calcium sulphate and in general RO cannot be used for concentrating the streams for further treatment/disposal. However it was felt that NF could be used as NF membranes can preferentially retain multivalents compared to monovalents thus affording better volume reduction overcoming the osmotic pressure limitations to a reasonable extent. Study of the calcium sulphate precipitation characteristics in the literature indicated that some significant gelation time is required for the precipitates to

form. Thus making use of these two information, it was decided to study the NF-RO hybrid system for the recovery of water and make use of the concentrated stream containing sodium chloride for softener regeneration. It was also decided to develop the mathematical model for wider application and in situ optimization of parameters depending on effluent concentrations. Accordingly, it was decided to study the treatment of effluents through hybrid membrane systems; one for the recovery of water from bulk scaling contaminants and the other for the removal & separation of trace contaminants and develop mathematical models for their wider applicability.

The mathematical model existing in the literature is based on the basic assumption that the complexing agent is fully rejected either as complexed or uncomplexed form and the metal ions are not at all rejected in its uncomplexed state. However, this assumption does not hold good whenever higher recoveries of water or high volume reduction factors are expected. Our initial experiments have shown very large errors compared to the model prediction based on the model with the above mentioned assumptions. This was attributed to the pore-size distribution which is always inherent in the membranes formed by phase inversion technique. Similarly any high molecular weight complexing polymer has a molecular weight distribution. These two factors were introduced into the basic irreversible thermodynamic model by modifying solute permeability ( $\omega$ ) in terms of discretised pore size distribution and the reflection coefficient ( $\sigma$ ) in terms of molecular weight distribution of ligand. The experimental results obtained have validated the model and it was also possible to show that the model could predict the performance for mixed solute systems. The mathematical model developed in this present studies can predict the experimental rejection value of different trace metals (copper, cobalt and iron) complexed with polyethyleneimine below 4 % error range. This model can also predict the fractionation potential of intra membrane hybrid membrane system by predicting the rejection behaviour of multicomponent solute mixture

through different molecular weight cut-off membranes. Thus, we could not only demonstrate that trace element contamination can easily be removed using complexation–UF with a good volume reduction at lower energy cost compared to RO but the model developed incorporating the basic membrane morphological characteristics and complexing polymer characteristics in terms of molecular weight heterogeneity can predict the performance of the membranes both for individual contaminants and mixed contaminants.

Our studies have indicated that it is possible to treat saturated calcium sulphate such as those encountered in mining effluents can be treated through membrane processes for the recovery of water as well make use of the concentrated salt solution for softener regeneration. Use of NF has not only mitigated the osmotic pressure constraints but also limited the concentration build up of calcium & sulphate species due to the presence of surface charge. The experimental studies have identified the three resistances namely osmotic pressure, boundary layer (scaling) and the membrane resistance. Efforts were made to mitigate the scale resistance. Supported by the studies on the calcium sulphate agglomeration studies it was inferred that the membrane does not phase the scale threat upto about 12.5 degree of supersaturation. Accordingly it was demonstrated that it is possible to recover about 70% of solution without significant calcium and sulphate contamination. Hence it was concluded that by optimising the operating pressure (which controls the flux) and the flowrate (to ensure that the boundary is not allowed to build up fast), it would be possible to recover water for reuse. Further it was demonstrated that the permeate stream of NF processed through RO can yield nearly pure water ( about 6 ppm) for reuse and the concentrate containing NaCl can be sent for regeneration of the softeners. The concentrate of NF system is passed through lime column where the supersaturated levels of calcium sulphate is reduced to unsaturated levels and could be recycled through NF. A small amount requires to be bled in order to maintain the total TDS levels within operable limits.

Thus the membrane based scheme emerged through experimental study consists of NF and RO and a lime column and provides an approach to zero release concept besides allowing the recovery of value through purified water and sodium chloride for reuse in the process.

Mathematical model has been developed not only to predict the behaviour of NF system but also to optimise the operating conditions for a given feed composition to minimise the scale threat for achieving the specific separation objective. Assessment of different resistance terms (intrinsic membrane resistance, osmotic and scale resistance) were carried out experimentally in nanofiltration membrane and by incorporating these resistance terms in mathematical model, experimental flux decline has been predicted for the entire recovery range including post scaling phase. Different operating conditions have been thermodynamically optimised for obtaining maximum recovery at minimum scale threat by thermodynamic parameter 'exergy'. This exercise also concludes that 9 lpm feed flow and 9 bar operating pressure as the optimised condition for the assumed composition of effluents at which thermodynamic efficiency of the system is maximum. Incorporation of an existing mathematical model for reverse osmosis for optimizing the operating pressure for obtaining required product quality and quantity has been carried out. The optimised pressure for reverse osmosis system is obtained as 10 bar for getting sulphate concentration in product water less than 10 ppm.

The reject management of supersaturated stream coming from NF module has been studied under different conditions including free settling, seeded settling and through lime column. It is observed that the lime column is the best suited as it can bring down the calcium sulphate concentration below the super saturation levels at the minimum possible time and is amenable to integrate with the membrane system for continuous operation. This scheme opens up the possibility of approaching Zero Liquid Discharge for such difficult effluents.

Mathematical model developed for water recovery and reuse from near saturated sparingly soluble mine effluents by hybrid NF-RO system is unique for its novel attempt to demonstrate the potential of membrane for sparingly soluble salt removal by optimizing the hydrodynamics, without addition of antiscalant. Application of NF prior to RO is critical step in which most bivalent load can be eliminated by high flux NF keeping RO at minimum scale threat. Incorporation of resistance terms for evaluation of flux decline in NF improves the model predictability.

## Nomenclature

$A$	Molecular weight PEG/PEO
$A_k$	Ratio of total cross sectional pore area to the effective membrane area
$A_t$	Membrane area, $m^2$
$A_w$	Solvent permeability constant, $m/hr\text{-bar}$
$C_b$	Bulk concentration, $kg/m^3$
$C_s$	Saturation concentration, $kg/m^3$
$C_w$	Wall concentration, $kg/m^3$
$(C_s)_{ln}$	Logarithmic solute concentration, $kgmole/m^3$
$C_m$	Concentration on membrane surface, $kgmole/m^3$
$C_p$	Product concentration, $kgmole/m^3$
$D$	Diffusivity, $m^2/sec$
$d_h$	Hydraulic diameter, $m$
$f(q)$	Correction factors for effect of cylindrical walls for filtration flow
$g(q)$	Correction factors for effect of cylindrical walls for convection flow
$[H]$	Hydrogen ion concentration, $kgmole/m^3$

$[HL]$	Concentration of protonated ligand, $\text{kgmole/m}^3$
$J_b$	Bulk flux, $\text{m/hr}$
$J_c$	Bulk flux due to cake resistance, $\text{m/hr}$
$J_w$	Pure water permeability, $\text{m/hr}$
$J_v$	Solvent flux, $\text{m/s}$
$J_s$	Solute flux, $\text{m/s}$
$k$	Mass transfer coefficient, $\text{m/sec}$
$K_s$	Saturation constant, $\text{sec}^{-1}$
$K_{i,n}$	Equilibrium constant of complex, $(\text{kgmole/m}^3)^{-n}$
$K_a$	Equilibrium constant of protonated ligand, $(\text{kgmole/m}^3)^{-1}$
$[L]$	Concentration of ligand in feed, $(\text{kgmole/m}^3)$
$[L]_{free}$	Concentration of free ligand, $(\text{kgmole/m}^3)$
$L_p$	Solvent permeability constant, $\text{m/s-Pa}$
$m_s$	Weight of scale formed, $\text{kg}$
$[Me]$	Concentration of metal in feed, $(\text{kgmole/m}^3)$
$[MeL_n]$	Concentration of metal ligand complex, $(\text{kgmole/m}^3)$

$[Me]_{free}$	Concentration of free metal, (kgmole/m <sup>3</sup> )
$M_w$	Molecular weight, kg/kgmole
$M$	Molecular wt. of PEG/PEO kg/kgmole
$n$	Coordination number
$N_A$	Avogadro's number
$\Delta P$	Pressure difference, bar
$q$	Ratio of solute radius and pore radius
$R$	Recovery
$R_c$	Cake resistance, m <sup>-1</sup>
$R_m$	Membrane resistance, m <sup>-1</sup>
$R_L$	Rejection of ligand
$R_{Me}$	Rejection of metal
$R_{Mefree}$	Rejection of free metal
$r_s$	Solute radius, m
$r_p$	Pore radius, m
$S_D$	Steric hindrance factor for diffusive flow

$S_F$	Steric hindrance factor for filtration flow
$SR$	Salt rejection
$u$	Velocity, m/sec
$V_b$	Volume of feed tank, m <sup>3</sup>
$V_p$	Volume of product tank, m <sup>3</sup>
$\beta$	Area occupied per unit mass m <sup>2</sup> /kg
$\Delta\pi$	Osmotic pressure, bar
$i$	No. of species
$[\eta]$	Specific viscosity, m <sup>3</sup> /kg
$\omega$	Solute permeability constant, kgmole/N-s
$\mu_p$	Mean pore size of membranes
$\sigma$	Reflection coefficient
$\Delta p$	Effective operating pressure, Pa
$\Delta X$	Membrane thickness, m

## References

1. Mark Wilf, Leon Awerbuch, Craig Bartels, Mike Mickley, Graeme Pearce, Nikolay Voutchkov, The Guidebook to Membrane Desalination Technology: Reverse Osmosis, Nanofiltration and Hybrid Systems Process, Design, Applications and Economics, Balaban Publishers, 1st edition, January 1, 2007
2. Steven Till, Henry Mallia, Membrane Bioreactors: Wastewater treatment applications to achieve high quality effluent, 64th Annual Water Industry Engineers and Operators' Conference, 5 and 6 September, 2001
3. Anil K. Pabby, Syed S.H. Rizvi, Handbook of membrane separations: Chemical, Pharmaceutical, and Biotechnological Applications, CRC Press, 07 July 2008
4. Chiranjib Gupta, Harbinderpal Singh, Uranium resource processing: secondary waste, Springer, 12-Feb-2003
5. D. Rana, T. Matsuura, M.A. Kassim, A.F. Ismail Radioactive decontamination of water by membrane processes — A review, Desalination 321 (2013) pp77–92
6. A.G. Chmielewski, M. Harasimowicz, G. Zakrzewska-Trznadel, Membrane technologies for liquid radioactive waste treatment, Czech. J. Phys. 49 (S1) (1999) pp979–985
7. Zaidi, Javaid, Matsuura, Takeshi, Polymer membranes for fuel cell, Springer, 2009
8. B. Jiao, A. Cassano, E. Drioli, Recent advances on membrane processes for the concentration of fruit juices: a review, Journal of Food Engineering, 63 3 (2004) pp303–324
9. Hanki Kim, Jooyoung Jeong, Jawon Shin and Jooyang Park, Effect of the Applied Electric Potential on Nitrate Removal in Bipolar Electrolysis Using ZVI Packed Bed, 2012, 2nd International Conference on Environmental and Agriculture Engineering IPCBEE volume 37 (2012) IACSIT Press, Singapore

10. Jovan Matovic, Nanomembranes-an overlooked 2D nanostructure, Viena University of Technology, EuroNanoForum2011-Budapest
11. Ronald W. Rousseau, Handbook of Separation Process Technology, Wiley, 13-May-1987
12. Nadine Schmeling, Roman Konietzny, Daniel Sieffert, Patrick Rölling and Claudia Staudt, Functionalized copolyimide membranes for the separation of gaseous and liquid mixtures, Beilstein J. Org. Chem. 2010 (6) pp 789–800
13. Junbai Li, Qiang He, and Xuehai Yan, Molecular Assembly of Biomimetic Systems. © 2011 WILEY-VCH Verlag GmbH & Co. KGaA, Weinheim
14. Hendrik Verweij, Inorganic Membranes, Current Opinion in Chemical Engineering, 2012 12 pp 156–162
15. Jiyong Heo, Linkel K. Boateng, Joseph R.V. Flora, Heebum Lee, Namguk Her, Yong-Gyun Park, Yeomin Yoon, Comparison of flux behavior and synthetic organic compound removal by forward osmosis and reverse osmosis membranes, Journal of Membrane Science, 443 (2013) pp 69-82
16. Libin Yang, Junke Tang, Lei Li, Fei Ai, Xiaoyong Chen, Wang Zhang Yuan and Yongming Zhang; Properties of precursor solution cast PFSI membranes with various ion exchange capacities and annealing temperatures, RSC Adv., 2013 3 pp 7289-7295
17. Ulrich Siemann, Solvent cast technology – a versatile tool for thin film production; Progr Colloid Polym Sci (2005) 130 pp 1–14
18. M Buczkowski, BSartowska, D Wawszczak, W Starosta, Radiation resistance of track-etched membranes, Radiation Measurements, 34 (2001) 1-6 pp 597-699
19. [www.separationprocesses.com](http://www.separationprocesses.com)
20. S. Loeb, S. Sourirajan, Preparation of asymmetric Loeb-Sourirajan Membranes, Polymer Letters Edition, 11(1973) pp 201-205

21. [www.lenntech.com](http://www.lenntech.com)
22. Tzahi Y. Cath, Amy E. Childress, Menachem Elimelech, Forward Osmosis: Principles, applications and recent developments; *Journal of Membrane Science*, 281 (2006) 1-2 pp70-87
23. H. Strathmann, Electromembrane Processes: Basic Aspects and Applications; *Comprehensive Membrane Science and Engineering*, 2 (2010) pp391-429
24. M. Tomaszewska, Membrane Distillation - Examples of Applications in Technology and Environmental Protection, *Polish Journal of Environmental Studies* 9 (2000), pp27-36
25. W. Kamiński, W. Kwapiński, Applicability of Liquid Membranes Environmental Protection, *Polish Journal of Environmental Studies* Vol. 9, No. 1 (2000), pp37-43
26. <http://www.emis.vito.be>
27. De Carvalho, A study of retention of sugars in the process of clarification of pineapple juice (*Ananas comosus*, L. Merrill) by micro- and ultra-filtration, *Journal of Food Engg*, 87(4) (2008) pp447-454
28. Puliot Y. et.al, Membrane processes in dairy technology—From a simple idea to worldwide panacea *International Dairy Journal*, 18 7(2008)pp735-740
29. Wolters, R. et.al, Rinsing water recovery in the steel industry — a combined UF/NF treatment, *Desalination*, 224(1-3)(2008)pp209-214
30. Govalvez et.al, Nanofiltration of secondary effluent for wastewater reuse in the textile industry *Desalination*, 222(1-3) (2008) pp272-279
31. Walha et.al, Treatment by nanofiltration and reverse osmosis of high salinity drilling water for seafood washing and processing Abstract, *Desalination*, 219 (1-3) (2008)pp231-239
32. [www.synderfiltration.com](http://www.synderfiltration.com)

33. Douglas M. Ruthven, Diffusion through Porous Media: Ultrafiltration, Membrane Permeation and Molecular Sieving; diffusion-fundamentals.org 11 (2009) 13 pp1-20
34. Takeshi Matsuura; Membrane Separation Technologies; Water Sciences, Engineering and Technology Resources-2004 EOLSS Publishers
35. Rajinder Singh, Hybrid Membrane Systems for Water Purification: Technology, Systems Design and Operations; February 22, 2006
36. Osman A. Hamed, Overview of hybrid desalination systems- current status and future prospects- Presented at “Chemistry & Industry” Conference, King Saud University, Riyadh, on 11 to 15 Dec., 2004
37. M.Soltanieh et.al., Review of reverse osmosis membranes and transport model, Chemical Engineering Communication, <http://www.tandfonline.com/loi/gcec20>
38. Katchalsky and O. Kedem, Thermodynamics of flow processes of biological systems, Membrane Biophysics, 1958 pp 53-78
39. M.Kargolet.al., Mechanistic Formalism for Membrane Transport Generated by Osmotic and Mechanical Pressure, Gen. Physiol. Biophys. (2003), 22, pp51-68
40. ANDRZEJ ŚLĘZAK<sup>1</sup> et.al., A development of the generalized Spiegler-Kedem-Katchalsky modelequations for interactions of hydrated species in transport through polymeric membranes, [www.polimery.am.wroc.pl/2006/405](http://www.polimery.am.wroc.pl/2006/405)
41. Baburao.S. Mohite et.al , Column chromatographic separation of uranium(VI) and other elements using poly(dibenzo-18-crown-6) and ascorbic acid medium, Journal of Chromatography A , 983 (2003) pp277–281
42. Nalini P et.al, Permeation liquid membrane for trace metal speciation in natural waters, Transport of liposoluble Cu(II) complexes, Journal of chromatography A, 1025 (2004) pp33–40

43. Juang,Chen et.al, Measurement of Binding Constants of Poly(ethyleneimine) with metal ions and metal chelates in aqueous media by ultrafiltration , Ind.Eng.Chem.Res.35(1996) pp1935-1943
44. Pieter Vonk et.al., Ultrafiltration of a polymer-electrolyte mixture, Journal of Membrane Science, 130(1997) pp249-263
45. R. Molinari et.al., Metal-ions removal from wastewater or washing water from contaminated soil by ultrafiltration-complexation, Water Research 38 (2004) pp593-600
46. P. Canizares et.al., A semicontinuous laboratory-scale polymer enhanced ultrafiltration process for the recovery of cadmium and lead from aqueous effluents, Journal of Membrane Science, 240(2004) pp197-200
47. P.Canizares et.al., Improvement and modeling of a batch polyelectrolyte enhanced ultrafiltration process for the recovery of copper, Desalination 184(2005) pp357-366
48. P.Canizares et.al., Selective separation of Pb from hard water by a semi-continuous polymer-enhanced ultrafiltration process (PEUF), Desalination 206(2007) pp602-613
49. P. Canizares et.al., Simultaneous recovery of cadmium and lead from aqueous effluents by a semi-continuous laboratory-scale polymer enhanced ultrafiltration process, Journal of Membrane Science,320(2008)pp520-527
50. Javier Llanos et.al., Copper recovery by polymer enhanced ultrafiltration (PEUF)and electrochemical regeneration,Journal of Membrane Science 323 (2008) pp28–36
51. Javier Llanos et.al., Polymer supported ultrafiltration as a technique for selective heavy metal separation and complex formation constants prediction, Separation and purification technology,73(2010) pp126-134
52. S.Singh et.al., Membrane characterization by solute transport and atomic force microscopy, Journal of Membrane Science 142(1998) pp111-127

53. Michales et.al., Analysis and prediction of Sieving Curves for ultrafiltration membranes: A universal correlation?, Separation Science and Technology, 15 (6) 1980 pp1305-1322
54. Katsumi Kaneko, Review determination of pore size and pore size distribution 1. Adsorbents and Catalysts, Journal of Membrane Science 96 (1994) pp59-89
55. Youm et.al., Prediction of Intrinsic Pore Properties of Ultrafiltration Membrane by solute rejection curves: Effects of operating conditions on pore properties, Journal of Chemical Engineering of Japan 24, 1 (1991) pp1-7
56. E.A. Mason et.al., Statistical- Mechanical Theory of Membrane Transport, Journal of Membrane Science, 51(1990) pp1-81
57. Noordman et.al., Transport of large molecules through membranes with narrow pores- The Maxwell-Stefan description combined with hydrodynamic theory, Journal of Membrane Science, 210(2002)pp227-243
58. Gill et.al., Review of Reverse Osmosis Membranes and Transport Models, Chem. Eng. Commun. 12 (1981) pp 279-363
59. Pappenheimer Jr. Passage of molecules through capillary walls, Physiol. Rev. 333 (1953) pp387-423
60. Verinory et.al. Measurement of the Permeability of Biological Membranes— Application to the Glomerular Wall, J. Gen. Physiol. 62 (1973) pp489-507.
61. Nakao, Kimura, Analysis of solute rejection in ultrafiltration, Journal of chemical Engg. Japan, 141(1981) pp32-37
62. Shiro Kobayashi et.al., Chelating properties of linear and branched polyethyleneimine, Macromolecules, 20(1987) pp1496-1500
63. Hatsuo Ishida, Properties of Polymers, Department of Macromolecular Science, Western Reserve University, Cleveland, Ohio.

64. R.J.Bowell, Review of sulphate removal options for mine waters, [www.imwa.info/docs/imwa\\_2004/IMWA2004\\_43\\_Bowell.pdf](http://www.imwa.info/docs/imwa_2004/IMWA2004_43_Bowell.pdf)
65. Mpinga, CleophaeNgoie, "Removal and recovery of aluminium and sulphate ions from an alkaline medium using solvent extraction"(2009). CPUT Theses & Dissertations. Paper 125.[http://dk.cput.ac.za/td\\_cput/125](http://dk.cput.ac.za/td_cput/125)
66. Godfrey Madzivire, Removal of sulphates from South African mine,water using coal fly ash,etd.uwc.ac.za/usrfiles/.../etd\_gen8Srv25Nme4\_1231\_1297840178.
67. Awadalla, F. T. and Kumar, A., Opportunities for Membrane Technologies in the Treatment of Mining and Mineral Process Streams and Effluents, Separation Science and Technology, 29 10(1994)pp 1231-1249.
68. Antonio Pérez Padilla, Eduardo L. Tavani,Treatment of Industrial effluents by Reverse Osmosis, Desalination 126(1999) pp219-226
69. AndityaRahardianto, JunboGao, Christopher J. Gabelich, Mark D. Williams and Yoram Cohen, High recovery membrane desalting of low-salinity brackish water: Integration of accelerated precipitation softening with membrane RO, Journal of Membrane Science 289 (2007) pp123–137
70. EfremCurcio, Hybrid nanofiltration-membrane crystallisation system for the treatment of sulphate wastes, Journal of Membrane Science, 360 1-2 (2010) pp493-498
71. GJG Juby et.al., Membrane life in a seeded slurry reverse osmosis system, Water SA Vol. 26 No. 2 April 2000
72. Mark Williams, Non-thermal Process for Recovering Reverse Osmosis Concentrate: Process Chemistry and Kinetics, Presented at the 2002 Water Quality Technology Conference, American Water Works Association, November 10-14, 2002, Seattle, Washington.

73. Sandeep Sethi, Existing & Emerging Concentrate Minimization & Disposal Practices for Membrane Systems, June 2006, Florida Water Resources Journal
74. Wen-Yi-Shih et.al., A dual probe approach for evaluation of gypsum crystallization in response to antiscalant treatment, *Desalination*, 169 3(2004)pp 213-221
75. Marina Prisciandaro et.al., Retardant effect of different additives on gypsum nucleation, [www.aidic.it/icheap9/webpapers/432Prisciandaro.pdf](http://www.aidic.it/icheap9/webpapers/432Prisciandaro.pdf)
76. A. Kavitskaya, Reverse Osmosis of concentrated calcium sulphate solutions in the presence of iron (III), *Desalination* 132 (2000) pp281-286
77. Wen-Yi-Shih et.al., Ranking of antiscalant performance for gypsum scale suppression in the presence of residual aluminium 1961-3 (2006)pp280-292
78. Julius Glater, John Schwartz, High temperature solubilities of calcium sulphate hemihydrate and anhydrite in natural sea water concentrates, *Journal of Chem. Engg. Data*, 21 1(1976) pp-47-52
79. R. Sheikholeslami, Assessment of the scaling potential for sparingly soluble salts in RO and NF units , *Desalination* 167 (2004)pp247-256
80. NuralKuyuck et al, Lime neutralisation process for treating acidic waters, US Patent Issued on June 27, 1995
81. Sangho Lee et.al., Analysis of Calcium sulphate scale formation mechanism in various nanofiltration module, *Journal of Membrane Science* 163 (1999) pp63–74
82. T. Chaabane et.al, Contribution to the comprehension of the calcium ions transfer phenomena through a nanofiltration spiral wound membrane, *Desalination* 167 (2004) pp361-368

83. T. Chaabane et.al, Modelling of the concentration polarization of the bivalent salts using a Nanomax50 membrane in nanofiltration process, *Desalination* 200 (2006) pp406–408
84. T. Chaabane et.al., Retention modelling of the bivalent cations in crossflownanofiltration investigation in the porous models, *Desalination* 204 (2007) pp359–367
85. Yann A. Le Gouellec et.al. Control of Calcium Sulfate (Gypsum) Scale in Nanofiltration of Saline Agricultural Drainage Water, *Environmental Engineering Science*, Volume 19, Number 6, 2002
86. M.S.H. Bader, Analysis of the Paradox Valley brine desulfation by nanofiltration, *Desalination* 229 (2008) pp33–51
87. C.A.C. van de Lisdonk et.al. Prediction of supersaturation and monitoring of scaling in reverse osmosis and nanofiltration membrane systems, *Desalination* 138 (2001) pp259-270
88. Sébastien Déon, A transport model considering charge adsorption inside pores to describe salts rejection by nanofiltration membranes, *Chemical Engineering Science* 66 (2011) pp2823–2832.
89. Benito J. Marinas et al., Modeling concentration–polarization in reverse osmosis spiral wound elements, *J. Environ. Eng.*, 122 (4)(1996) pp292–298.
90. SJoan D. Willey : The Effect of ionic strength on the solubility of an electrolyte, *J. Chem. Educ.*, 81 11 (2004)pp 1644
91. Michael Uchymiak et.al., Kinetics of gypsum crystal growth on a reverse osmosis membrane, *Journal of Membrane Science*, 3141-2 (2008)pp163-172
92. Amedeo Lancia et.al, Measuring induction Period of calcium sulphate dihydrate precipitation, *AIChE Journal*, 452 (1999)pp 390-397

93. F.Alimi et al., Kinetics of the precipitation of CaSO<sub>4</sub> dihydrate in a desalination unit, Desalination 157 (2003) pp9-16
94. Sangho Lee and Chung-Hak Lee, Effect of operating conditions on CaSO<sub>4</sub> scale formation mechanism in nanofiltration for water softening, Water Resource 34 15 (2000) pp3854-3866
95. Che-Jen Lin et.al., Discussion of “Mechanistic Model for CaSO<sub>4</sub> Fouling on Nanofiltration Membrane, J. Envir. Engg. 133 9 (2007)pp941-942
96. Che-Jen Lin et.al , Effects of operational parameters on cake formation of CaSO<sub>4</sub> in nanofiltration, Water Research 40 (2006) pp806-816
97. David Hassan et.al, Mechanism of calcium sulphate scale deposition on heat transfer surface, I&EC Fundamentals, 9 1 (1970)pp 1-10
98. Baohong Guan, Liuchun Yang et al., Effect of Mg<sup>2+</sup> Ions on the Nucleation Kinetics of Calcium Sulfate in Concentrated Calcium Chloride Solutions, Ind. Eng. Chem. Res., 49 12 (2010)pp 5569-5574
99. S.He. et.al., The nucleation kinetics of calcium sulfate dehydrate in NaCl solution upto 6 m and 90°C, Journal of colloid and Interface science, 162(1994) pp297-303
100. Tiwari et.al, Evaluation of design parameters of backwashable ultrafiltration system as pretreatment approach to Reverse Osmosis, presented in National symposium “Water For All”, 2009, Coimbatore
101. Vogel's Quantitative Chemical Analysis (6th Edition)
102. Tomi Gominsek, Andrej Lubej et.al., Continuous precipitation of calcium sulphate dehydrate from waste sulphuric acid and lime, Journal of chemical technology and biotechnology: 80 (2005)pp939-947
103. Lorax 2003, A review of sulfate treatment. Report to INAP by Lorax consultants. Electronic document, INAP website [www.inap.com](http://www.inap.com)

104. Benito J. Marinas et al.: Modeling concentration- polarization in Reverse Osmosis Spiral Wound Elements: Journal of Environmental Engineering, 122 4 (1996) pp 292-298
105. www.dow.com ,ROSA 6.0 Manual
106. S. Sourirajan, Reverse Osmosis, Academic Press,1970
107. <http://www.ktf-split.hr/periodni/en/abc/kpt.html>
108. Z.Kovacs et.al, Modeling of batch and semi batch membrane filtration processes, Journal of membrane science,327(2009)pp164-173
109. Z.Kovacs et.al., Numerical simulation and optimization of multi-step batch membrane processes, Journal of Membrane Science,324(2008)pp 50-58
110. [http://en.wikipedia.org/wiki/Euler\\_method](http://en.wikipedia.org/wiki/Euler_method)
111. Alessandra Criscuoli et.al., Energetic and exergetic analysis of an integrated membrane desalination system: Desalination 124 (1999) pp243-249
112. K.S. Spiegler et.al, Energetics of Desalination Process: Desalination 134(2001) pp109-128
113. Yunus Cerci et.al., Exergy analysis of a Reverse Osmosis Desalination Plant in California: Desalination 142 (2002) pp257-266
114. NafizKahraman et.al., Exergy analysis of a combined RO,NF, EDI Desalination Plant:Desalination 171(2004) pp217-232
115. O. Ignatenko et.al., Exergy as a tool for evaluation of the resource efficiency of recycling systems Minerals Engineering 20 (2007) pp862–874
116. H. Mehdizadeh et.al, Membrane desalination plants from an energy–exergy viewpoint: Desalination 191 (2006) pp200–209
117. ZahidAmjadet.al., Performance of polymers as precipitation inhibitors of calcium phosphonate,Canadian Journal of Chemistry,66 (1988) pp1529-1536